Functional and Structural Characterisation of *Streptococcus pyogenes* Nuclease A (SpnA)

Ann (Yu-ming) Chang

A thesis submitted in fulfilment of the requirements for the degree of Doctor of Philosophy

Department of Molecular Medicine and Pathology
The University of Auckland
2013

Abstract

Streptococcus pyogenes, or Group A streptococcus (GAS) is a major human pathogen that is responsible for a wide range of diseases. GAS produces a large arsenal of virulence factors that interferes with the host immune system. *Streptococcus pyogenes* nuclease A (SpnA) is a recently discovered DNase that plays a role in virulence as shown in a mouse infection model. SpnA is the only cell wall-anchored DNase identified in GAS thus far.

The 910-amino acid protein is predicted to contain a N-terminal signal peptide that is followed by three oligonucleotide binding (OB) domains. A predicted exo/endonuclease nuclease is located in the C-terminus with a conserved Gram-positive sortase cell wall anchoring motif, LPKTG, and a cell wall spanning domain. The C-terminal nuclease domain alone is enzymatically inactive. SpnA requires at least two out of the three OB-domains in the N-terminus to be nuclease active. The N-terminal OB-domains are involved in DNA binding as a large amount of DNA is found bound to the peptide.

Using a combination of a *spnA*-knockout mutant and a *Lactococcus lactis* gain-of-function mutant, this study has shown that SpnA promotes bacterial survival in human whole blood and in neutrophil killing assays. The protective effect of SpnA on bacterial cells against killing by blood and NETs is, at least partially, due to its destructive nuclease activity on NETs. SpnA expression is found on the cell surface of GAS as well as in the culture supernatant. Heterologous expression of secreted SpnA in *L. lactis* reveals that the protein is able to protect bacterial cell against killing by blood in both secreted and cell surface anchored forms. A zebrafish embryo infection model is able to present a significant difference between the virulence between GAS wildtype and the *spnA*-knockout.

Structural prediction of SpnA's nuclease domain based on the structure of bovine pancreatic DNase I (BP DNase I) reveals several conserved catalytic activity/Mg^{2+} binding/substrate-binding sites between the two proteins. Site directed alanine mutagesis at these conserved functional residues in SpnA can significantly reduce the nucleolytic activities of the protein. One of the nuclease inactive mutants, SpnA_H716A, appears to inhibit bacterial killing by blood, suggesting SpnA may possess mechanisms other than the nuclease activity that contribute to the overall virulence of GAS.

With the results from this study, we have a more comprehensive understanding in the complex interaction between GAS and its human host. Characterising these pathogen-host interactions may assist in the identification of novel therapeutic targets against GAS infection.

Acknowledgement

I would like to acknowledge and thank my supervisor, Associate Professor Thomas Proft, for providing me with the opportunity to work on this challenging and exciting project. His enthusiasm in science has inspired me, and his continued guidance, patience, and encouragement have supported me through the project.

Thank you to my co-supervisor Dr. Chris Hall for the technical advice in setting up the zebrafish embryo infection model. Thank you to Dr. Hae-Joo Kang for providing the construct of SpnA. And a very special thank you to Dr. Jacelyn Loh for the continued support, the encouragement in times of difficulties, and for proof reading this manuscript.

Thank you to Adrina Khemlani for all the late night platings we did together, and all the technical assistance. Thank you to Weilin Hou, Natalie Lorenz, and Richard Sequeira for the help with phlebotomy, and to all the volunteers who kindly donated blood. Thank you to Leslie Sanderson for assistance with preparing zebrafish embryos.

And thank you to all the past and present members of Proft lab for all the memorable times we spent together. It has been a great pleasure working with all of you! The times we spent together would be one of the most unforgettable parts of my life.

A warm thank you to the friends from Evangelical Formosan Church of North Shore, for supporting me through the prayers in the past five years, this would not be possible without your prayers.

I would like to thank my parents, Eric and Tracy, for being my biggest support throughout the Ph.D. course and for their unconditional love. Thank you to my sister, Angela, for always know how to make me happy. And thank you to my husband, Mike, for his unconditional love, patience and encouragement that make me believe in myself.

Dear God, thank you for leading me onto this path, so I could learn your faithfulness and your abundant grace. May you get all the glory and praise!

This work was made possible through the financial support from the Marsden grant awarded to Associated Professor Thomas Proft by the Royal Society of New Zealand.

Table of Contents

List of Figures

List of Tables

Abbreviations

◦C	Degrees Celsius
%	Percent
Amp	Ampicillin
ATCC	American type cell culture collection
bp	Base pair
BSA	Bovine serum albumin
C-terminal	Carboxy terminus
DNA	Deoxyribonucleic acid
dNTP	Deoxynucleotide triphosphate
FCS	Fetal calf serum
Fig	Figure
g	Gram
g	Gravitational force
GAS	Group A streptococcus
hr/hrs	Hour/hours
IDA	Iminodiacetic acid
Ig	Immunoglobulin
IPTG	Isopropyl β-D-thiogalactopyranoside
kDa	Kilodalton
L	Litre
LB	Luria-Bertani broth
LPS	Lipopolysaccharide
M	Molar
mA	Milliampere
mg	Milligram
MHC	Major histocompatablity complex
min	Minute(s)
µL	Microlitre
mL	Milliliter
µM	Micromolar
mM	Millimolar
ng	Nanogram
NE	neutrophil elastase
NETs	neutrophil extracellular traps

N-terminus	Amino-terminus
OB-fold	Oligosaccharide/oligonucleotide binding fold
PBS	Phosphate buffered saline
PCR	Polymerase chain reaction
pg	Picogram
PMSF	Phenylmethylsulfonyl fluoride
Pmol	Picomol
RBC	Red blood cell
RBS	Ribosomal binding site
rpm	Revolutions per minute
RPMI	Roswell Park Memorial Institute Medium - 1640
s	Second(s)
SDS	Sodium dodecyl sulphate
SDS-PAGE	Sodium dodecyl sulphate-polyacrylamide gel electrophoresis
SpnA	*Streptococcus pyogenes* nuclease A
TBS	Tris buffered saline
TCA	Trichloroacetic acid
TCR	T-cell receptor
TEMED	N,N,N,N – teramethylethylenediamine
THY	Todd-Hewitt broth
TNFα	Tumor necrosis factor alpha
V	Volts
w/w	Weight per weight
w/v	Weight per volume
v/v	Volume per volume

Chapter 1
Introduction

1.1 Streptococcus pyogenes, Group A streptococcus

1.1.1 Classification of the bacterium

Streptococcus pyogenes, also known as Group A streptococcus (GAS), is a Gram-positive, capsulated, facultative anaerobic bacterium that has been recognized as one of the most ubiquitous and versatile human pathogen. Streptococcal bacteria can be classified into different groups according to their haemolytic-activity and antigenic differences in their cell wall carbohydrate composition (Lancefield, 1933). *S. pyogenes* belongs to the β-haemolytic streptococci family, and it is the only member of GAS, characterised by a group-specific carbohydrate composed of N-acetyl β-D-glucosamine and rhamnoase on the surface of the bacterium (Barkulis, Boltralik, Hankin, & Heymann, 1967; Zeleznick, Boltralik, Barkulis, Smith, & Heymann, 1963). In the early 20th century, Dr. Rebecca Lancefield developed a method to further classify GAS into M and T serotypes based on the immunological differences two surface components, M protein, and the T antigen (Lancefield, 1928). The T antigen was later found to be the backbone protein of GAS pilus (Mora et al., 2005). The serotype classification of GAS has been expanded greatly with advanced bioinformatic technology that allows genotyping of GAS by the cloning and sequencing of the M protein (*emm*) gene. There are currently more than 100 M genotypes being identified based on the variable N-terminal sequences of M protein (Facklam et al., 2002).

1.1.2 Streptococcal infections and post-infection sequelae

Humans are the only natural host of GAS. The pathogen is responsible for a broad spectrum of diseases ranging from uncomplicated superficial infections, including pharyngitis and impetigo, to life-threatening invasive illness, such as necrotizing fasciitis and streptococcal toxic shock syndrome (STSS). GAS is also capable of triggering two post-infection sequelae, acute rheumatic fever and acute glomerulonephritis, typically three to four weeks after the initial streptococcal infection (Cunningham, 2008). The cause of acute rheumatic fever is partly due to the production of auto-reactive antibodies that cross-react with GAS components and host tissues. GAS infected hosts may produce antibodies targeting the surface M protein that shares similar antigenic epitopes with tissues in the heart valves, brain and synovium of joints of human. Therefore, a portion of M protein specific antibodies can cross-react with host tissues that

results in immune responses directed at host tissue leading to tissue destruction (Cunningham, 2008). In severe cases of acute rheumatic heart disease the heart valves may be permanently damaged, and require surgical replacement of the damaged valves.

1.1.3 The burden of GAS infections

There are more than 700 million new cases of uncomplicated GAS infections each year, and the direct medical cost for streptococcal non-invasive infections in the United States alone is between 1 to 2 billion USD dollars (Musser & Shelburne, 2009) (Carapetis, Steer, Mulholland, & Weber, 2005). A study in 2005 showed the prevalence of severe GAS diseases, which include acute rheumatic fever (ARF), acute glomerulonephritis and invasive GAS infections, was at least 18 million cases globally, with an increase of 1.78 million new cases every year (Carapetis et al., 2005). With repeated episodes of ARF, patients may develop rheumatic heart disease. Among these severe GAS diseases, rheumatic heart disease is the greatest medical burden which has a prevalence of at least 15.6 million cases globally and causes more than 200 000 deaths each year (Carapetis et al., 2005). All the data suggest GAS is a major cause of mortality and morbidity globally, and more studies in this pathogen are required to reinforce and develop new control and prevention strategies of GAS. Studies in how the pathogen interacts with the immune system of the human host may provide insights to the mechanisms GAS employs to cause diseases. Novel therapeutic methods or vaccine targets against GAS infection might be discovered through such studies.

1.2 Defense mechanisms of human innate immunity

The innate immune system is the major defense line against streptococcal infections. The system is a complex cellular and molecular network that has evolved to specialize in immediate elimination of invading pathogens in events where the physical barriers, such as skin and mucosal layers, are breached. The complement cascade system of the innate immune defense labels microbes and chemotactically attracts phagocytic cells, including neutrophils and macrophages, to migrate to the site of infection and eradicate invading pathogens (Nizet, 2007).

1.2.1 Anatomical barriers and antimicrobial factors

The epithelial layer acts as impermeable physical barrier that prevent microbial invasion. Saliva production in the oral cavity, where microbes can easily access, transports microbes to stomach where the acidic environment inhibits microbial growth; while constant upward cilial movement in the respiratory tract actively removes microbes from the host. Humans express cationic antimicrobial peptides in the epithelial cells of skin and in the gastrointestinal tract to further eliminate microbes, cathelicidin is one of them (Kosciuczuk et al., 2012). Bacterial surfaces are usually negatively charged that is distinctive to host cells.

The positively charged cathelicidin thus targets and interacts with negatively charged bacterial lipid membranes specifically leading to neutralization of membrane charge and resulting in membrane disruption (Kosciuczuk et al., 2012).

1.2.2 The complement system

The complement system is a complex and elegantly arranged reaction network mediated by over 30 serum proteins that produces acute inflammatory responses to eliminate invading microbes through multiple mechanisms. There are three distinct pathways facilitating the effect of complement system: the classic, lectin and the alternative pathways (Walport, 2001).

The complement system eradicates foreign invaders through direct and indirect mechanisms. The end result of the three pathways is the formation of hydrophobic membrane attack complexes (MACs) on bacterial surfaces. Formation of MAC on the bacterial surface produces a transmembrane channel that leads to osmotic imbalance in the bacterial cell and subsequently kills the bacterium (Walport, 2001). This mechanism is especially effective in eliminating Gram-negative bacteria that have thin cell walls, whereas the thick peptidoglycan cell walls of Gram-positive bacteria prevent killing through such mechanism.

The complement system can also indirectly kill microbes by attracting phagocytic cells to infection sites, where the phagocytic cells engulf microbes labeled by surface-associated complement proteins. An enzyme complex called C3 convertase is another end product of all three complement pathways. The activated C3 convertase complex functions to cleave the central component of complement system C3 into C3a and C3b fragments (Pangburn & Muller-Eberhard, 1986). The C3b fragment binds to C3 convertase and forms C5 convertase, which cleaves the C5 protein into C5a and C5b fragments. The C5b fragment is one of the building blocks of the transmembrane MAC that lyses bacterial cells (Kolb & Muller-Eberhard, 1975). The resultant C3a and C5a fragments are potent anaphylatoxins that attract phagocytic cells to the site and stimulate proinflammatory responses in these cells (Manthey, Woodruff, Taylor, & Monk, 2009; Sahu & Lambris, 2001). The production of anaphylatoxins by complement cascade and the subsequent activation of phagocytic cells is one of the major defenses against streptococcal infection.

1.2.3 Neutrophil mediated intracellular bacterial killing

Neutrophils are key effector cells for the innate immune system and are essential for the immediate response against intruding microbes. Neutrophils migrate along an ultrafine gradient of chemoattractants,

including C5a of the complement system and interleukin-8 (IL-8), to the site of infection. The chemotactic molecules also stimulate the signaling pathways in neutrophils that induce rearrangement of the cytoskeletons and enable the movement of neutrophils toward higher concentration of chemotactic molecules at the site of infection (Cowburn, Condliffe, Farahi, Summers, & Chilvers, 2008).

Activation of neutrophils could lead to the production of reactive oxygen species (ROS) that are extremely destructive for bacterial cells as well as host tissues. Thus, the activation of neutrophil degranulation and respiratory burst is tightly controlled by a two-stage process. The contact with activated epithelium, components of microbes or elevated concentration of chemoattractants mildly activates the NADPH oxidase in neutrophils.

Full activation of neutrophils is induced by the subsequent recognition of pathogen specific patterns, including peptidoglycan of bacterial cell wall and lipopolysaccharide, at site of infection (Amulic, Cazalet, Hayes, Metzler, & Zychlinsky, 2012). The complement protein fragments and immunoglobulins (Ig) that are disposed on bacterial surfaces promote phagocytosis by neutrophils. The NADPH oxidase on phagosomal membrane is further activated after the engulfment of opsonized bacteria, resulting in the production of superoxide radicals and ROS in the phagosome. In addition to the production of ROS, the phagosome containing engulfed microbes fuses with intracellularly stored granules. The antimicrobial peptides stored in granules are released into the phagosome, and efficiently kill microbes that are contained in the vacuole lumen (Cowburn et al., 2008).

Apart from the intracellular killing of microbes through the activities of ROS and antimicrobial peptides from the granules, neutrophils also exhibit an extracellular killing mechanism named neutrophil extracellular traps (NETs). This antimicrobial mechanism will be described in section 1.4.1.

1.3 Virulence factors of GAS

Virulence factors are bacterial components that contribute either to the establishment of infections or the manifestation of diseases. As a pathogen, it is crucial for GAS to adapt to the host environment in order to survive and further invade the host. The process of a GAS infection starts firstly from the adherence and colonization to host epithelial surfaces, such as skin and pharynx, where the pathogen has to compete with existing normal flora for resources and to overcome any physical forces that may dislodge it. On top of being able to persist on the epithelial surfaces, GAS also require mechanisms that evade host immune responses and allow the bacterium to disseminate from the sites of infection to cause systematic infections.

It is therefore not a surprise to find GAS producing a large arsenal of virulence factors that function in various ways to facilitate the bacterium in surviving and establishing infections. A summary of surface exposed and secreted virulence factors of GAS is listed in Figure 1.1.

In 2001 Ferretti and coworkers published the complete genome of a GAS M1 strain that was then followed by the completion of genomes in other M types, including M3, M5, M6, M12, M18 and M28 (Ferretti et al., 2001). Completion of GAS genome sequencing opens up opportunities for identifying novel virulence factors through advanced bioinformatic technology. Intensive research on GAS virulence factors was carried out to expand understanding in the molecular basis underlying the pathogenesis of the bacterium. Through studies in GAS virulence factors, there is the hope to develop sustainable treatment and efficient prevention of GAS diseases.

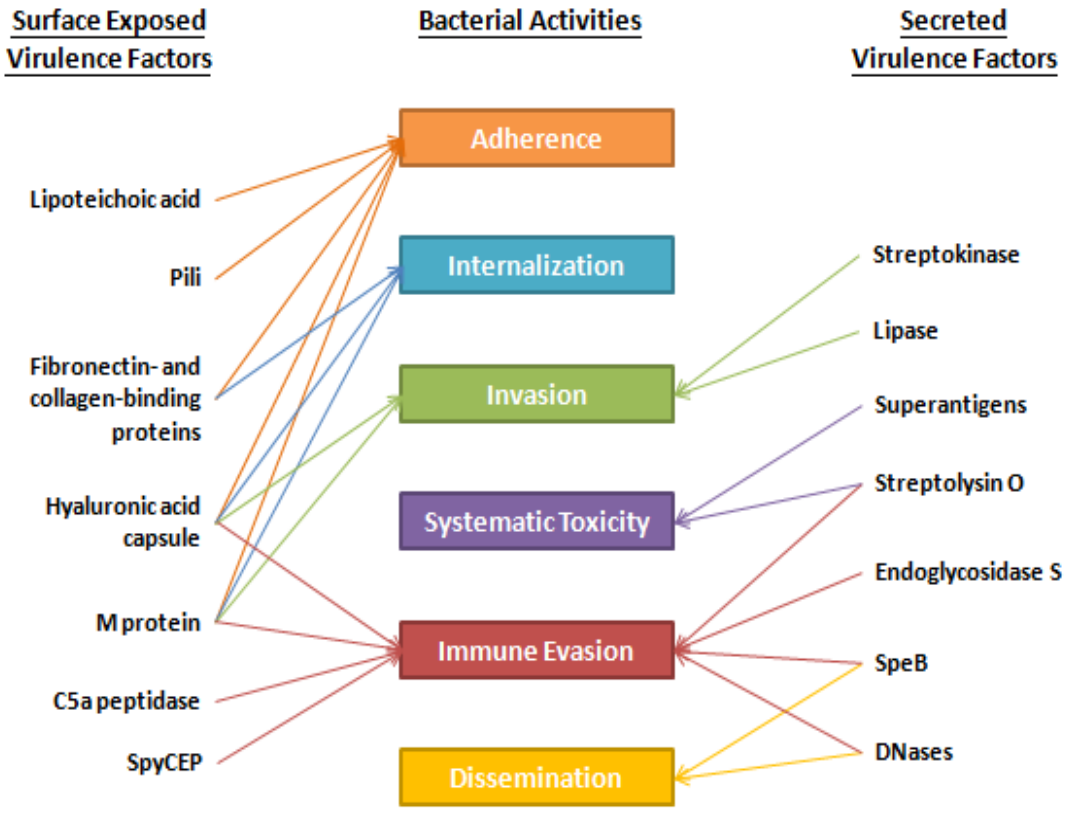

Figure 1.1 Summary of surface exposed and secreted virulence factors of GAS, and their corresponding activities

GAS produces a large arsenal of virulence factors that function to mediate bacterial adherence to host cells, evasion of the host immune responses and bacterial spreading. These virulence factors can be put into two categories: cell wall-associated virulence factors and secreted virulence factors. Figure modified from Tart et al, 2007 (Tart, Walker, & Musser, 2007)

1.3.1Secreted virulence factors

Secreted virulence factors of GAS are a collection of toxins, proteases, DNases, and superantigens that mainly contribute in immune evasion and dissemination of the bacteria, while some of them are responsible for host tissue destruction and massive non-specific immune activation that can lead to systematic toxicity and shock, even death.

1.3.1.1 Streptolysin O and Streptolysin S

Streptolysin O (SLO) and Streptolysin S (SLS) are both haemolysins of GAS. SLO is an oxygen-labile haemolysin that belongs to a Gram positive secreted toxin family, called Cholesterol Depending Cytolysins (CDCs) (Billington, Jost, & Songer, 2000). This cytolysin binds to cell membranes that contain cholesterol as a monomer, it then polymerizes with 40 to 80 membrane bound SLO monomers to form large ring-shape pores, of about 30 nm, which result in cell lysis (Meehl & Caparon, 2004). The characteristic β-haemolytic activity of GAS is a result of SLO induced erythrocyte lysis; while components of immune system such as polymorphonuclear leucocytes (PMN) and lysosomes are also targets of SLO, making it a virulence factor that evade host immunity (Timmer et al., 2009). SLO has an additional contribution in the active translocation of another GAS virulence factor, NAD^+-glycohydrolase, into the cytoplasm of host cells in a manner that is independent of the SLO-induced pore formation (Magassa, Chandrasekaran, & Caparon, 2010). Translocation of NAD^+-glycohydrolase accelerates the death of host cells, and results in further cytotoxicity. SLO is expressed in almost all GAS strains and it is antigenic; therefore, the anti-streptolysin O (ASO) titre is one of the indicators for the diagnosis of GAS infection, especially for acute rheumatic fever and acute glomerulonephritis.

Streptolysin S (SLS) is a small oxygen-stable haemolysin in contrast to SLO. It shares the same cytolytic targets with SLO, including erythrocytes, leucocytes and platelates (Keiser, Weissmann, & Bernheimer, 1964) (Hryniewicz & Pryjma, 1977). The haemolytic activity of SLS contributes to the GAS β-haemolysis character together with SLO. However, SLS forms smaller transmembrane pores on host cells in comparison to SLO, and the pores eventually induce osmotic cell lysis. SLS participates in evading host immune system through the lysis of immune cells, such as macrophages, T- and B-lymphocytes (Hryniewicz & Pryjma, 1977). Further studies on SLS reveal the virulence factor also facilitates bacterial invasion of GAS from epithelial surface to deeper tissue by recruiting a host protease, calpain, to plasma membrane. The proteolytic activities of calpain disrupt the intercellular junctions in plasma membrane, allowing the pathogen to invade deeper tissue through a paracellular pathway (Sumitomo et al., 2011).

1.3.1.2 Streptococcal pyrogenic exotoxin B

Streptococcal pyrogenic exotoxin B (SpeB) was originally thought to be one of the GAS superantigens, however it was later found to be a highly conserved cysteine protease that is expressed in almost every strain of GAS (Gerlach, Reichardt, Fleischer, & Schmidt, 1994). SpeB has a huge spectrum of substrates, it cleaves both human and bacterial proteins to alter their activities; thus, SpeB has been considered one of the most important secreted virulence factors of GAS (Nelson, Garbe, & Collin, 2011).

Antibodies, or immunoglobulins, are major components of the adaptive immune system against infections. Collin *et al* show that SpeB is able to degrade immunoglobulins A, D, E, G, and M into smaller fragments, hence inhibits immunoglobulin-induced opsonophagocytosis (Collin & Olsen, 2001; Collin et al., 2002). SpeB further disrupts the host immune response to GAS invasion by degrading other crucial components of the defense network, include the opsonin C3b of complement pathway and many chemokines (Kuo, Lin, Chuang, Wu, & Tsao, 2008) (Egesten et al., 2009), and effectively inactivate the host anti-microbial mechanisms.

SpeB plays a role in tissue invasion for GAS as it degrades a wide range of human proteins, including extracellular matrix (ECM) proteins fibronectin and vitronectin (Kapur et al., 1993), that allow the pathogen to penetrate tissues directly. SpeB is also able to contribute in tissue destruction and bacterial invasion indirectly by activating host proteases, such as human matrix metalloproteases. The activated human matrix metalloproteases could damage extracellular matrix and lead to apoptosis (Tamura et al., 2004).

SpeB is also a potent modifier of GAS proteins. It cleaves GAS adhesins, such as fibronecting-binding proteins, thereby reduces bacterial adhesion to host cell and promotes bacterial dissemination from the original sites of infection (Chiang-Ni & Wu, 2008). However, a study by Walker *et al* also showed the SpeB's proteolysis inactivates several virulence factors, including superantigens and DNase Sda1, and may hinder the virulence of GAS (Walker et al., 2007). They found SpeB expression was down regulated due to mutations in two-component *covRS* regulator in some hypervirulent strains of GAS. The down regulation of SpeB in the *covRS* mutants appeared to involve in the switch from a local infection phenotype to a hypervirulent phenotype (Walker et al., 2007).

1.3.1.3 Superantigens

Bacterial superantigens are secreted protein toxins that are able to excessively and non-specifically stimulate T-lymphocytes in an uncontrolled manner through the binding to major histocompatibility complex

(MHC) class II on host antigen presenting cells (APCs) and the T-cell receptor (TCR) (Fraser & Proft, 2008). Superantigen toxins are mostly expressed by *Staphylococcus aureus* and GAS, and GAS has been found to produce at least 12 distinct superantigens (Proft & Fraser, 2007). These superantigens are small in size, ranging from 23 to 27 kDa in molecular weight, but they are extremely potent in T-cell simulation. Under normal circumstances, 1 in 10,000 T-cells would be stimulated in response to the recognition of a specific antigen. The process involves APCs engulfing an antigen and presenting it on the surface MHC class II molecule, and only T-cells that have the TCR specific for the antigen would recognize it and become activated. However, superantigens can activate more than 20% of the T-cell population through this non-specific and uncontrolled cross-link between APCs and TCR (Figure 1.2) (McCormick, Yarwood, & Schlievert, 2001).

This strong T-cell activation stimulates a massive production of cytokines that can reach toxic levels. The massive influx of inflammatory cytokines IL-2, interferon-gamma (INF-gamma) and tumour necrosis factor-α (TNF-α) have been recognized as the major cytokines responsible for toxicity (Fraser & Proft, 2008). The excessive production of immune modulators can cause abnormal activation of complement and coagulation pathways, as well as the life threatening condition streptococcal toxic shock syndrome (STSS) with the typical manifestation of hypotension and multiple organ failure (Sriskandan, Faulkner, & Hopkins, 2007).

The exact role of superantigens in GAS pathogenesis is still unclear after decades of study. There is the speculation that superantigen induced-inflammatory activities will subvert the normal innate and adaptive immune responses, and thus undermine the host immune activity to the invading pathogen (Fraser & Proft, 2008). More studies will have to be done to define why GAS produces superantigens.

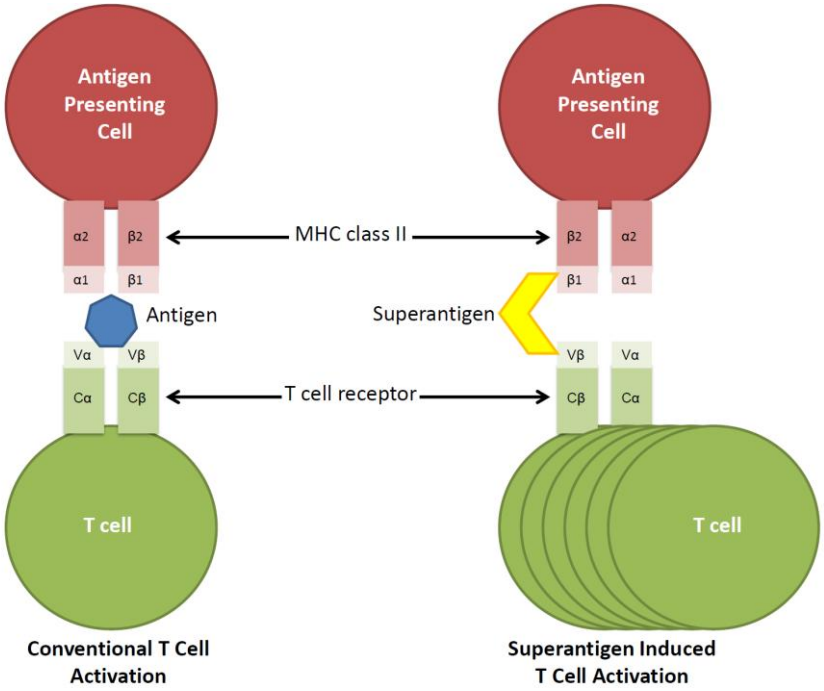

Figure 1.2The conventional T cell activation and superantigen induced T cell activation

The conventional T cell activation involves the presentation of an antigen by the MHC class II molecule on surface of APCs. Only T cells with TCR that recognizes the antigen specifically will be activated. The activation is highly regulated and specific. The superantigen induced T cell activation starts with the superantigen forming a strong association with MHC class II molecules on the APC surface. The accumulation of superantigens on the APC surface leads to cross-linking between the MHC class II molecule and multiple TCRs, and induces massive T cell activation. Figure adapted from Sriskandan *et al*, 2007 (Sriskandan et al., 2007)

1.3.2 Cell surface virulence factors

Surface attached virulence factors have crucial roles in the interaction between the bacteria and the environment. These virulence factors are most likely involved in bacterial adhesion, colonization, host cell invasion and, sometimes, immune evasion. Thus, surface exposed virulence factors have the potential to be drug targets and vaccine candidates as they often interact with host immune system (Rodriguez-Ortega et al., 2006). Many of these cell surface virulence factors, M protein, pili and C5a peptidase for example, are attached to the cell wall via a Gram positive-conserved LPXTG motif that is recognized and covalently linked to cell wall by the cell surface sorting enzyme, sortase A (Patti, Allen, Mcgavin, & Hook, 1994).

1.3.2.1 M protein

M protein is one of the major virulence factors of GAS as it is involved in multiple aspects of pathogenicity of the pathogen, including adhesion, cell invasion, immune evasion, and may trigger ARF due to its molecular mimicry property (Cunningham, 2008).

The structure of M protein has been studied extensively and shown to be a homodimer of polypeptide chains arranged in alpha-helical coiled-coil configuration that is covalently linked to the cell wall at the C-terminus via a sortase mediated transpeptidation process (Bisno, Brito, & Collins, 2003). Each of the polypeptide chains are made with four repeating blocks, A to D. The N-terminal end of M protein is highly variable, and the difference in the amino acid sequence of this region is the basis of M serotyping. The C-terminus of M protein however is highly conserved among different M types (Cunningham, 2008) (refer to Figure 1.3).

M protein is well known for its role in adhesion during the early stage of GAS infection. A two step mechanism of GAS adhesion to host cells was proposed, that a non-specific and reversible binding between the bacterium and host cell occurs first and a second more specific and irreversible adhesion follows (Courtney, Hasty, & Dale, 2002). M protein has been shown to be involved in the strong and irreversible second step of the adhesion mechanism and binds to epithelial cells (Ellen & Gibbons, 1972). The receptors on host cells for M protein binding are M serotype-dependent due to the hypervariable amino acid sequences on the N-terminus of the protein. For example, only M1, M3 and M6 are able to bind to firbonectin on epithelial cells and establish a firm adhesion. In contrast, CD46 and glycosaminoglycans are receptors that are more commonly shared among M serotypes (Feito et al., 2007) (Frick, Schmidtchen, & Sjobring, 2003). In addition to its role in adhesion, M protein binding to either fibronectin or laminin was shown to induce internalization of GAS into human epithelial lung cells (Cue, Dombek, Lam, & Cleary, 1998).

GAS has evolved multiple pathways for anti-phagocytic mechanisms that are essential for the pathogen to survive in human blood. Both M protein and the hyaluronic acid capsule contribute to this virulence mechanism (Moses et al., 1997). The complement system of the host innate immunity has a crucial role in recruiting phagocytes to the site of infection during the early stages of bacterial infection. M protein has evolved to inhibit the complement system and the subsequent phagocytosis through various mechanisms. Firstly, M proteins are able to bind to one or more inhibitory regulators of the complement system to prevent complement activation on the surface of GAS (Oehmcke, Shannon, Morgelin, & Herwald, 2010).

For example, M protein binds to the classic complement pathway inhibitor C4-binding protein (C4BP) through its hypervariable N-terminus that results in limited classical pathway activation and confers resistance to phagocytosis (Carlsson, Berggard, Stalhammar-Carlemalm, & Lindahl, 2003). The second mechanism of complement inhibition by M protein is mediated by binding to host protein fibrinogen. The binding of fibrinogen to surface exposed M protein reduces the accessibility of opsonin C3b to GAS; this in turn blocks activation of the alternative pathway and inhibits phagocytosis (Horstmann, Sievertsen, Leippe, & Fischetti, 1992). Lastly, a number of M proteins are able to impede phagocytosis by binding to the Fc region of IgA, hence prevent the normal opsonization activity of IgA and the recruitment of phagocytes (Horstmann et al., 1992).

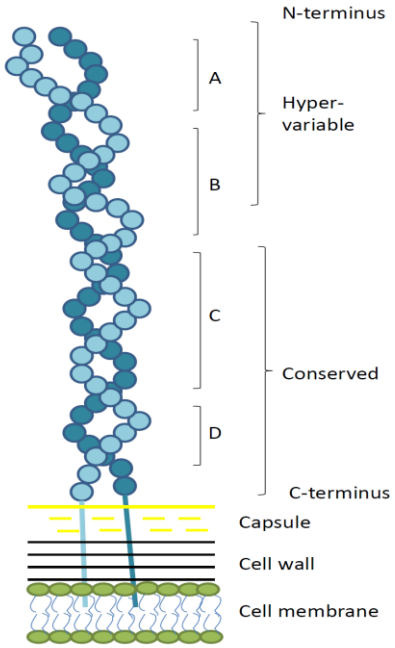

Figure 1.3 Structure of M protein

M protein is a homodimer of polypeptide chains arranged in alpha-helical coiled-coil configuration that its C-terminus is covalently linked to the cell wall. Each polypeptide chains are made with four repeating blocks, A to D. The N-terminus of the protein is hyper-variable, while the C-terminus is highly conserved.

Figure adapted from Georgousakis *et al*, 2009 (Georgousakis, McMillan, Batzloff, & Sriprakash, 2009)

1.3.2.2 Protease SpyCEP

IL-8 is a major chemokine responsible for the recruitment of neutrophils to the sites of infection and for neutrophil activation. Inhibition of IL-8 activities would significantly reduce the host immune defense against invading microbes. It is therefore not a surprise to find GAS developing mechanisms that inhibit IL-8 activities in order to survive in the host. A report by Edwards *et al* has demonstrated that IL-8 is inactivated by a proteinase, SpyCEP, found in the culture supernatant of the bacterium (Edwards et al., 2005). The report also shows that proteinase cleaves the C-terminus of mature IL-8 polypeptide at position Q50 and R60, and the resultant IL-8 fragment is unable to promote neutrophil migration to infected sites (Edwards et al., 2005).

The expression of SpyCEP was found to be strongly upregulated *in vivo* in the hypervirulent GAS M1T1 strains associated with life-threatening infections (Sumby, Whitney, Graviss, DeLeo, & Musser, 2006). A follow-up study on SpyCEP activities by Zinkernagel *et al* reveals the IL-8 protease is important for the virulence of GAS (Zinkernagel et al., 2008). The GAS M1T1 knockout mutant lacking SpyCEP expression failed to induce a skin necrotic infection in a murine model (Zinkernagel et al., 2008). The results from the report indicate SpyCEP promotes bacterial survival by decreasing IL-8 dependent neutrophil endothelial transmigration and therefore reduces bacterial killing through phagocytosis at site of infection (Zinkernagel et al., 2008). Further studies reveal the SpyCEP cleaves other chemokines, including granulocyte chemotactic protein 2 and growth-related oncogene alpha (Sumby et al., 2008), and prevents the priming and activation of neutrophils. The proteolytic activities of SpyCEP on host chemokines detrimentally alter the innate immune response to invading GAS, and effectively promote bacterial survival in the host.

The protease possesses a C-terminal LPXTG cell wall attachment motif, and the surface localisation of SpyCEP was detected in GAS M1 strains 3348 and SF370 by Chiappini and colleagues (Chiappini et al., 2012). The study indicates that protease is firstly expressed as a surface-associated protein and later being shed off into the culture supernatant. Their work shows the protease is capable of cleaving IL-8 in surface-bound status as well as in its shed form. Moreover, they have also shown the specific antibodies to SpyCEP can counteract the inhibitory effects on neutrophil recruitment *in vitro* and such antibodies can also recognise surface-bound SpyCEP (Chiappini et al., 2012). Chiappini and colleagues proposed that the inclusion of SpyCEP as a component of vaccine against GAS may exert a dual effect by promoting opsonophagocytosis and reducing virulence of the pathogen.

1.3.2.3 C5a peptidase

While M protein targets the C3b-mediated opsonization of phagocytes, GAS has other virulence factors that aim to paralyze the phagocytosis process. C3b is one of the building blocks of the C5 convertase complex, which cleaves the complement protein C5 into two fragments, C5a and C5b. C5a is a potent PMN chemoattractant that recruits the phagocytes to the site of infection. GAS expresses C5a peptidase, a highly conserved and cell wall anchored 130 kDa serine protease, in a serotype independent manner to counteract this anti-microbial mehcanism (Cleary, Prahbu, Dale, Wexler, & Handley, 1992). C5a peptidase specifically cleaves the chemotactic complement factor C5a thereby inhibit the recruitment of phagocytes to infectious sites (Cleary, Prahbu, et al., 1992). The streptococcal cysteine protease SpeB can release functional fragments of C5a peptidase from the cell wall and inhibit C5a chemotactic activity at a distance from the bacterium (Berge & Bjorck, 1995).

1.3.2.4 Hyaluronic acid capsule

All GAS strains produce a capsule on their surface composed of hyaluronic acid (HA), a high molecular weight polymer of glucuronic-β-1,3-*N*-acetylglucosamine (Cole et al., 2010). Encapsulation of GAS strains may vary greatly, and the heavy encapsulated strains are frequently linked with hypervirulence suggesting an important role of HA capsule in virulence (Alberti, Ashbaugh, & Wessels, 1998). HA capsule is encoded by a highly conserved *has* operon and the chemical composition of streptococcal HA is almost identical to mammalian polysaccharide in connective tissue of ECM (Bisno et al., 2003). The molecular mimicry of HA enables GAS to blend in as part of the host tissue in order to avoid the host immune surveillance and the subsequent phagocytosis (Wessels, Moses, Goldberg, & DiCesare, 1991). It has been shown that the acapsular isogenic GAS mutant fails to prevent phagocytosis, and is 100-fold more susceptible to killing by immune system (Wessels et al., 1991).

Apart from its contribution in immune evasion, HA has another role in bacterial adhesion and invasion that involves the binding to a widely distributed adhesion molecule, CD44, of human epithelial cells (Oliferenko, Kaverina, Small, & Huber, 2000). HA capsule of GAS mediates the binding to keratinocytes via the ligation with CD44 on cell surface to generate a weak first step adhesion to the host epithelium. The HA-CD44 interaction can further enhance bacterial invasion through activating actin rearrangement. In the mammalian system, the binding of HA in the connective tissue to cell surface receptor CD44 triggers a local signal cascade that leads to the rearrangement of actin cytoskeleton (Oliferenko et al., 2000). Such HA-CD44-induced actin cytoskeleton rearrangement can be found in various physiological processes, including tumour metastasis, wound repair and lymphocyte adhesion (Oliferenko et al., 2000). Bacterial

HA ligation to CD44 can also induce this cytoskeletal rearrangement marked by membrane ruffling and disruption of cellular junctions which allows the pathogen to penetrate into deeper tissues through a paracellular route (Cywes & Wessels, 2001).

1.4 NETs and streptococcal nucleases

1.4.1 Antimicrobial extracellular traps produced by neutrophils - NETs

Neutrophils of the innate immune system have long been appreciated for their antimicrobial activities through phagocytosis and the subsequent intracellular killing through antimicrobial peptides from granules and production of ROS (Segal, 2005). However, recent studies showed neutrophils are capable of conducting efficient extracellular pathogen entrapment and destruction through the production of NETs (Brinkmann et al., 2004).

NETs are extracellular fibrous structures released by neutrophils upon stimulation by a number of chemical substances, host and microbial components, including IL-8, phorbol myristate acetate (PMA), and LPS (Brinkmann et al., 2004) (Brinkmann & Zychlinsky, 2007). NETs are composed of nuclear DNA/histone complex and antimicrobial proteins, such as neutrophil elastase, myeloperoxidase and peptidoglycan recognition protein S (Brinkmann & Zychlinsky, 2007). The web-like structure of NETs allows the entrapment of microbes, while the structure also promotes accumulation of antimicrobial peptides at high concentrations that optimizes their bactericidal activities (Brinkmann & Zychlinsky, 2007) (refer to Figure 1.4).

Studies showed that NET production can be induced by fungus (Bruns et al., 2010) (Urban, Reichard, Brinkmann, & Zychlinsky, 2006), bacteria (Brinkmann et al., 2004) and protozoa (Baker et al., 2008) (Guimaraes-Costa et al., 2009) through a programmed cell death that is different from apoptosis, named NETosis. Neutrophils undergoing NETosis do not display the normal apoptotic PS signal, which attracts phagocytes for the engulfment of dead neutrophils, nor show sign of membrane blebbing or nuclear chromatin condensation that are morphological characterisations of apoptotic cells (Fuchs et al., 2007). Instead, NETosis cells maintain the plasma membrane integrity while the nuclear and granular membranes disintegrate allowing the mix of nuclear DNA with components in the antimicrobial granules to form NETs (Fuchs et al., 2007).

Although NETs have been shown to be an effective novel antimicrobial mechanism in *ex vivo* experiments,

some bacteria have developed strategies to counteract such entrapment and killing. Strains of GAS and *Staphylococcus aureus* have been shown to produce deoxyribonucleases (DNases) that degrade the nuclear chromatin backbone structure of NETs. The production of these DNases allows the evasion of bactericidal trapping by NETs and promotes bacterial dissemination from the site of infection (Buchanan et al., 2006) (Berends et al., 2010).

Production of extracellular traps was also observed in mast cells and these structures were able to trap and kill GAS (von Kockritz-Blickwede et al., 2008). Mast cells are often found at infection portals, such as the skin and the mucosa of the gastrointestinal and respiratory tracts. Like neutrophils, they are among the first lines of immune defense against invading pathogens.

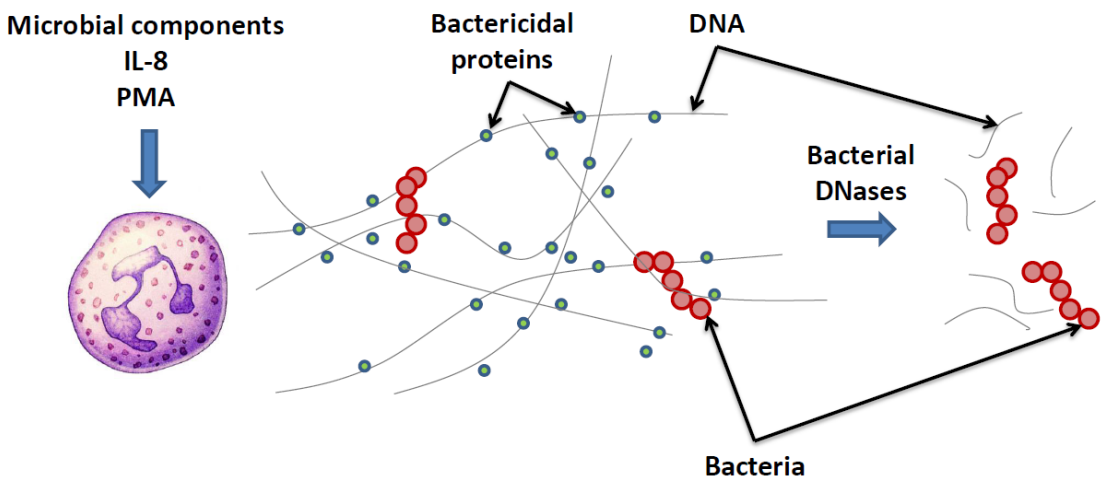

Figure 1.4 The production and structure of NETs

Production of NETs could be stimulated by chemical agents, cytokine IL-8 or microbial components, such as LPS. The extracellular trap consists of nuclear DNA as the backbone of the fibrous network, with bactericidal granular proteins accumulated on the backbone. The network traps microbes at site of infection and bacterial killing is mediated by the attached granular proteins. Some bacterial DNases are capable of degrading the DNA framework of NETs, thus allowing bacteria to escape from killing by NETs.

Figure adapted from Wartha et al, 2007 (Wartha, Beiter, Normark, & Henriques-Normark, 2007)

1.4.2 Streptococcal DNases

All GAS strains produce one or more soluble DNases. DNases are among the earliest identified virulence factors of GAS (McCarty, 1948) (Tillett, Sherry, & Christensen, 1948), as DNase activity was found regularly and abundantly in growth cultures of almost every GAS strain. Early studies on GAS reveal that the pathogen secretes four distinct subgroups of DNases into the supernatant fluid, they are designated DNase type A, B, C and D and each has different preferential substrates, pH ranges for optimal activity, and requirement of various metal ions for their DNase activity (Table 1.1) (Wannamaker, 1958) (Wannamaker, Hayes, & Yasmineh, 1967). Among the various GAS DNases, DNase B occurs in all the strains of GAS; hence, the DNase B antibody-titre has been employed as a clinical diagnostic marker for previous GAS infection in post-streptococcal ARF and acute glomerulonephritis (Eriksson, Eriksson, Holm, & Norgren, 1999).

The precise characterisation and function of GAS DNases in pathogenesis remains poorly understood after years of study. It was suggested that GAS DNases promote bacterial spreading from purulent material by degrading DNA released from dead neutrophils and bacteria thereby decreasing the viscosity of pus to enhance bacterial dissemination (Tillett et al., 1948). Sumby *et al* was able to demonstrate that an isogenic triple-mutant of a GAS M1 strain, in which the expression of three extracellular DNases were inactivated, was significantly less virulent in mouse infection model compared to the wildtype strain that was partially due to the impaired resistance against extracellular killing by human PMNs (Sumby et al., 2005). The result can be correlated to the recent discovery that some bacteria, including GAS and *Streptococcus penumoniae*, produce extracellular DNases that are able to disrupt the innate immune mechanism of NETs by destroying the DNA framework of the extracellular trap thereby releasing bacteria from entrapment and killing by NETs, hence enhancing bacterial survival in host.

Table 1.1 A summary of enzymatic specificity for the four GAS DNases

	DNase A	DNase B	DNase C	DNase D
Optimal pH	pH 8 – 9	pH 8 – 9	pH 5 – 6	pH 6 – 7
Cation dependency	Ca^{2+} and Mg^{2+}	Ca^{2+} and Mg^{2+}	Ca^{2+} and Mg^{2+}	Ca^{2+} and Mg^{2+}
Substrate specificity	DNA	DNA and RNA	DNA	DNA and RNA
Specificity of action at 5'-phosphate terminus	Phosphodiester bonds adjacent to deoxyguanosine	Phosphodiester bonds adjacent to deoxyguanosin	None specific	Phosphodiester bonds adjacent to deoxyadenosine

1.4.2.1 Streptodornase 1, Sda1

In the past 20 years, severe GAS infections have re-emerged with the strain M1T1 being found to be the most frequently isolated strain from both invasive and non-invasive streptococcal infections (Aziz & Kotb, 2008; Cleary, Kaplan, et al., 1992; Muotiala, Seppala, Huovinen, & Vuopio-Varkila, 1997). The hypervirulence of the M1T1 strain has been linked to the acquisition of novel virulence factors. Cleary et al found the M1T1 strain contains an additional 70 kb phage DNA sequence in its genome that makes the strain unique from other M1 subtypes (Cleary, LaPenta, Vessela, Lam, & Cue, 1998). Later studies by Aziz et al. further illustrated that two prophages had integrated into the genome of M1T1 and introduced the genes of two virulence factors into the strain, the superantigen SpeA and DNase Sda1 (Aziz et al., 2005).

Aziz and colleagues first observed the culture supernatant of M1T1 possessed DNase activity in the presence of Ca^{2+} and Mg^{2+} at a wide pH range, from 5.5 to 8.8 (Aziz, Ismail, Park, & Kotb, 2004). The addition of EDTA could partially inhibit such DNase activity at pH 6.8 to 7.2, however the inhibition was lost at pH 5.5 and 6.1. These results suggested M1T1 secretes several DNases. A novel protein found only in M1T1 but not from the ancestral SF370 strain was isolated and identified from other extracellular proteins of M1T1 by a matrix-assisted laser desorption ionization time-of-flight mass spectroscopy (MALDI-TOF MS) as a 40 – 45 kDa protein, with an approximate pI of 5.9. The MS peptide pattern of this novel protein was very similar to the theoretical peptide pattern of streptodornase D (SdaD) from *S. pyogenes* M49 (Aziz, Ismail, et al., 2004). The novel protein also shared high sequence similarity with SdaD-M49 and was named Sda1. Sda1 was found to be a phage-encoded novel DNase as the DNA sequences flanking the *sda1* gene showed typical phage features, and that the two highest scored-homologues of Sda1 were in fact phage-encoded DNases, Sda of GAS M18 and Sdα of GAS M3 (Aziz, Ismail, et al., 2004).

The role of Sda1 in the pathogenicity of the hypervirulent M1T1 strain was investigated by Buchanan and colleagues as they hypothesised that the DNase activity of Sda1 could destroy the DNA structure of NETs allowing the pathogen to escape from NET-mediated killing (Buchanan et al., 2006). A *sda1* isogenic knockout M1T1 mutant was generated and the mutant was significantly more susceptible to killing by human neutrophils and whole blood in comparison to the wildtype M1T1 (Buchanan et al., 2006). In concordance, when *sda1* was heterologously expressed in a non-invasive GAS M49 isolate and in non-pathogenic Gram positive bacterium *Lactococcus lactis*, both M49 and *L. lactis* gain-of-function mutants acquired enhanced resistance to killing by human neutrophils comparing to the controls

(Buchanan et al., 2006). The contribution of Sda1 to M1T1 virulence was further revealed in a mouse infection model of necrotising fasciitis, in which the average necrotic lesion size on skin of mice infected with *sda1* isogenic knockout mutant was vastly smaller than the lesions found on mice infected with wildtype M1T1; while the M49 *sda1*$^{+}$ mutant caused considerably larger skin lesions on mice than M49 transformed with empty vector (Buchanan et al., 2006). Degradation of the DNA framework of NETs appeared to be the underlying mechanism of how Sda1 contributes to M1T1 resistance to neutrophil killing and virulence. The wildtype M1T1 strain was able to degrade NETs in a dose-dependent manner in the report, whereas a considerable amount of NET persisted after incubation with the *sda1* knockout mutant. Although M1T1 wildtype and *sda1* isogenic mutant were equally capable in recruiting and stimulating leucocytes in a mouse subcutaneous challenge model, there was no NETs being detected in the purulent exudates of early stage abscess from mice inoculated with wildtype M1T1 in contrast to the visualisation of NETs in significant amounts from the abscess of mice inoculated with the *sda1* knockout mutant (Buchanan et al., 2006). These results were in support of the hypothesis of Buchanan et al that the DNase activity of Sda1 mediates enhancement of M1T1 bacterial survival and virulence potential through the destruction of the host innate immune response NETs.

M1T1 strains have been linked to life threatening infections, including necrotising fasciitis, as well as uncomplicated infections (Johnson, Wotton, Shet, & Kaplan, 2002). Studies on M1T1 clinical isolates revealed the transition from local to systematic infection could be associated with mutations in the *covRS* two-component regulator of GAS, which regulates the expression of various virulence factors (Sumby et al., 2006). Mutations in the *covRS* regulator result in a clear shift in the transcriptional profile of M1T1 isolates found in invasive diseases compared to M1T1 clones that colonize the mucosal surface. It was reported a strong upregulation of *sda1* expression and a decreased expression of the gene encoding for the cysteine protease SpeB were observed in invasive M1T1 isolates (Sumby et al., 2006). Interestingly, SpeB has been shown to be able to degrade Sda1 (Aziz, Pabst, et al., 2004). Walker and colleagues investigated the hypothesis that Sda1 provides selection pressure for the loss of SpeB expression *in vivo*, as SpeB-deficient clones are able to accumulate Sda1 for resistance against NET-mediated killing at sites of infection (Walker et al., 2007). They demonstrated that the isogenic *sda1*-knockout mutant did not undergo the switch to the SpeB-deficient phenotype (1/500 SpeB-negative colony) in a mouse subcutaneous infection model in comparison to the wildtype M1T1 strain (76/500 SpeB-negative colonies). DNA sequencing of the SpeB-negative colonies indicated mutations in the *covRS* regulator may be responsible for the loss of SpeB expression (Walker et al., 2007). The result suggests the acquisition and expression of the phage-encoded Sda1 in M1T1 provide evolutionary selection pressure for an enhanced

resistance to host immune response through the loss of SpeB expression. The resultant hyperinvasive phenotype may cause life-threatening invasive infections.

Sda1 not only assists GAS M1T1 in immune evasion by disrupting the NET-mediated killing, but also allows the pathogen to escape from host innate immune surveillance mediated through Toll-like receptor 9 (TLR9) (Uchiyama, Andreoni, Schuepbach, Nizet, & Zinkernagel, 2012). Toll-like receptors (TLRs) are pattern recognition receptors of the host innate immune system, which recognize conserved molecular pattern from pathogens. Toll-like receptor 9 is an intracellular receptor that recognizes unmethylated CpG-rich DNA motif that is frequently found in microbial DNA but rare in the human genome (Hemmi et al., 2000). The intracellular localisation of TLR9 suggested its role in recognizing intracellular pathogens, however recent studies indicated it also participates in the defense against extracellular pathogens, including GAS (Zinkernagel et al., 2012). Based on these findings, Uchiyama et al hypothesised that Sda1 of hypervirulent M1T1 could modify the bacterial unmethylated CpG-rich DNA fragment and prevent the pathogen from being recognised by TLR9 (Uchiyama et al., 2012). They reported that genomic DNA of GAS could induce murine bone-marrow derived macrophages (BMDMs) to produce proinflammatory cytokines, interferon-α (INF-α) and tumour necrosis factor-α (TNF-α), through a TLR9-dependent pathway, and such INF-α and TNF-α secretion was not observed when BMDMs were incubated with human DNA. The secretion of INF-α and TNF-α by BMDMs was diminished when GAS genomic DNA was pre-incubated with recombinant Sda1, which supported the hypothesis that Sda1 is capable of preventing TLR9-dependent recognition of the pathogen. Oxidative burst activity of murine macrophages has been identified as a TLR9-induced mediator for intracellular killing to eliminate pathogens following phagocytosis (Zinkernagel et al., 2012). Oxidative burst activity measured in BMDMs infected by Sda1 expressing M1T1 wildtype was significantly lower than the activity measure in BMDMs infected by the isogenic *sda1*-knockout mutant, while the expression of Sda1 also prevented the pathogen from intracellular killing by macrophages (Uchiyama et al., 2012).

These findings suggest Sda1 is an important virulence factor of hypervirulent GAS M1T1 strains through multiple mechanisms. The enzymatic activity of Sda1 modifies GAS genomic DNA to prevent TLR9-depedent innate immune recognition and the subsequent intracellular killing by macrophages during the initial infection process. DNase activity of Sda1 also facilitates bacterial survival and dissemination from extracellular traps produced by neutrpohils through destroying the DNA framework of NETs. The crucial role of Sda1 in pathogenesis of epidemic M1T1 strains makes it a possible therapeutic target.

1.4.2.2 EndA of *Streptococcus pneumoniae*

Streptococcus pneumoniae is a human pathogen and the most common cause of community-acquired pneumonia and meningitis in children and elderly according to the World Health Organisation (WHO). The pathogen is closely related to GAS, and has similar capacity in causing morbidity and mortality in humans. The organism has naturally occurring genetic transformation capacity that allows the pathogen to uptake non-homologus DNA from the environment through the activity of a cell wall-anchored nuclease, EndA (Lacks, Greenberg, & Neuberger, 1975). The uptake of foreign DNA is a two-step process, that double-stranded DNA molecule firstly binds to receptors on the bacterial surface and the cell wall-embedded EndA degrades one strand of the DNA while the complementary strand is internalised into bacterial cell (Mejean & Claverys, 1993). Such genetic transformation ability of *S. pneumoniae* was linked to the pathogen's resistance against oxidative stress. The uptake of foreign DNA allows repairing of bacterial DNA damaged by oxidative stress (Michod, Bernstein, & Nedelcu, 2008).

After the discovery of NETs and its defensive role in innate immunity, the enzymatic activity of EndA was re-examined especially for its potential in interrupting the DNA structure of NETs. A study by Beiter and colleagues showed EndA was able to degrade NETs, by measuring the release of neutrophil elastase (NE) from NETs after incubating activated neutrophils with EndA-expressing *S. pneumonia*e (Beiter et al., 2006). Immunofluorescent microscopy demonstrated EndA-expressing *S. penumoniae* was able escape from NET entrapment by degrading the DNA backbone of the fibrous extracellular structure. Expression of the DNase also enhanced bacterial survival in a mouse intranasal infection model, while the *endA*-deficient pneumococcous mutant was significantly less virulent than the EndA-expressing wildtype *S. pneumoniae* (Beiter et al., 2006).

Although earlier studies on EndA indicated the protein had no access to extracellular DNA when the bacterial cell was not competent for transformation (J. D. Chen & Morrison, 1987), the recent report by Zhu *et al* has demonstrated the existence of EndA-mediated the nucleolytic activity independent of the competence status of the bacterium (Zhu, Kuang, Wilson, & Lau, 2013). A *S. pneumoniae* strain was genetically modified in this study to remove its competence development. The competence-deficient strain was shown to retain extracellular nuclease activity comparable to the parental strain, including the ability to destroy NETs. The study also showed EndA was secreted into culture medium during growth, and the EndA-mediated nuclease activity was responsible for the rapid degradation of NETs. The extracellular nucleolytic activity of EndA was also demonstrated to be essential for the full virulence of *S. pneumoniae* during lung infection in mice (Zhu et al., 2013).

1.5 Streptococcus pyogenes nuclease A, SpnA

The *spy0747*/*spnA* gene was originally identified as a 2736 bp open reading frame (ORF) that encodes a potential 910-amino acid precursor protein. The *spnA* ORF was found in the genome of more than 41 GAS strains with limited sequence variation, indicating the gene is well conserved in the species (Reid et al., 2002). Further bioinformatic analysis on the *spnA* ORF showed the gene product might be a novel cell-wall anchored DNase of GAS.

In silico analysis with the N-terminal sequence using the SignalP 3.0 software revealed a signal peptide with a cleavage probability of 0.877 at a site between position 27 and position 28 of the SpnA precursor protein (Figure 1.5). An InterProScan and a conserved domain (CD) sequence search showed significant similarities with two known protein domains: an endonuclease/exonuclease/phosphatase domain (PF03372) at position 549 – 851 with an E-value of 2.4^{-17}, and a Gram-positive LPXTG cell wall-anchor domain (PF00746) at position 877 – 908 with an E-value of 2.4^{-5}, which contains the sortase recognition motif LPKTG at position 877 – 881. In addition, there are three predicted OB (oligonucleotide/oligosaccharide binding)-fold motifs within the N-terminal domain of SpnA. One predicted OB-fold (OB2) is located at position 217 – 271 and weakly resembles the nucleic acid binding superfamily motif SSF50249 (E = 1.3). This is flanked by two predicted OB-folds at position 99 – 171 (OB1) and position 310 – 395 (OB3) that both resemble the YhcR-OBF-like domain CD04486 (E = 2 x 10^{-9} and 6 x 10^{-10} respectively).

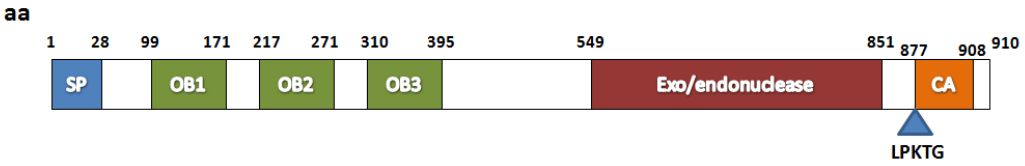

Prediction	Position	Motif	Server	Probability	E-value
Signal peptide (SP)	1 – 28		SignalP 3.0	0.877	
Oligonucleotide biding (OB) fold 1	99 - 171	YhcR-OBF-like domain CD04486	BLAST search		2 x 10^{-9}
OB-fold 2	217 – 271	SSF 50249	Superfamily 1.69		1.3
OB-fold 3	310 - 395	YhcR-OBF-like domain CD04486	BLAST search		6 x 10^{-10}
Exo/endonuclease	549 - 851	PF03327	Pfam 22.0		2.4^{-17}
Gram-positive cell wall anchorage (CA)	877 - 908	PF00746	Pfam 22.0		2.4^{-5}

Figure 1.5 Bioinformatic analysis of spy0747/spnA gene

The *spy0747/spnA* gene was predicted to encode for a 910-aa precursor protein. The encoded protein was predicted to have a signal peptide (SP) and three OB-fold motifs in the N-terminal domain. An exo/endonuclease domain was predicted to be located in the C-terminus, followed by a conserved Gram-positive cell wall anchorage motif, LPKTG, and a cell wall spanning domain (CA).

The mature full-length SpnA was expressed as a recombinant protein through the *E. coli* pProExHtb expression system for the preliminary study on the protein's character (Chang, Khemlani, Kang, & Proft, 2011). Functional characterisation of recombinant SpnA (rSpnA) revealed that the protein possessed Ca^{2+} and Mg^{2+}-dependent nuclease activity on circular and linear DNA molecules, as well as on RNA molecules. It was also found that the C-terminal endo/exonuclease domain alone does not exhibit any nuclease activity, suggesting the N-terminal OB-fold motifs are crucial for the enzymatic activity of the protein. SpnA-specific antibodies were found in convalescent serum of a patient with STSS indicating the protein is expressed during GAS infection and is immunogenic (Chang et al., 2011).

A report by Hasegawa and colleagues in 2010 has identified SpnA as a cell wall associated nuclease. A *spnA* isogenic knockout mutant was generated and shown to be less virulent in an *in vitro* whole blood bactericidal assay and in a mouse infection model in comparison to the parental GAS M1 strain (Hasegawa et al., 2010). However, the exact mechanism of SpnA in promoting bacterial survival was not identified.

1.6 Research aim and objectives

S. pyogenes is a human pathogen that causes high morbidity and mortality rates in both developing and developed countries. Virulence factors produced by the pathogen contribute greatly to its potency in causing diseases, and our understandings of the virulence factors may assist the development of effective prevention and therapeutic strategies against streptococcal infections. The recently identified novel streptococcal nuclease SpnA is conserved among all serotypes of GAS, and the protein has been shown to be important to the pathogen's virulence. The project, therefore, has the following aim, hypothesis and objectives:

The hypothesis

SpnA is a novel GAS virulence factor that promotes bacterial survival in host by destroying NETs and allowing the pathogen to disseminate from the site of infection.

The aim

To investigate the functional and structural properties of SpnA and the mechanism it employs to contribute

to the virulence of GAS.

The objectives

1. To investigate if recombinant SpnA could disrupt NETs framework *in vitro* (refer to Chapter Three)
2. To create GAS *spnA*-knockout mutant and complement strains, and *Lactococcus lactis* gain-of-function mutants for the study of SpnA's role in GAS virulence (refer to Chapter Four)
3. To investigate if the expression of SpnA could enhance bacterial survival in *in vitro* killing assays (refer to Chapter Five)
4. To establish a GAS-zebrafish embryo infection model to study the effect of SpnA expression in GAS virulence *in vivo* (refer to Chapter Five)
5. To solve the structure of SpnA through crystallography (refer to Chapter Six)
6. To investigate if SpnA possessed additional activities than digesting DNA molecules that may further contribute to the virulence of GAS (refer to Chapter Six)

Chapter 2

Materials and Methods

2.1 Materials

2.1.1 Molecular biology

2.1.1.1 Reagents

TAE	2 mM EDTA, 0.1 % (v/v) glacial acetic acid, 40 mM Tris pH 8.0
DNA loading dye (6x)	30 % (v/v) glycerol, 0.25 % (w/v) bromophenol blue, 0.25 % (w/v) xylee cynaol, 50 mM Tris pH 7.6
PCR buffer (10x)	500 mM KCl, 0.1 % (v/v) Triton-X 100, 100 mM Tris pH 8.3
Plasmid prep solution A	50 mM glucose, 10 mM EDTA, 25 mM Tris pH 8.0
Plasmid prep solution B	0.2 M NaOH, 1% SDS
Plasmid prep solution C	3 M potassium acetate, 11.5% glacial acetic acid
TFB I (sterile filter)	30 mM potassium acetate, 50 mM $MgCl_2$, 100 mM RbCl, 5 mM $CaCl_2$, 15 % (v/v) glycerol Adjusted to pH 5.8 with 1 M HCl, stored at -20°C
TFB II (sterile filter)	10 mM MOPS pH 7.0, 75 mM $CaCl_2$, 10 mM RbCl, 15 % (v/v) glycerol, stored at -20°C

2.1.1.2 Plasmids

Plasmid vectors used in this project for protein expressions and DNA manipulation

Table 2.1 Plasmid vectors used for protein expression and DNA manipulation

Name	Selection marker	Source	Details
Plasmid vectors for protein cloning and protein expression			
pBlueScript	Ampicillin	Stratagene	Cloning vector
pProExHtB	Ampicillin	Life technologies	An *E. coli* expression vector. Expression is controlled by *lac* promoter.
Heterogeneous expression in *L. lactis*			

pOri23T	Erythromycin	Prof. Philippe Moreillon, University of Lausanne, Switzerland Modified by Asso. Prof. Thomas Proft	A modified version of *L. lactis* expression vector pOri23 with additional terminator sequence from *S. pyogenes* M1 pilus operon
Construction of isogenic knockout mutant and complementation in GAS			
pFW11	Spectinomycin	Prof. Andreas Podbielski, University of Rostock, Germany	An *E. coli* – GAS suicidal vector used for knocking out the target gene and replaces the target gene with specitnomycin resistance gene, *aad9*
pLZ12km2	Kanamycin	Prof. Nobuhiko Okada Kitasato University	An *E. coli* – GAS shuttle vector used for complementation

2.1.1.3 Oligonucleotide primers

Table 2.2 Oligonucleotide primer sequence

Primer used for amplification of *spnA* (Sigma-Genosys, Australia). The restriction enzyme recognition site is underlined.

Name	**Sequence 5' – 3'**	**Restriction site**
Spy0747.fw*	CCGCTCGAGATGATTAACAAGAAATG	*Xho*I
Spy0747.rev*	CGGGATCCCTATGATTCCTTTTTGC	*Bam*HI
rSpnA.fw*	CGGGATCCGAAGAAGTTACTTCAC	*Bam*HI
rSpnA.rev*	CCCAAGCTTCTACAGTTTTCCTTTTGAAG	*Hind*III
$SpnA_{99}$.fw	GCGGATCCCCCTATACTGTTACTGGCAAG	*Bam*HI
$SpnA_{217}$.fw	GCGGATCCGATGATAGTGGTAAAAG	*Bam*HI

$SpnA_{310}$.fw	GCGGATCCACCGTAGAACAGGTTGTTG	*Bam*HI
$SpnA_{396}$.fw	GCGGATCCCAAGTTCCATCACCGCTTGTTTTAG	*Bam*HI
$SpnA_{395}$.rev*	CCAAGCTTCTAAGCTGTCCCTGTTTTGGTC	*Hind*III
SpnA_F1.fw	GCGTCGACTGTAGGATTTGTTGCTTTTAC	*Sal*I
SpnA_F1.rev	GCCTCGAGGATATCTCCTTTTAATGTGATTAG	*Xho*I
SpnA_F2.fw	GCCTGCAGTGGTTGTGTGCAACCAGTCAC	*Pst*I
SpnA_F2.rev	GCCCCGGGTCATTTCAGATATTCTAAATTG	*Xma*I
SpnA_LL.fw*	GGATCCAAAAGGAGATATCATGATTAACAAGAAATG	*Bam*HI
SpnA_LL.rev	CGCTCGAGTATGATTCCTTTTTGC	*Xho*I
SpnAsec_LL.rev	GGGCTCGAGCTACAGTTTTCCTTTTGAAG	*Xho*I
SpnA_rbs.fw	CGCTCGAGAAAAGGAGATATCATGATTAACAAGAAATG	*Xho*I
SpnAsec.rev	CGGGATCCCTACAGTTTTCCTTTTGAAG	*Bam*HI

Table 2.3 Primers for mutagenesis

Primers used for site directed mutagenesis of *spnA* (Sigma-Genosys, Australia)

Mutant	**Forward primer 5' – 3'** **Reverse primer 5' – 3'**
R696A	GATGTTGCTAAATCACTAGCAGCAG GATTTAGCAACATCTTTCCAAGCGG
N769A	GTGACTTTGCTGATTTTGAATTCACAAAG ATCAGCAAAGTCACCTAGCATCACAATATTAG
H716A	CAAATGCTTTGAACTCTAAGCGTGGG GTTCAAAGCATTTGCAACAACAACGAC
D767A	CTAGGTGCCTTTAATGATTTTGAATTC ATTAAAGGCACCTAGCATCACAATATTAG
D810A	CCCTTGCTAATATATTAGTTTCACGC TATATTAGCAAGGGTTCGATTATTGC
E592A	TTAATTGCAGTCCAAGATAATAATG GGACTGCAATTAATCCAATAATGTC
D842A	GCATCAGCTCATGATCCATTGTTACTTC ATCATGAGCTGATGCGCGTCCGTGAGC

2.1.1.4 Bacterial strains

Table 2.4 List of bacterial strains used in this study

Bacterial strain	Characteristics	Source
E. coli DH5α	Strain used for cloning	ATCC
E. coli BL21	Strain used for expression recombinant protein	Novagen
L. lactis M1363	Strain used for heterogeneous expression	Nicolas Heng, Otago University, Dunedin, New Zealand
GAS M1 SF370	Wildtype GAS	ATCC

2.1.1.5 Bacterial growth medium

Luria-Bertani broth	1 % (w/v) Bacto-tryptone, 0.5 % (w/v) Bacto-yeast extract, and 1 % (w/v) NaCl
Todd-Hewitt (THY) medium	3 % (v/v) Bacto-Todd Hewitt Broth (Becton Dickinson), 0.2 % Bacto-yeast extract
GM17 broth	3.725 % (w/v) M17 powder, 0.5 % (w/v) glucose
Agar plates	Growth media prepared as outlined above / 1.5 % (w/v) bacto-agar (Becton Dickinson)

2.1.1.6 Selective antibiotics

Ampicillin (Amp)	Final concentration 50 ug/mL
Chloramphenicol (Cm)	Final concentration 30 ug/mL
Erythromycin (Ery)	Final concentration 500 ug/mL (*E. coli* culture)
	Final concentration 5 ug/mL (*L. lactis* culture)
Spectinomycin (Spec)	Final concentration 100 ug/mL
Kanamycin (Kan)	Final concentration 50 ug/mL (*E. coli* culture)
	Final concentration 200 ug/mL (GAS culture)

2.1.2 Protein expression and analysis

2.1.2.1 Reagents

Protein purification buffer I	40 mM Tris pH 7.4, 200 mM NaCl, 10 mM $CaCl_2$, 10 mM imidazole, 1 % (v/v) Triton-X100, 0.1 mM PMSF
Protein purification buffer II	40 mM Tris pH 7.4, 200 mM NaCl, 10 mM $CaCl_2$, 10 mM imidazole
Protein purification buffer III	40 mM Tris pH 7.4, 200 mM NaCl, 10 mM $CaCl_2$, 20 - 200 mM imidazole
SDS-PAGE gel solution A	30% (w/v) acrylamide, 0.8% (w/v) bisacrylamide
SDS-PAGE gel solution B	0.4% (w/v) SDS, 1.5M Tris.HCl pH8.8
SDS-PAGE gel solution C	0.4% (w/v) SDS, 0.5M Tris.HCl pH6.8
Protein loading buffer	125 mM Tris pH 6.8, 20 % (v/v) glycerol, 0.3 M 2-mercaptoethanol, 4 % (w/v) SDS, 0.0001 % (w/v) bromophenol blue
SDS-PAGE running buffer	0.1 % (w/v) SDS, 250 mM glycine, 25 mM Tris pH 8.0
Coomassie stain	0.06 % (w/v) Brilliant Blue R-250 (Sigma Aldrich, USA), 50 % (v/v) ethanol, 7.5 % (v/v) acetic acid
Coomassie destain	25 % (v/v) ethanol, 8 % (v/v) acetic acid

2.1.3 Functional analysis

2.1.3.1 Reagents

Towbin transfer buffer	25 mM Tris.HCl pH8.3, 192 mM glycine, 0.375% (w/v) SDS, 20% (v/v) methanol
TBS	10 mM Tris pH 8.0, 120 mM NaCl
TBS-T	TBS with 0.1 % (v/v) Tween 20
Blocking solution	TBS-T with 5% (w/v) non-fat dairy milk powder
Probing solution	TBS-T with 2.5% (w/v) non-fat dairy milk powder
PBS	2.7 mM KCl, 150 mM NaCl, 10 mM phosphate salts pH 7.4
Silver staining sol A	6 % Na_2CO_3, 0.0008 % $Na_2S_2O_3$
Silver staining sol B	0.1 % formaldehyde
Protoplast buffer	40 % (w/v) sucrose, 100 mM K_2HPO_4, 10 mM $MgCl_2$, 2 mg lysozyme, 40 U mutanolysin, 1 X protease inhibitor cocktail

2.1.3.2 Antibodies

Table 2.5 List of commercial antibodies used in this study

	Species	Source	Dilution	Catalogue No.
Anti-rabbit Igs:HRP	Goat	BD Biosciences	1:1000	554021
Anti-human neutrophil elastase	Rabbit	Calbiochem	1:1000	481001
Anti-rabbit IgG:FITC	Goat	AD Serotec	1:40	401002

2.1.4 Materials for zebrafish infection

2.1.4.1 Reagents

E3 0.33 mM $CaCl_2$, 0.33 mM $MgSo_4$, 0.14 mM KCl , 5 mM NaCl

Phenol red 0.5% (w/v) phenol red in 0.2 M KCl

2.1.4.2 Zebrafish line

Table 2.6 Zebrafish line used in this study

Zebrafish line	Source
Wildtype (AB line)	Zebrafish international resource centre, USA

2.2 Methods

2.2.1 DNA purification

2.2.1.1 Plasmid extraction by alkaline lysis

Overnight culture of *E. coli* containing the plasmid of interest was made with LB broth, containing the appropriate antibiotics, and incubated at 37ºC with constant shaking. The following instruction is for plasmid preparation from 1 mL of overnight culture. Bacterial cells were collected by centrifugation at 5,000 rmp for 10 min. Supernatant was removed and cells were resuspended in 100 µL plasmid prep solution A. Cells were lysed by addition of 200 µL of plasmid prep solution B with gentle inversion and incubated on ice for 10 min. Addition of 150 µL plasmid prep solution C, with gentle inversion, precipitated bacterial debris and proteins. Debris was removed by centrifugation at 13,000 rmp for 20 min at 4ºC. The supernatant was transferred to a new tube and 1 mL of pure ethanol was added and incubated on ice for 10 min. The solution was centrifuged at 13,000 rmp for 10 min. Supernatant was removed and the DNA pellet was resuspended in 10 µL of milliQ water for future use.

2.2.1.2 Phenol/Chloroform purification

DNA fragments were separated from proteins and other substances by phenol/chloroform purification. Equivalent volume of chloroform and Tris-saturated phenol (1:1) was added to DNA sample (with a minimum volume of 100 µL), and vortex for 20 s, followed by centrifugation at 13,000 rpm for 1 min. The aqueous phase was transferred into a new tube for further ethanol precipitation.

2.2.1.3 Ethanol precipitation

To precipitate DNA from aqueous solution, sodium acetate was added at the concentration of 0.3 M, and 100 % ethanol at 2 to 2.5 volumes were added and incubated on ice for 10 min. The mixture was then centrifuged at 13,000 rpm for 10 min and the supernatant was removed. Precipitated DNA pellet was then resuspended with milliQ water.

2.2.2 DNA amplification and analysis

2.2.2.1 DNA amplification by polymerase chain reaction (PCR)

PCRs were performed with 2.5 U Taq polymerase (produced in *E. coli* by Prof. John Fraser, University of

Auckland), 1× PCR buffer (10 mM Tris.HCl pH 8.3, 50 mM KCl), 2.5 mM $MgCl_2$, 100 uM of each dNTP, 0.2 uM of reverse and forward primers respectively and 25-50 ng template DNA in a total volume of 100 µL. The reactions were performed with MyCycler™ thermal cycler (Bio-rad). Reactions were run in the following cycles,

- Step 1 (single cycle): at 94ºC for 5 min
- Step 2 (multiple cycle): at 94ºC for 30 s
  at 53ºC for 1 min
  at 72ºC for 1 min
- Step 3 (single cycle): at 72ºC for 7 min

Number of repetitive cycles was dependent on the nature of amplification. For amplification from genomic DNA, 30 cycles of Step 2 were required. For single colony PCR or amplification from plasmid DNA, 15 cycles were performed.

2.2.2.2 Site directed mutagenesis by overlap PCR

A two-step overlap PCR was employed to introduce specific mutation into the *spnA* sequence. These mutations were incorporated in the design of overlapping primer sets in the forward and reverse orientation by altering the first two bases in the amino acid codon to produce an alanine. The upstream and downstream fragments of the *spnA* sequence were separately amplified using each mutant primer together with the appropriate outer primer. The amplified fragments were gel purified to remove any contaminating plasmid DNA or primers. Approximately 5 µL of the suspension from gel purification (section 2.2.5) was used for the second round of PCR. When added together the complimentary regions of these fragments overlap and can be used as the template. As a result, the outer primers of the gene amplify a single fragment containing the introduced mutation.

2.2.2.3 Agarose gel electrophoresis

DNA samples were mixed with 6× DNA loading dye at a ratio of 6:1 and loaded into a 1 % (w/v) agarose in TAE buffer. The gel was electrophoresed at 100 V for around 30 min. Gel was stained in TAE buffer containing 5 ug/mL ethidium bromide (Promega) for 10 min. DNA was visualized under UV light using the software Gel Doc 2000 (Bio-rad).

2.2.2.4 DNA extraction from agarose gel

The desired DNA fragment was cut from the gel under UV light after ethidium bromide staining. DNA fragments were extracted from gel using the freeze-and-thaw method. Following the addition of 10 µL

milliQ water, the gel slice was frozen at -80°C for 10 min. The gel slice was thawed at 37°C for 1 min and smashed. This process was repeated 2 times. DNA was collected by centrifuging at 13,000 rpm for 10 min to separate agarose gel and aqueous solution containing the desired DNA fragment. The aqueous portion was transferred to a new tube for future use.

2.2.3 Ligation and transformation

2.2.3.1 Restriction endonuclease digestion

Restriction enzymes (Invitrogen, USA or Roche) were used with corresponding reaction buffers according to manufacturers' instructions. Reactions were incubated for 2 hrs at 37°C. If enzymes/buffers were incompatible, two digestions were carried out respectively. Phenol/chloroform purification and ethanol precipitation were performed after the first digestion to remove the enzyme/buffer; then the second digest was performed. Total volume of enzymes added did not exceed 10 % of the final reaction volume. In some cases, 5 U of calf intestinal alkaline phosphatase (CIP) were added to either insert DNA or linearised plasmid for another 30 min at 37ºC to prevent self-ligation. DNA was extracted through phenol/chloroform and ethanol precipitation.

2.2.3.2 Ligation

Linearised vector and DNA insert were mixed at a molar ratio of 3:5 and 1 µL of T4 ligase (Invitrogen, USA) with compatible reaction buffer to make a final volume of 10µL. The mixture was incubated for at least 3 hrs at room temperature.

2.2.3.3 Preparation of chemically competent *E. coli*

Overnight starter culture of *E. coli* DH5α or BL21 was prepared with LB broth containing 10 mM KCl and 20 mM $MgSO_4$ with appropriate antibiotics at 37°C with shaking (200 rpm). One mL of the overnight starter culture was used to inoculate 100 mL of LB broth containing 10 mM KCl and 20 mM $MgSO_4$, and the culture was further incubated at 37°C with shaking (200 rpm) until the optimal density of 0.4 - 0.6 at 600 nm (OD_{600}) was reached. Cells were collected by centrifugation at 5,000 rmp for 10 min at 4°C. The cell pellet was gently resuspended in 60 mL of ice-cold TFB I and incubated on ice for 10 min. Bacteria were centrifuged at 4,000 *g* for 5 min at 4°C. The supernatant was discarded, and cell pellet was carefully resuspended in 4 mL ice cold TFB II. The resuspension was aliquoted, then flash frozen in a dry ice/ethanol bath and stored at -80°C. The whole procedure was performed in sterile hood.

2.2.3.4 Transformation of chemically competent *E. coli*

Chemically competent cells (50 µL) were thawed on ice, and then incubated with 5 µL of ligation mixture on ice for 5 min. Bacteria were heat shocked by water bath at 42°C for 45 s, then immediately placed onto ice for 5 min. LB broth at 500 µL was added to the cells and incubated at 37°C for 30 min for recovery. Bacteria were collected by centrifugation at 5,000 rpm for 10 min, then removing 400 µL of the supernatant. Bacteria were resuspended in the remaining 100 µL LB broth. For blue/white selection of pBlueScript vectors, 40mM IPTG and 0.8 % (v/v) X-gal were added before plating. Bacteria were plated onto LB agar plates containing the appropriate antibiotics and grown overnight at 37°C.

2.2.3.5 Preparation of electrocompetent *L. lactis*

To prepare electrocompetent *L. lactis*, 1.5 mL of GM17 medium was inoculated with *L. lactis* MG1363 and grown overnight at 28˚C. On the second day, 1 mL of overnight culture was used to inoculate 50 mL of fresh GM17 medium and incubated at 28˚C until the optimal density of 0.4 - 0.6 at 600 nm (OD_{600}) was reached. The cells were then harvested by centrifugation at 4000 *g* for 10 min at 4˚C. The cells were kept on ice or in cooling centrifuge for centrifugation from this point onwards. The cells were then washed twice with 4 mL of milliQ water, once with 2 mL of 50 mM EDTA and once with 2 mL of 0.3 M sucrose. Finally, the cells were resuspended in 0.4 mL of 0.3 M sucrose solution and used immediately for eletroporation.

2.2.3.6 Electroporation of electrocompetent *L. lactis*

Electroporation cuvettes (2 mm, Bio-rad) were cooled on ice for 10 min before use. Purified plasmid DNA at 1 ug was added to 50 µL of electrocompetent *L. lactis* cells and incubated on ice for 5 min. The DNA/bacteria mixture was transferred to the cuvette. The eletroporation was performed through the Gene Pulser XCell (Bio-Rad) at 1.05 kV/mm, 25 mF capacitance

and 200 W resistance. Immediately after electroporation 1 mL of GM17 medium was applied to the bacterial cells, cells were transferred into a microtube and incubated at 28˚C for 2 hrs. Cells were collected by centrifugation at 5000 rpm for 10 min, then removing 950 µL of the supernatant. The cells were resuspended in the remaining 100 µL medium and plated onto GM17 agar with appropriate antibiotics.

2.2.3.7 Preparation of electrocompetent GAS

To prepare electrocompetent GAS, 2 mL of THY medium was inoculated with GAS and grown overnight at 37˚C. On the second day, 2 mL of overnight culture was used to inoculate 20 mL of fresh THY medium

and incubated at 37˚C until the optimal density of 0.4 - 0.5 at 600 nm (OD_{600}) was reached. The cells were then harvested by centrifugation at 4000 *g* for 10 min at 4˚C. The cells were kept on ice or in cooling centrifuge for centrifugation from this point onwards. The cells were then washed twice with 2 mL of 0.5 M sucrose buffer. Finally, the cells were resuspended in 0.4 mL of 0.5 M sucrose solution and used immediately for eletroporation.

2.2.3.8 Electroporation of electrocompetent GAS

Electroporation cuvettes (2 mm, Bio-rad) were cooled on ice for 10 min before use. Purified plasmid DNA at 1 ug was added to 50 µL of electrocompetent GAS cells and incubated on ice for 5 min. The DNA/bacteria mixture was transferred to the cuvette. The eletroporation was performed through the Gene Pulser XCell (Bio-Rad) at 1.05 kV/mm, 25 mF capacitance

and 200 W resistance. Immediately after electroporation 1 mL of THY medium was applied to the bacterial cells, cells were transferred into a microtube and incubated at 37˚C for 3 hrs. Cells were collected by centrifugation at 5000 rpm for 10 min, then removing 950 µL of the supernatant. The cells were resuspended in the remaining 100 µL medium and plated onto THY agar with appropriate antibiotics.

2.2.3.9 Plasmid analysis by sequencing

The plasmids were further cleaned up through Zyppy^{TM} plasmid miniprep kit for sequencing purpose. The plasmid DNA was quantified by UV spectroscopy and sequenced at the Allan Wilson Centre, Massey University, Palmerstone North, New Zealand using a capillary ABI3730 Genetic Analyzer (Applied Biosystems Inc.).

2.2.4 Protein expression and purification

2.2.4.1 Protein expression

E. coli transformed with expression vectors pProExHtb containing the fragment of interest were cultured overnight at 37°C with shaking (200 rpm) in 100 mL LB broth containing 50 ug/mL ampicillin. On the second day, the overnight culture was added to 900 mL of LB broth containing the 50 ug/mL ampicillin to make up the total volume of 1 L and allowed to grow continuously at 37°C with shaking at 200 rpm. The cells were incubated at 37°C until the optimal density at 600 nm (OD_{600}) = 0.8 – 0.9 was reached. IPTG was added to 0.1 mM as final concentration and the culture was allowed to grow continuously for 4 hr at 28°C with shaking. Bacterial cells were harvested by centrifugation at 5000 rmp for 10 min at 4°C, the supernatant was removed and the pellet frozen at -20°C for overnight.

2.2.4.2 Protein purification

The cell pellet was resuspended in 100 mL of protein purification buffer I. The cells were lysed by sonication using a Misonix XL2015 sonicator over 4 × 30 s at high power with a 75 % pulse. The lysate was centrifuged at 10000 rmp for 10 min to separate the insoluble fraction and bacterial debris from the supernatant containing the soluble proteins. The His-tag protein in the supernatant was purified by metal affinity chromatography, using an IDA sepharose column (Bio-rad) pre-charged with 10 column volumes of 100 mM $NiSO_4$ and equilibrated with protein purification buffer II. The column was washed with 10 column volumes of protein purification buffer II, and the supernatant was passed through then washed with another 10 column volumes of NTA I buffer. The column was further washed with 10 column volumes of protein purification buffer III, with imidazole concentration at 20 mM, 50 mM, and 70 mM to remove residual *E. coli* proteins. The protein was eluted with 10 column volumes of protein purification buffer at 100 mM imidazole and 150 mM imidazole. The eluted protein was dialyzed overnight at 4°C in 40 mM Tris buffer pH 7.4, 1 mM $CaCl_2$ after the elution was confirmed by sodium dodecyl sulphate polyacrylamide gel electrophoresis (SDS-PAGE).

2.2.5 Protein characterisation and analysis

2.2.5.1 Preparation of SDS-PAGE

The 12.5 % running gel was made by 2.1 mL solution A, 1.25 mL solution B and 1.6 mL milliQ water. To polymerize the gel, 4 µL TEMED and 30 µL 10 % ammonium persulphate (APS) were added immediately before the pouring. The gel was poured into the Hoefer SE 245 dual gel caster unit (Amersham Biosciences, USA). Water saturated butanol was added to level the surface. Butanol was removed after the gel was solidified, and the stacker gel, containing 0.25 mL solution A, 0.415 mL solution C, 1.0 mL milliQ water, 1.65 µL TEMED, and 20 µL10 % APS, was poured onto the running gel with either 10 or 15 well comb.

2.2.5.2 Protein separation by SDS-PAGE

Non-reducing or reducing SDS-PAGE loading buffer was added to protein samples at 1:1 ratio, and heated at 94°C for 2 min to denature the protein. Protein samples were electrophoresed at 200 V at 20 mA per gel in SDS-PAGE running buffer.

2.2.5.3 Coomassie blue staining of SDS-PAGE gels

Proteins on SDS-PAGE gel were visualised by staining the gel with coomassie stain for at least 30 min at room temperature with shaking (~45 rpm). The gel was rinsed with deionised water and destained in destaining solution with tissue paper overlaid to absorb excess dye with shaking.

2.2.5.4 Western Blotting analysis

Proteins were separated by SDS-PAGE gel and transferred onto nitrocellulose membrane using a TE77 semi-dry transfer unit (Hoefer) with Towbin's buffer. Efficiency of protein transfer was checked by reversibly staining the membrane with Ponceau red stain and destained by rinsing with deionized water. The membrane was blocked with 5% blocking solution for at least 60 min; then incubated in 2.5 % probing solution containing 1:1000 dilution of probe with constant shaking at room temperature. The membrane was washed twice with TBS-T, and followed by 3 times 5 min incubation in TBS-T with shaking. If additional layers were required for HRP detection, a 40 - 50 min incubation with secondary or tertiary antibodies was performed with the 2.5 % probing solution following the manufacturer's instruction. This was followed by rinsing and incubation in TBS-T as above. The fixed protein-antibody complexes were visualized by chemiluminescence, ECL western Blotting Detection Reagents (Amersham) and exposed with Fujifilm LAS-3000 Scanner (Alphatech).

2.2.5.5 Trichloroacetic acid protein precipitation

Proteins in the culture supernatant (1 mL) of GAS or *L. lactis* were precipitated with 10 % (v/v) ice cold trichloroacetic acid (TCA). The supernatant was mixed well and incubated at 4^{o}C for 30 min. The sample was spun at 13000 rpm for 10 min at 4°C. The supernatant was discarded and the pellet was resuspended in SDS-PAGE loading buffer for analysis in Western Blotting.

2.2.6 Blood and cell based methods

2.2.6.1 Human whole blood preparation

Blood was taken from healthy donors and collected into Vacutainer® tube with 150 USP units of sodium heparin (BD) to prevent blood coagulation. Blood was kept at room temperature for immediate use.

2.2.6.2 Isolation of human neutrophils

Human neutrophils were isolated from heparinised whole blood using Histopaque density centrifugation according to the manufacturer's instructions. Typically, 5 mL of heparinised blood was layered on top of a two layer Histopaque gradient, which typically consisted of 2.5 mL Histopaque-1077 over 2.5 mL

Histopaque-1119 (Sigma-Aldrich). Blood gradient was centrifuged at 700 *g* for 30 min at room temperature with no brake. Neutrophils were collected from the interface between the Histopaque-1119 and Histopaque-1077 and washed once with PBS pH 7.4 (328 *g* for 10 min at room temperature). Residual erythrocytes were removed by mild osmotic lysis by resuspension of the cells in 0.2 % (w/v) NaCl for 30 s before buffering by the addition of an equal volume of 1.6 % (w/v) NaCl. Neutrophils were washed one final time in PBS (328 *g* for 10 min at room temperature) before being resuspended in the required assay buffer.

2.2.6.3 PMA-induced NET production by human neutrophils

Human neutrophils were isolated from heparinised blood according to the method mentioned above, and resuspended in RPMI, 10 mM HEPES, 2 % HSA to a concentration of 1 x 10^6 cells/mL. Each well was loaded with 200 µL neutrophils and activated by the addition of PMA at a final concentration of 100 nM and incubated at 37°C for 4 hrs with 5 % CO_2.

2.2.7 Functional assay methods

2.2.7.1 SDS-PAGE nuclease assay

To examine the nuclease activity of a protein with known molecular weight, the SDS-PAGE nuclease assay was performed. Special SDS-PAGE gel was prepared with sheared salmon sperm DNA (Sigma, USA) incorporated into the gel at a concentration of 10 ug/mL. SDS-PAGE reduced loading buffer was added to protein samples at 1:1 ratio and loaded without boiling the protein, electrophoresed at 200 V and a current less than 10 mA per gel until the dye front reached the bottom of the gel. The proteins on SDS-PAGE were renatured by incubation with 20 volumes renaturation buffer (40 mM Tris at pH 7.4, 0.001% w/v casein, 0.04% v/v 2-mercaptoethanol) 15 min for 8 times at room temperature with shaking. The nucleases in SDS-PAGE gel were activated by incubation with renaturation buffer containing 2 mM $MgCl_2$ and 1 mM $CaCl_2$ for 1 hr at 37°C with shaking. The gel was stained in 5 ug/mL ethidium bromide for 5 min and destained in water for 5 min with shaking. Observation was made under UV illumination, where the nuclease activity was detected as non-fluorescent regions on the gel.

2.2.7.2 Biochemical analysis of SpnA

Recombinant SpnA was added to Lambda DNA (Promega) to a final concentration of 10 ug/mL of enzyme and 50 ug/mL of DNA in a nuclease reaction buffer (50 mM Tris pH 7.4,
150 mM NaCl, 5 mM $MgCl_2$, 1 mM $CaCl_2$). and incubated for 1 h at 37°C. For Mg^{2+} and Ca^{2+} titrations, $MgCl_2$ and $CaCl_2$ were omitted from the reaction buffer and added separately at various concentrations.

For pH titrations, the Tris-HCl in the reaction buffer was replaced with 40 mM acetate buffer, pH 4.0 or with 40 mM Tris buffer, pH 7–9.

To quantify SpnA activity, a serial dilution of the enzyme was incubated in nuclease reaction buffer containing 1 mM $CaCl_2$, 3 mM $MgCl_2$ and 1 mg of lambda DNA for 1 h. All enzyme reactions were stopped by addition of EDTA to a final concentration of 20 mM.

After incubation, samples were loaded and separated on a 1 % agarose gel. Lambda DNA, without addition of rSpnA, was loaded as a control. DNA bands were visualized after ethidium bromide staining using a Gel imager 2000™ (Bio-rad) and quantified using ImageQuant V4.3 software (Bio-rad). Relative SpnA activity was calculated as 1 - (band $density_{+SpnA}$/band $density_{-SpnA}$) x 100. All samples were analysed in triplicates.

2.2.7.3 Measuring DNA binding to rSpnA proteins

Purified rSpnA proteins in 25 mM Tris pH 7.4 at final concentration of 3 uM was incubated with DAPI at 0.05 ug/mL for 15 min before the fluorescence was measured at a excitation/emission wavelength of 350/470 nm using a fluorescence microplate reader (Synergy HT Multi-Detection Microplate reader, Bio-Tek Instruments). Another set of wells were prepared in the same condition with the addition of BP DNase I at 6 ug/mL final concentration.

Both sets were incubated at 37°C for 2 hrs and the fluorescence was measured again at 350/470 nm for the reduction in fluorescence. All samples were analysed in triplicates.

2.2.7.4 Visualisation of NET destruction by rSpnA

Eight-well chamber slides (BD Biosciences) were coated with 250 µl per well of 0.001% poly-L-lysine (Sigma) for 1 h at 37°C. Unbound poly-L-lysine was removed by washing with milliQ water. Human neutrophils were isolated from heparinized blood according to the method mentioned above (section 2.2.9.2). The neutrophils were activated by addition of PMA (Sigma) at 100 nM and incubated for 4 hrs at 37°C and 5 % CO_2. Neutrophils were rinsed gently with PBS and resuspended in activity buffer (0.1 M HEPES pH 7.5, 0.15 M NaCl, 3 mM $MgCl_2$, 1 mM $CaCl_2$, 1% BSA). Recombinant SpnA or BP DNase I (Roche) were added at 0.5 uM and cells were incubated for a further 1 hr at 37°C and 5 % CO_2. After washing with PBS, the neutrophils were fixed with 4 % paraformaldehyde/PBS for 30 min and washed again with PBS. Cells were permeabilized with PBS, 0.05% Triton X-100 and blocked overnight with PBS, 1 % bovine serum albumin (BSA, Invitrogen) at 4°C. Rabbit anti-human neutrophil elastase (NE) antibody (Calbiochem) (1:1000 dilution) was added and incubated for 1 hr at 37°C followed by an incubation with anti-rabbit IgG-FITC (AD serotec) at 1:40 dilution. After 1 h, ProLong® Gold Antifade Reagent (Molecular

Probes) containing DAPI was added and the slides were analysed using a Nikon Eclipse E600 fluorescent microscope.

2.2.7.5 Quantification of NETs

For quantification of DNA release, 200 µL of neutrophils were seeded in a 96-well plate and allowed to settle for 30 min at 37°C and 5 % CO_2. The neutrophils were activated by addition of PMA at 100 nM and incubated for 4 hrs at 37°C and 5 % CO_2. Recombinant SpnA or BP DNase I (Roche) was added at 0.5 uM. $MgCl_2$ and $CaCl_2$ were added to a final concentration of 3 mM and 1 mM, respectively, per well. The neutrophils were incubated for a further 1 hr at 37°C and 5 % CO_2. Sytox Orange (Invitrogen) was added to a final concentration of 0.1 uM and, after 10 min incubation, fluorescence was measured (excitation 530 nm, emission 590 nm) using a fluorescence microplate reader (Synergy HT Multi-Detection Microplate reader, Bio-Tek Instruments). Three replicates per treatment were performed.

2.2.7.6 Methyl green-DNase activity assay

(a) Bacterial cell-based DNase activity assay

The Methyl green assay was performed as described by Sinicropi *et al* (Sinicropi, Baker, Prince, Shiffer, & Shak, 1994). *L. lactis* or GAS was grown to a density of OD_{600} = 0.6 and washed in PBS. Then, 3.3 x 10^8 cells were resuspended in triplicates of 50 µL of DNA-methyl green substrate (1.54 mg/mL salmon testes DNA (Sigma), 0.02 % methyl green (Sigma), 25 mM HEPES, 3 mM $MgCl_2$, 1 mM $CaCl_2$, 0.1% BSA, 0.05% Tween-20, pH 7.5) and transferred into a 96-well plate. After 24 hrs incubation at 37°C, absorbance was measured at 492 nm and 620 nm using a Synergy HT Multi-Detection plate reader (Bio-Tek). The absorbance measured at 492 nm was subtracted from the absorbance at 620 nm.

(b) Protein-based DNase activity assay

Recombinant SpnA protein at 50 µL in 25 mM Tris pH 7.4, 3 mM $MgCl_2$, 1 mM $CaCl_2$ was added to equal volume of DNA-methyl green substrate to reach a final concentration of 1.5 uM and transferred into a 96-well plate. After 24 hrs incubation at 37°C, absorbance was measured at 492 nm and 620 nm using a Synergy HT Multi-Detection plate reader (Bio-Tek). The absorbance measured at 492 nm was subtracted from the absorbance at 620 nm.

2.2.7.7 SpnA surface detection by flow cytometry

GAS cells were grown to appropriate growth phase and cells from 1 mL of culture were harvested by centrifugation at 10000 rpm for 10 min. The cell pellet was washed twice with PBS and resuspended in 1

mL of newborn calf serum (NCS). Cells were incubated at room temperature for 30 min with gentle rotation. Cells were collected by centrifugation at 10000 rpm for 10 min and washed twice with PBS before resuspension in PBS with 0.1% BSA, to reach an optical density of 0.15 at 600 nm. About 200 µL of bacterial resuspension was taken and incubated with rabbit anti-SpnA antibodies at 1:200 dilution for 30 min on ice. Cells were collected by centrifugation and washed twice with 0.1 % BSA in PBS, and resuspended in 100 µL PBS with 0.1 % BSA. A FITC-labeled anti-rabbit IgG (AD serotec) was added to the cells at 1:40 dilution, and incubated for 30 min on ice. The cells were washed twice in PBS with 0.1 % BSA and resuspended in 500 µL of PBS with 0.1 % BSA for analysis on a LSR II flow cytometer with FACSDIVA software v6.1.1. (BD) by acquiring 10000 events.

2.2.8 *In vitro* killing assays

2.2.8.1 Whole blood killing assay with bacteria

Approximately 1000 cfu of GAS or *L. lactis* grown to the late exponential phase were added to 1 mL of heparinised human whole blood and incubated at 37°C. Diluted blood samples were plated in triplicates onto appropriate agar plates at selected time points to enumerate the surviving bacteria. The survival rate was calculated as [cfu (at a given time point)/cfu (at the start)] × 100.

2.2.8.2 Whole blood killing assay with rSpnA

L. lactis 1363 was grown overnight in GM17 at 28 °C without agitation. The following day a fresh culture was inoculated and growth was monitored by regular OD600 readings using an Ultraspec 2100pro (Ambersham Bioscience). Once late exponential phase (OD600 ~ 0.8) was reached, bacteria were pelleted by centrifugation for 5 min at 5500 *g* and resuspended in HBSS (Sigma) to reach 1 x 10^8 cfu/mL. Heparinised blood at 350 µL was added to 10 µL bacterial resuspension, 90 µL of HBSS and 50 µL of recombinant protein in PBS for a total volume of 500 µL. Immediately, 10 μL of blood and bacteria mix was taken from each sample and diluted for plating in triplicates to calculate the initial bacterial dose. The remaining samples were incubated at 37°C for 3 hrs with slow rotation before another serial dilution was plated in triplicates. Plates were incubated overnight at 28°C and the survival rates were calculated on the following day.

2.2.8.3 NET killing assay

This assay was adapted from Buchanan *et al* (Buchanan et al., 2006). Human neutrophils were isolated as described above and resuspended in RPMI, 10 mM HEPES, 2 % HSA to a concentration of 0.5 × 10^6 cells/mL. Cell suspension at 200 µL per well was seeded onto a poly-L-lysine-coated 96-well microtitre plate (BD Biosciences) and incubated for 30 min at 37°C. NET release was induced as

described above before cytochalasin D was added to a final concentration of 10 ug/mL in RPMI, 10 mM HEPES, 2 % HAS and incubated for 15 min. One hundred microlitre of bacterial cells (2×10^5 cfu) grown to mid-logarithmic phase were added and incubated for 1 hr at 37°C. Neutrophils were lysed by adding 100 ul of 2.7 % NaCl, 0.03% Triton X-100 for 2 min. For enumeration of the surviving bacteria, the complete content of one well was transferred into a reaction tube and dilutions were plated in triplicates onto agar plates with appropriate antibiotics and grown for 24 hrs at 30°C for *L. lactis*, or at 37°C for GAS. Control wells without neutrophils were used to determine baseline bacterial counts at the assay end-points. Percent survival of the bacteria was calculated as [(cfu/mL test well)/(cfu/mL control well)] × 100.

2.2.9 Methods for zebrafish embryo infection model

2.2.9.1 Maintenance of adult zebrafish

Adult zebrafish (*Danio rerio*) were maintained in a custom designed zebrafish facility on a 14 hr light : 10 hr dark automated lighting cycle. Water conditions were maintained between 25.5 - 29.5°C, 250 - 500 uS conductivity and pH 7.2 - 7.6. The feeding regime consisted of live artemia (Artemia International) supplemented with tetramin (Tetra) and ZM300 (ZM Systems) dry food supplemented with tetramin and Cyclop-eeze (Argent Laboratories).

2.2.9.2 Breeding

Adult zebrafish were paired for spawning late in the afternoon. Upon “dawn” at the facility, water in the spawning tanks was manually replaced to stimulate spawning. Eggs were collected after 1 – 3 hrs. Embryos were manually collected from spawning tanks, rinsed in cold tap water and E3 with methylene blue. Embryos were raised in Petri dishes in E3 with methylene blue at 28.5 °C for one day and dechorionated manually. Zebrafish embryos were transferred into E3 buffer without methylene blue for further use.

2.2.9.3 Microinjection of bacteria

Bacterial cells were grown to late exponential phase (OD_{600} ~ 0.8) and washed twice with PBS before resuspension in PBS with 0.2 % (v/v) phenol red to desired dose. A P-80 micropipette puller (Sutter Instruments) was used to pull borosilicate glass capillaries to make microinjection needles. Tops of the needles were removed with forceps and backloaded with 2 µL bacterial resuspension. Injection volume was calculated by measuring the diameter of an injection into mineral oil solution with a haemocytometer. Embryos were anesthetized with tricaine and mounted in 3 % (w/v) methyl cellulose for microinjection. Injection was made with a Narishige micromanipulator (type GJ) connected to a MPPI-2 Milli-Pulses

Pressure Injector (Applied Scientific Instrumentation). Infection innoculum was determined by injection of one bolus into sterile PBS, spot plating onto agar plate and incubated overnight for enumeration.

2.2.10 Statistic analysis

Statistical significance was calculated using the two-tailed T-test provided by Microsoft Excel software for all the experiments, except for the zebrafish embryo infection model. Survival graphs and statistical significance for the infection model was performed through Statistical analyses were performed using GraphPad Prism version 5 for Mac OS X (GraphPad Software, San Diego California USA). A *P* value of < 0.05 was considered to be significant.

Chapter 3
Production and Characterisation of Recombinant SpnA Proteins

3.1 Introduction

Many cell wall anchored proteins of *S. pyogenes* are important virulence factors of the pathogen. The cell surface localisation enables direct association between virulence factors and proximal host components for bacterial adhesion, internalization of bacterial cells and neutralizing host immune defense mechanisms. An ORF, *spy0747*/*spnA*, in GAS M1 SF 370 was predicted to be a cell wall anchored nuclease as the DNA sequence indicated the presence of an exo/endonuclease domain and a sortase cell wall anchorage motif, LPXTG, that is conserved in Gram-positive bacteria.

Preliminary functional characterisation of rSpnA from GAS M1 SF370 by our lab (Chang et al., 2011) and by Hasegawa *et al* (Hasegawa et al., 2010) has revealed the protein to be a novel GAS cell surface nuclease. The full-length mature rSpnA was able to digest linear and circular DNA molecules, as well as RNA, in the presence of Ca^{2+} and Mg^{2+} ions (Chang et al., 2011). Further investigation demonstrated the recombinant C-terminal exo/endonuclease domain ($rSpnA_{549-877}$) by itself was enzymatically inactive, suggesting the N-terminus of the protein is essential for the nuclease activity of SpnA (Chang et al., 2011).

Bacterial DNases were thought to assist in bacterial dissemination by decreasing the viscosity of purulent material at site of infection. Bacterial DNases may also be beneficial for bacterial growth as degraded DNA could be uptaken as nutrient. Recent studies have also shown that some bacterial DNases were able to promote bacterial survival by neutralizing the DNA-based extracellular bactericidal mechansim, NETs (Beiter et al., 2006; Buchanan et al., 2006; Sumby et al., 2005). Therefore, the cell wall localisation and the nuclease activity of SpnA made this novel nuclease an interesting research target as a potential virulence factor of GAS that mediates evasion of host immunity.

In order to further understand the mechanism of SpnA's nucleases activity, and to determine if SpnA had destructive activities on NETs, recombinant proteins of SpnA in full-length and truncated forms were constructed and expressed in *E. coli* BL21. This chapter outlines the purification and characterisation of SpnA recombinant proteins, and the ability of full-length rSpnA in degrading the DNA framework of NETs.

3.2 Results

3.2.1 Production of rSpnA proteins

3.2.1.1 Cloning and expression of recombinant SpnA proteins

The preliminary study on SpnA by our lab showed that the three N-terminal OB-folds are crucial for the nuclease activity of SpnA. As OB-folds are often involved in nucleic acid binding, it is hypothesized that at least one of the three OB-fold domains in the N-terminal region is required for the nuclease activity of SpnA. To investigate the significance of the OB-folds to SpnA nuclease activity, truncated rSpnA proteins were constructed (Figure 3.1).

The genomic DNA of *S. pyogenes* SF370 was the template to clone *spnA* in various lengths for expression in *E. coli* strain BL21. Four N-terminally truncated SpnA proteins were generated in addition to the previously constructed full-length rSpnA and the C-terminus nuclease domain, $rSpnA_{549-877}$. These four recombinant proteins all end immediately before the Gram-positive cell wall anchorage LPKTG motif at the 877^{th} residue. Recombinant $SpnA_{99-877}$ starts at residue 99, where the first predicted OB-fold begins (OB1), and contains all three OB-fold domains (OB1, OB2 and OB3). Recombinant $SpnA_{217-877}$ starts at the beginning of the second OB-fold motif (OB2) at the 217^{th} residue and consists of two OB-folds (OB2 and OB3). Recombinant $SpnA_{310-877}$ starts at the beginning of predicted OB3 domain and has only one OB-fold (OB3). Recombinant $SpnA_{396-877}$ starts immediately after the end of predicted OB3 domain, thus contains no OB folds. The DNA fragments encoding for these protein constructs were cloned into pProExHtB vector between the *Bam*HI and *Hind*III sites. In addition to the above four constructs, the DNA fragment encoding for the N-terminus alone was introduced into the same position in pProExHtb vector for the expression of $rSpnA_{99-395}$.

The truncated rSpnA proteins were expressed with an N-terminal polyhistidine tag under the control of an IPTG-inducible promoter. The N-terminal polyhistidine tag allows protein purification through Ni^{2+} affinity chromatography.

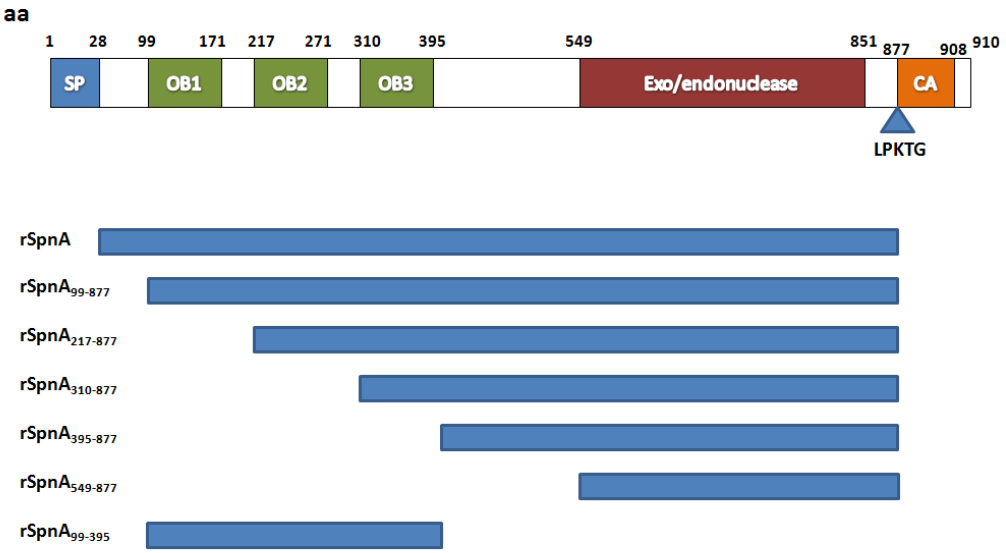

Figure 3.1 Predicted domain architecture of SpnA and the summary of truncated rSpnA proteins

The in silico analysis on the amino acid sequence of SpnA has predicted the domain architecture of the protein. SpnA has a signal peptide (SP) in the N-terminus end, followed by three OB-fold motifs (OB1, OB2 and OB3). An exo/endonuclease domain locates in the C-terminus of the protein together with the predicted cell wall anchorage domain (CA), which has a conserved Gram-positive cell wall sorting recognition motif LPKTG at amino acid position 873-877.

rSpnA – the full-length SpnA

$rSpnA_{99-877}$ – contains all three OB-fold motifs of SpnA (OB1, OB2 and OB3) and extends to the beginning of the cell wall anchorage motif

$rSpnA_{217-877}$ – the protein extends from OB2 domain to the beginning of the cell wall anchorage motif

$rSpnA_{310-877}$ – the protein extends from OB3 domain to the beginning of the cell wall anchorage motif

$rSpnA_{396-877}$ – the protein extends at the end of OB3 domain to the beginning of the cell wall anchorage motif

$rSpnA_{549-877}$ – the C-terminal nuclease domain of SpnA

$rSpnA_{99-395}$ – the protein represents the N-terminus of SpnA, containing all three OB-fold domains

3.2.1.2 Purification of rSpnA proteins

The protein purification method for truncated rSpnA proteins is similar to the purification for full-length rSpnA described previously (Chang, 2007). The recombinant proteins were purified through Ni^{2+} affinity chromatography by the interaction between the N-terminal polyhistidine tag and Ni^{2+} IDA sepharose. A titration of imidazole at 20 mM, 50 mM, 75 mM, 100 mM, 150 mM was employed for competitive elution of the polyhistidine-tagged recombinant proteins from the IDA spharose after washing the column with 10 mM imidazole. The fractions eluted with 100 mM and 150 mM contain clean soluble recombinant SpnA proteins, as the fractions eluted with lower imidazole concentrations removed most impurities. Figure 3.2 shows the purification of $rSpnA_{99\text{-}877}$ as an example of other rSpnA proteins listed in this chapter. Recombinant proteins $rSpnA_{99\text{-}350}$, $rSpnA_{99\text{-}877}$, $rSpnA_{217\text{-}877}$ and $rSpnA_{396\text{-}877}$ were expressed as stable soluble proteins similar to the full-length rSpnA, with a 1 L *E. coli* culture typically producing 2 mg of clean soluble recombinant protein. Recombinant $SpnA_{310\text{-}877}$ was an exception as it has poor solubility and stability compared to other truncated versions of SpnA. The protein $rSpnA_{310\text{-}877}$ appeared as a double band on the SDS-PAGE gel, most likely due to disruption of protein structure that resulted in instability of the protein (Figure 3.4 A). The yield of $rSpnA_{310\text{-}877}$ from a 1 L *E. coli* culture is typically 1 mg.

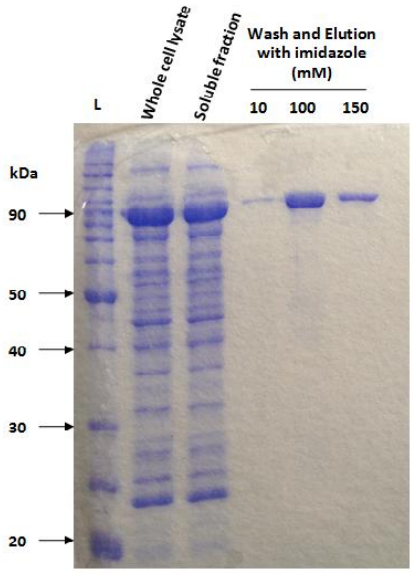

Figure 3.2 Protein purification for $rSpnA_{99\text{-}877}$ through Ni^{2+} affinity chromatography

Benchmark protein ladder was applied to estimate molecular weight of $rSpnA_{99\text{-}877}$ in 10 % SDS-PAGE gel stained with coomassie blue. The $rSpnA_{99\text{-}877}$ at around 90 kDa was mostly found in the soluble fraction. The column was washed with imidazole at 10 mM to remove residues of *E. coli* protein. Elution with 100 mM and 150 mM imidazole produced clean $rSpnA_{99\text{-}877}$.

3.2.2 Functional analysis on truncated rSpnA proteins

3.2.2.1 DNA binding assay of $rSpnA_{99-395}$ and full-length rSpnA

The N-terminus has been shown to be crucial for the nuclease activity of SpnA (Chang, 2007). The *in silico* analysis on SpnA amino acid sequence has predicated three OB-fold domains in the N-terminus of the protein (Figure 3.1). These OB-fold domains were thought to mediate DNA binding for SpnA. A DNA binding assay was designed to investigate if the predicted OB-fold domains could bind DNA molecules.

The purified full-length rSpnA protein was found to bind to a large quantity of *E. coli* DNA after purification process (personal communication with Professor John Fraser, University of Auckland, New Zealand), yet these DNA molecules were not hydrolysed, as rSpnA was nuclease inactive in the absence of Ca^{2+} ions. The DNA binding assay was thus designed to quantify DNA molecule binding to rSpnA and $rSpnA_{99-395}$ proteins before and after the addition of bovine pancreas DNase I (BP DNase I) with the DNA dye, DAPI. A decrease in the fluorescence after digestion with BP DNase I would indicate a reduction in DNA quantity; therefore, the decrease in fluorescence could be an indirect indication of the presence of DNA.

The full-length rSpnA and the N-terminus of SpnA, $rSpnA_{99-395}$, were purified through Ni^{2+} affinity chromatography as mentioned in the previous section. Equimolar amount of rSpnA and $rSpnA_{99-395}$ were incubated with DAPI respectively for the measurement of fluorescence at an excitation/emission wavelength of 350/470 nm. BP DNase I was added subsequently after the initial fluorescence reading for digestion of DNA molecules bound to the proteins. Measurement of fluorescence was taken again after 2 hrs.

Reduction in fluorescence was observed with both rSpnA and $rSpnA_{99-395}$ (Figure 3.3). The $rSpnA_{99-395}$ protein had a fluorescence reading at around 11000 at time 0, and the incubation with BP DNase I resulted in a 3-fold reduction in the measurement. The full-length rSpnA bound double the quantity of DNA than the N-terminus of SpnA alone, and the digestion by BP DNase I decreased the reading by 10-fold (Figure 3.3). The reduction in fluorescence observed with both rSpnA and $rSpnA_{99-395}$ was statistically significant ($P < 0.01$). This observation indirectly indicates the OB-fold domains in the N-terminus of SpnA bind to DNA molecules.

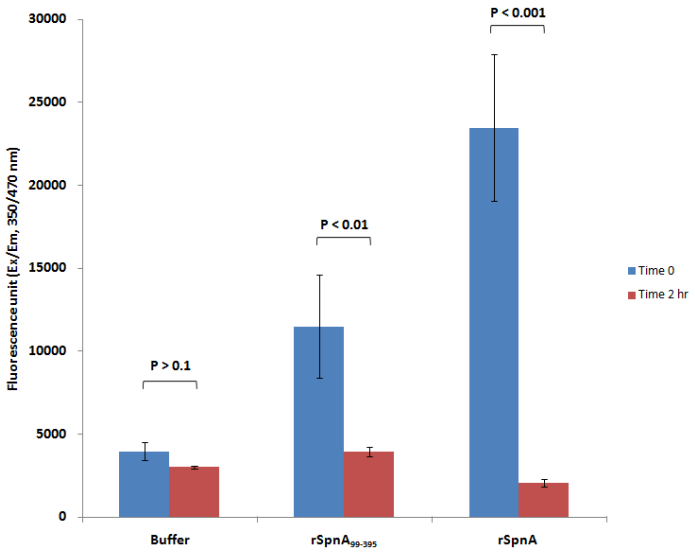

Figure 3.3 The DNA binding of rSpnA$_{99-395}$ and rSpnA measured by DAPI

DNA molecules bound to full-length rSpnA and rSpnA$_{99-395}$ after purification were measured by DAPI. The addition of BP DNase I hydrolysed the DNA molecules and resulted in decreased fluorescence unit readings, such reduction was an indirect indication of DNA binding to rSpnA proteins. The digestion by BP DNase I caused a 3-fold and a 10-fold decrease in fluorescence with rSpnA$_{99-395}$ and rSpnA respectively. The negative control had no protein in the incubation buffer and showed no significant change in fluorescence reading. The error bars show the standard deviation of three independent experiments.

3.2.2.2 Analysis on the nuclease activity of full-length and truncated rSpnA proteins

An in-gel nuclease activity assay was carried out to investigate the nuclease activity of the N-terminally truncated rSpnA proteins. Non-boiled recombinant proteins were loaded and analysed on a specially made SDS-PAGE gel containing sonicated salmon sperm DNA. The SDS-PAGE gel was washed repeatedly in a Tris-based buffer to renature the proteins in gel after electrophoresis. To activate the nuclease activity of the recombinant SpnA proteins, the gel was soaked in an activation buffer containing 2 mM $MgCl_2$ and 1 mM $CaCl_2$ and incubated at 37°C to allow nuclease activity. The gel was stained with either coomassie blue for the position of protein (Figure 3.4 A) or with ethidium bromide for the detection of DNA under UV light (Figure 3.4 B).

The enzymatically active full-length rSpnA was the positive control. A hollow area was found on the gel containing DNA after staining with ethidium bromide at the position corresponding to the molecular weight of full-length rSpnA (Figure 3.4 B). This is an indication of nuclease activity as DNA molecules around the protein band were hydrolysed. In contrast, no nuclease activity was observed in the enzymatically inactive rSpnA$_{549-877}$, which was the C-terminal nuclease domain alone (Figure 3.4 B). The rSpnA$_{99-877}$

(contains OB1, OB2 and OB3) and rSpnA$_{217-877}$ (contains OB2 and OB3) both showed similar nuclease activity to the full-length rSpnA, while rSpnA$_{310-877}$ (contains only OB3) and rSpnA$_{396-877}$ (contains no OB-fold) were without any enzymatic activity (Figure 3.2 B). This suggests that at least two of the three OB-fold domains (OB2 and OB3) are required for SpnA to be an active nuclease.

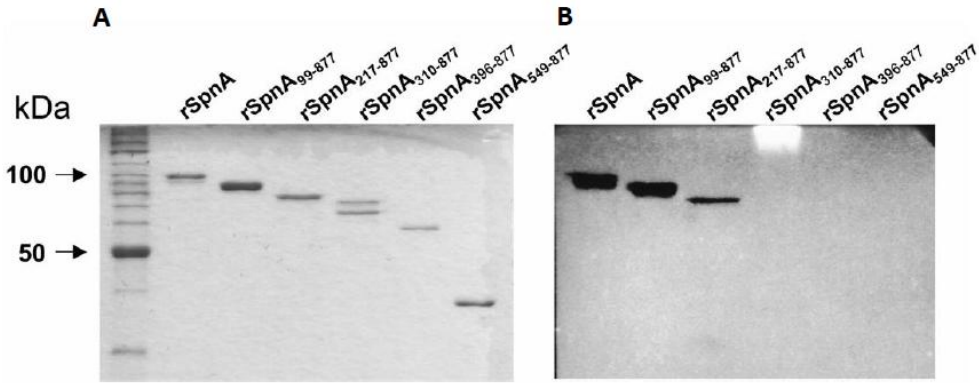

Figure 3.4 Nuclease activity assay with full-length and N-terminally truncated rSpnA proteins

A. Coomassie blue stained 10 % SDS-PAGE gel. The full-length and N-terminally truncated rSpnA proteins were analysed on a specially made SDS-PAGE gel, containing DNA. The gel was stained with coomassie blue to show the position of the proteins with corresponding molecular weight. The rSpnA$_{316-877}$ protein appeared as a double band on the gel, this is most likely caused by instability of the protein.

B. Ethidium bromide stained 10 % SDS-PAGE gel. The gel shows the nuclease activity of the rSpnA proteins. The full-length mature rSpnA, along with the truncated rSpnA$_{99-877}$ and rSpnA$_{217-877}$ are enzymatically active. In contrast, recombinant SpnA proteins that contains only one (OB3) or none of the OB-fold motifs are without enzymatic activity. This indicates that at least two OB-fold domains (OB2 and OB3) are required for nuclease activity.

3.2.3 The optimal conditions for nuclease activity of the full-length recombinant SpnA

3.2.3.1 The requirement of divalent cations for nuclease activity of full-length rSpnA

Preliminary studies on rSpnA showed the activity of the nuclease was Ca^{2+} and Mg^{2+}-dependent (Chang et al., 2011; Hasegawa et al., 2010). Here the requirement for divalent cations was further analysed in Ca^{2+} and Mg^{2+} titration assays using lambda DNA as a substrate (Figure 3.5 A and B). Recombinant SpnA showed maximal activity to lambda DNA at 0.78 mM Ca^{2+}, but significant enzyme activity was also observed between 0.15 – 3.13 mM Ca^{2+} (> 70 %). Only marginal DNase activity was detected above 12.5 mM or below 0.05 mM $CaCl_2$ (< 10 %), and the protein becomes inactive above 25 mM or in absence of Ca^{2+}. The optimal Mg^{2+} concentrations for SpnA nuclease activity lie between 1.5 – 3 mM (Figure 3.5 B). The activity showed reduced, but still significant activity at 0.2 mM (50 %) and 12.5 mM (60 %) $MgCl_2$. Recombinant SpnA is completely inactive in the absence of Mg^{2+}.

3.2.3.2 The optimal pH range for recombinant full-length SpnA enzymatic activity

The rSpnA nuclease activity against lambda DNA was also analysed at varying pH using optimal Ca^{2+} (at 1 mM) and Mg^{2+} (3 mM) concentrations. Recombinant SpnA showed maximal activity between pH 5.5 – 7, and reduced activity at pH 5 (60 %) and pH 8 (20 %). Enzymatic activity of rSpnA was completely inhibited at pH 8.5 and above (Figure 3.5 C).

3.2.3.3 The analysis of SpnA nuclease activity unit

The nuclease activity unit of SpnA was characterised using a serial dilution of rSpnA under the optimal reaction condition (1 mM $CaCl_2$, 3 mM $MgCl_2$, pH 7.4) with 1 ug Lambda DNA. The result indicated 2.5 ug (26 pmol) was required to completely digest 1 ug Lambda DNA in 1 h (Figure 3.5 D).

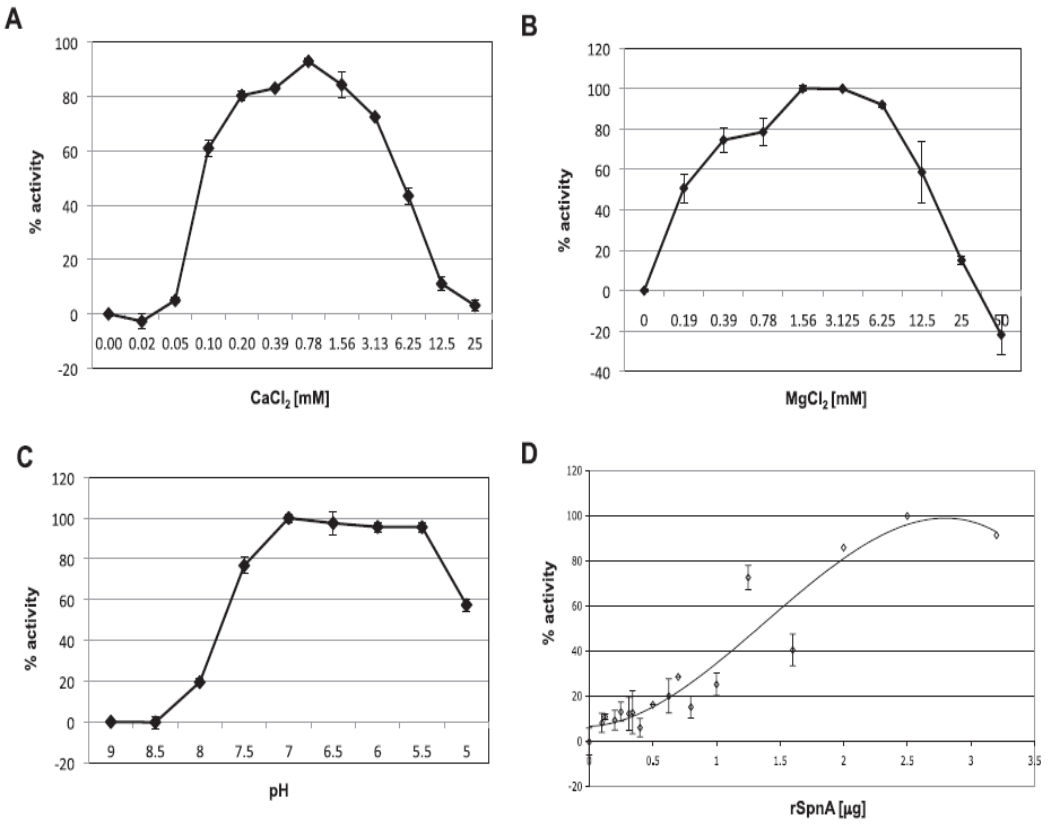

Figure 3.5 Biochemical analysis of rSpnA for the optimal reaction condition

A. DNA digestion by rSpnA with varying concentrations of $CaCl_2$. Optimal activity was observed at 0.78 mM Ca^{2+}, but significant enzyme activity was also observed between 0.15 – 3.13 mM Ca^{2+}.

B. DNA digestion by rSpnA with varying concentrations of $MgCl_2$. Optimal activity was observed between 1.5 – 3 mM.

C. DNA digestion by rSpnA with a varying pH. The nuclease was most active between pH 5.5 – 7.

D. Nuclease activity analysis indicated 2.5 ug (26 pmol) was required to completely digest 1 ug Lambda DNA in 1 hr.

The error bars show the standard deviation of three independent experiments.

3.2.4 Enzymatic activity of rSpnA on NETs

3.2.4.1 Production of NETs from human neutrophils and analysing rSpnA reactivity toward NET structure

Reports have shown that some bacteria, including strains of GAS, *S. pneumonia* and *S. aureus*, produce nucleases that degrade the DNA framework of NETs and allow bacteria to escape from the entrapment and killing by the extracellular trap (Beiter et al., 2006; Berends et al., 2010; Buchanan et al., 2006). The destruction of NETs has been believed to be an important immune evasion mechanism. To analyse if rSpnA is capable of destroying NETs we stimulated isolated human neutrophils with PMA for 4 hrs for NET

release. Extracellular fibrous structures were observed after incubating human neutrophils with PMA for 4 hrs (Figure 3.6 A, second panel), whereas no extracellular DNA was observed with the cells incubated with only PBS (Figure 3.6 A, first panel). The extracellular filamentous structures could be detected by DAPI for DNA (blue) and by neutrophil elastase-specific antibodies (green) confirming them to be NETs. When 0.5 uM rSpnA was added to the PMA activated neutrophils the extracellular structure disappeared, indicating that rSpnA is capable of destroying NETs (Figure 3.6 A, third panel). BP DNase I was employed as a positive control as its enzymatic activity on NETs has been demonstrated before (Beiter et al., 2006). The last panel in Figure 3.6 A showed that 0.5 uM BP DNase I could completely clear the extracellular traps.

3.2.4.2 Quantification of NET destruction by rSpnA

The release of DNA from neutrohpils was quantified using Sytox Orange, a DNA stain that does not penetrate cells (Figure 3.6 B). Activation of neutrophils with PMA led to a great increase in extracellular DNA from around 1400 to 4000 fluorescence units. The addition of rSpnA significantly ($P < 0.0001$) lowered the amount of extracellular DNA to around 3000 units in stimulated neutrophils indicating destruction of NETs. No significant change was observed when unstimulated neutrophils were treated with rSpnA. Equimolar amount of BP DNase I was added to stimulated neutrophils as the positive control and the amount of extracellular DNA dropped to around 1900 units.

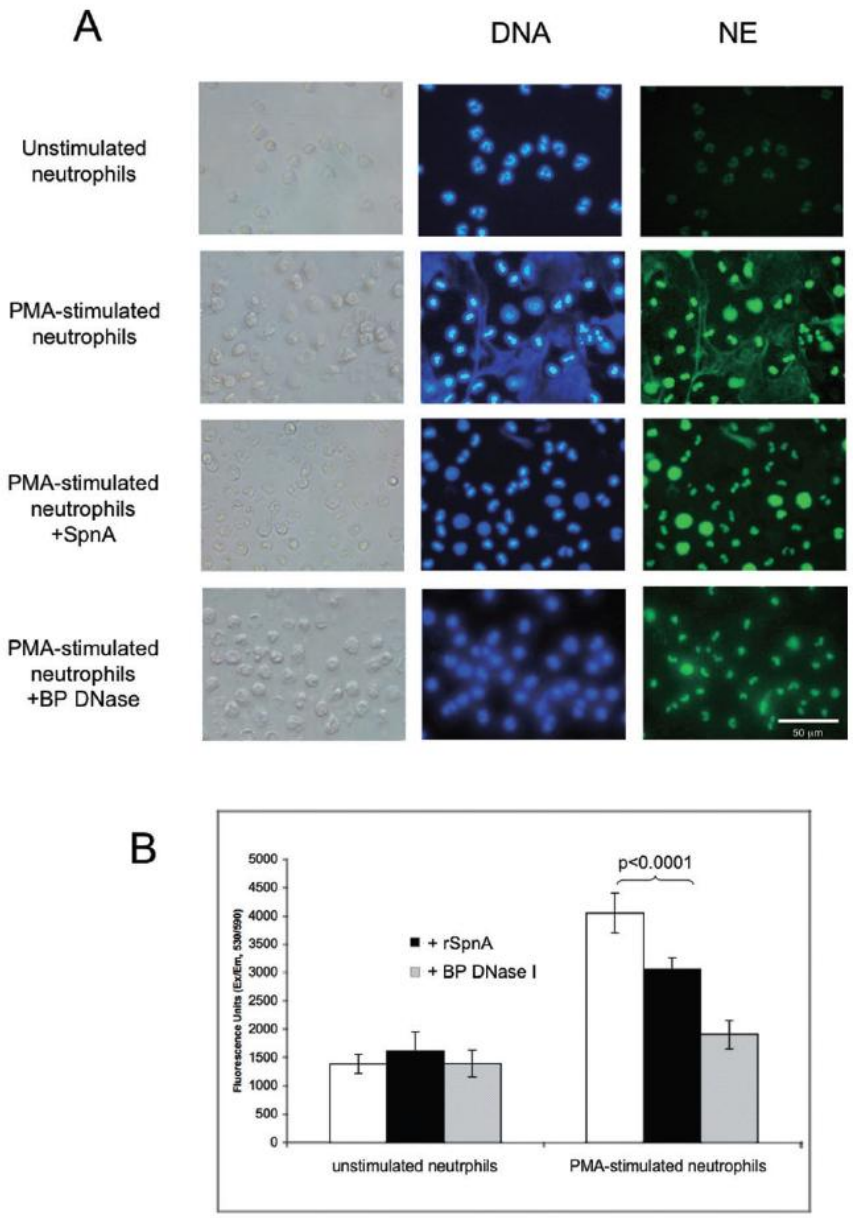

Figure 3.6 Release of NETs and destruction by rSpnA

A. Immunofluorescence microscopy of human neutrophils incubated for 4 hrs without stimulation (top panel) and with PMA treatment (second panel). NETs are released from neutrophil after PMA stimulation. The DNA was stained with DAPI (blue) and neutrophil elastase (NE) was detected by anti-human neutrophil elastase antibody and a FITC-labeled secondary antibody (green). Treatment with rSpnA (third panel) or BP DNase I (bottom panel) as a positive control both resulted in complete NET destruction.

B. NET release and destruction by rSpnA was quantified staining neutrophils with DNA stain Sytox orange, which is cellular impermeable. Activation of neutrophils with PMA stimulation resulted in a strong increase in extracellular DNA. Treatment with either rSpnA or BP DNase I leaded to significant decrease of extracellular DNA in stimulated, but not unstimulated neutrophils. The error bars show the standard deviation of three independent experiments.

3.3 Discussion

The cell wall localisation of SpnA and its nuclease activity made this newly discovered cell wall anchored nuclease an attractive research target as a potential virulence factor of GAS. The *spnA* gene was cloned and expressed as soluble recombinant proteins in *E. coli* BL21 in full-length or truncated forms to study the mechanism of its enzymatic activity.

The protein architecture of SpnA was predicted by computer program based on its amino acid sequence (listed in Figure 1.5), and the result indicated the presence of three OB-fold domains in the N-terminus of the protein. Previous functional analysis on rSpnA also concluded the N-terminus was essential for its nuclease activity. OB-fold domains are often involved in substrate binding; hence SpnA was speculated to bind DNA through the OB-domains in the N-terminus, while the exo/endonuclease domain in the C-terminus catalysed the degradation of DNA. The DNA binding assay indirectly quantified DNA bound to full-length rSpnA and the SpnA N-terminus, $rSpnA_{99\text{-}395}$, by digesting protein-bound DNA molecules with BP DNase I. The 2 hr digestion by BP DNase I decreased the fluorescence signal of DAPI by 3-fold and 10-fold for $rSpnA_{99\text{-}395}$ and rSpnA respectively, indicating the presence of DNA. The next question was whether SpnA required all three OB-domains for the nuclease activity.

Four N-terminally truncated SpnA recombinant proteins were expressed to investigate if enzymatic activity of SpnA required multiple OB-fold domains. In an in-gel nuclease activity assay, it was found SpnA requires at least two of the three OB-fold motifs (OB2 and OB3) to digest DNA. It is possible that the multiple OB-fold domains were acquired over evolutionary course for protective purpose against losing nuclease activity due to attack by proteases.

The optimal reaction conditions of rSpnA were characterisd in this chapter. SpnA's activity is dependent on Ca^{2+} and Mg^{2+} ions, with optimal activity observed between 0.15 – 3.13 mM Ca^{2+} and 1.5 – 3 mM Mg^{2+}. The nuclease is most active between pH 5.5 – 7, and with a nuclease unit of 26 pmol. SpnA appeared to share similar characters with the DNase D subgroup of GAS DNases according to the results gathered in this chapter and in the preliminary study of SpnA. Characteristics of DNase D subgroup include optimal activity occurring between pH 6 – 7, digesting both DNA and RNA, and the dependency on Ca^{2+} and Mg^{2+} for the nuclease activity.

The report by Hasegawa *et al* demonstrated that a *spnA*-knock out mutant was less virulent in blood bactericidal assay and in a murine infection model suggesting SpnA contributes in GAS virulence (Hasegawa et al., 2010). However, the exact role of SpnA in GAS virulence was never fully explored.

Recent identification and characterisation of streptococcal DNase Sda1 of GAS M1T1 strain indicates Sda1 protects the pathogen from NET killing by effectively cleaving the DNA framework of NETs that releases pathogen from entrapment and subsequent killing (Buchanan et al., 2006). A *sda1*-knockout mutant was shown to be more susceptible to killing in neutrophil and whole blood bactericidal assay, as well as in the mouse infection model (Buchanan et al., 2006). For these reasons, we have hypothesized that SpnA participates in the immune evasion process of GAS by destroying NETs and allowing the pathogen to escape from sites of infection. In this chapter, it was demonstrated that recombinant mature full-length SpnA was indeed capable of clearing NETs when added to PMA stimulated human neutrophils. The clearance of NETs by rSpnA could be observed under immunofluorescent microscopy and quantified using extracellular DNA stain Sytox Orange, in which rSpnA significantly decreased the amount of extracellular DNA in PMA-stimulated neutrophils. The result suggests SpnA might play role in evading NETs and thereby promote GAS survival in host.

Chapter 4

Construction of *spnA* Mutants in GAS and *Lactococcus lactis*

4.1 Introduction

The nuclease characteristics of SpnA have been closely investigated in the previous chapter, however the exact role of SpnA in the virulence of *S. pyogenes* was yet to be explored.

To further understand how SpnA might benefit *S. pyogenes* during the course of infection, a heterologous expression system was constructed to express SpnA in the Gram-positive bacterium *L. lactis*. The organism has been frequently used in the food industry, and has been considered as a possible drug and vaccine delivery system in therapeutic use (Le Loir et al., 2005). The bacterium has also been widely used as an exogenous expression system for studies of virulence factors from pathogenic Gram-positive bacteria, including *S. pyogenes* and *S. aureus*, as *L. lactis* shares similar protein expression and processing procedures with other Gram-positive bacteria (Le Loir et al., 2005). *L. lactis* lacks the expression of virulence factors; therefore it is an ideal system to study the effect of virulence factors in isolation. This chapter outlines the cloning and expression of SpnA in *L. lactis*.

In addition to the *L. lactis* gain-of-function mutants, an isogenic GAS M1 SF370 *spnA*-knockout mutant was constructed to study the changes in bacterial survival in the absence of SpnA. The expression of SpnA in the *spnA*-knockout mutant was subsequently restored through a plasmid-based expression system to confirm that any differentiation between the parental GAS M1 strain and *spnA*-knockout mutant was a result of *spnA* deletion. This chapter summarizes the construction of plasmids used for *spnA* gene replacement and complementation.

4.2 Results

4.2.1 Generation of SpnA expressing *L. lactis* strains

S. pyogenes expresses a wide range of virulence factors including secreted DNases that have been shown to disrupt the innate antimicrobial mechanism, NETs, and to assist bacterial spreading from sites of infection. In order to analyse the effect of SpnA on the pathogen's virulence without the interference from activities of other virulence factors and DNases, the gene was introduced and expressed in non-pathogenic Gram-positive *L. lactis* where the role of SpnA in virulence could be investigated in isolation.

4.2.1.1 Primer design and plasmid construction

An *E. coli* - *L. lactis* shuttle plasmid was constructed, pOri23T:s*pnA*, by inserting *spnA* gene amplified from the genomic DNA of GAS M1 SF370 strain along with its ribosomal binding site (RBS) between *Bam*HI and *Xho*I in the multiple cloning site of pOri23T vector. The pOri23T:*spnA* plasmid was designed to express cell wall-anchored SpnA in *L. lactis* that resembles the native SpnA expression in GAS.

Primers were designed to construct the lactococcal shuttle plasmid. The forward primer, SpnA_LL.fw, was designed to contain the *Bam*HI restriction sequence for cloning purpose, the RBS of *spnA* and the very first 17 bp from native *spnA* gene, including the start codon. The reverse primer, SpnA_LL.rev, has a *Xho*I restriction sequence and very last 17 bp from native *spnA* gene, including the stop codon.

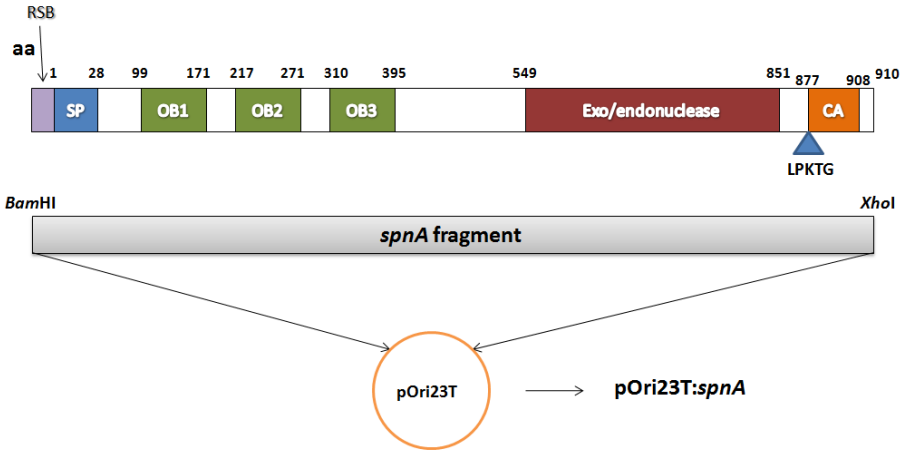

Figure 4.1 The construction of pOri23T:spnA plasmid

The entire *spnA* gene with its RSB was amplified from the genomic DNA of GAS M1. The DNA fragment was inserted into the pOri23T vector between *Bam*HI and *Xho*I sites in the multiple cloning site (MCS).

4.2.1.2 Expression of SpnA by *L. lactis* pOri23T:*spnA* gain-of-function mutant

The uptake of the pOri23T shuttle vector carrying *spnA* gene by *L. lactis* after electroporation was detected through single colony PCR by amplifying the *spnA* gene using SpnA_LL.fw and SpnA_LL.rev primers (Figure 4.2 A). Seven out of eighteen colonies screened were shown to be pOri23T:*spnA* positive. *L. lactis* pOri23T:*spnA* mutant was grown to late exponential phase (OD_{600} = 0.8 – 1.0) and treated with a protoplast buffer consisting of mutanolysin and lysozyme which solubilize the bacterial cell wall and release embedded proteins. Cell wall extract from the mutant was concentrated by TCA precipitation and subjected to Western blot analysis in comparison to *L. lactis* harbouring empty pOri23T as a negative control. Presence of SpnA at similar molecular weight to rSpnA (~100 kDa) was found in the cell wall fraction of *L. lactis* pOri23T:*spnA* as a double-band, this might be an artifact resulting from the precipitation process (Figure 4.2 B). No SpnA was detected from the cell wall fraction of *L. lactis* empty pOri23T vector control.

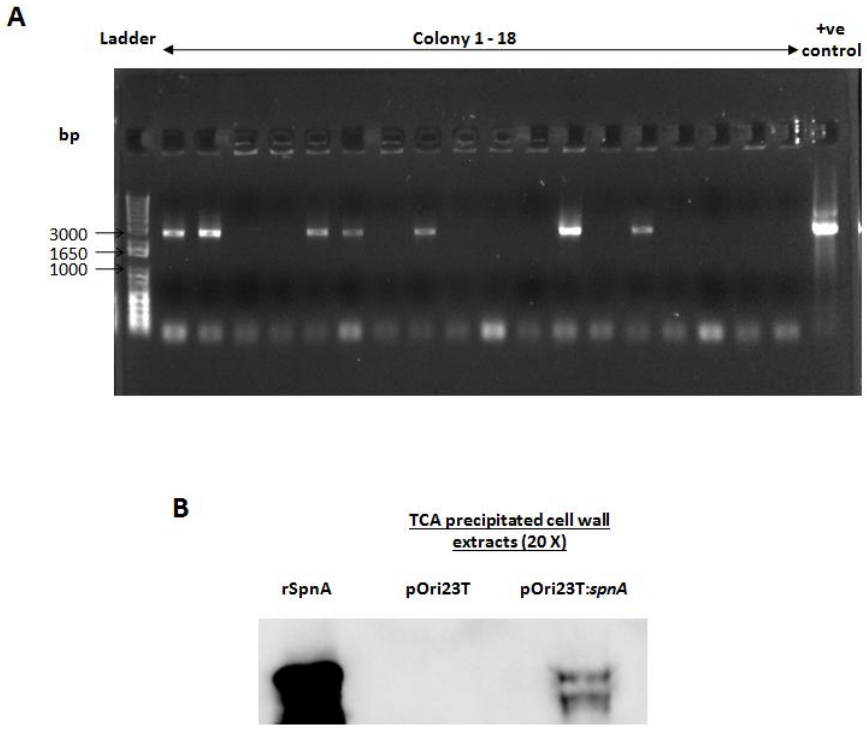

Figure 4.2 Screening of spnA gene and SpnA expression in L. lactis pOri23T:spnA mutant

A. Single colony PCR was performed to screen for *L. lactis* colonies containing pOri23T:*spnA* plasmid. A total of eighteen colonies were screened and seven among them were tested positive for the presence of *spnA* gene represented by a ~2.7K bp DNA fragment. The pOri23T:*spnA* plasmid was used as the template for the positive control in this PCR screening.

B. Expression of SpnA in the *L. lactis* gain-of-function mutant was detected through Western blot analysis. Expression of SpnA was found in the cell wall extraction from *L. lactis* pOri23T:*spnA*. No trace of SpnA expression was detected in the cell wall extraction of the pOri23T empty vector control. Recombinant mature full-length SpnA (10 ug) was used as the positive control.

4.2.1.3 Growth rate of *L. lactis* pOri23T:*spnA* and *L. lactis* pOri23T empty vector control

The growth rate of *L. lactis* pOri23T:*spnA* and the pOri23T empty vector control were compared with *L. lactis* wildtype. Mutant *L. lactis* pOri23T:*spnA* and the empty vector control were grown in the presence of erythromycin to positively select bacteria carrying pOri23T plasmid. The growth of the two pOri23T carrying strains was delayed when comparing to wildtype *L. lactis* possibly due to the extra energy expenditure on antibiotic resistance and the expression of SpnA (Figure 4.3). Wildtype bacterium reached stationary phase after 6 hrs of incubation at 28°C, while *L. lactis* pOri23T:*spnA* and the empty vector control reached stationary phase after more than 8 hrs of incubation.

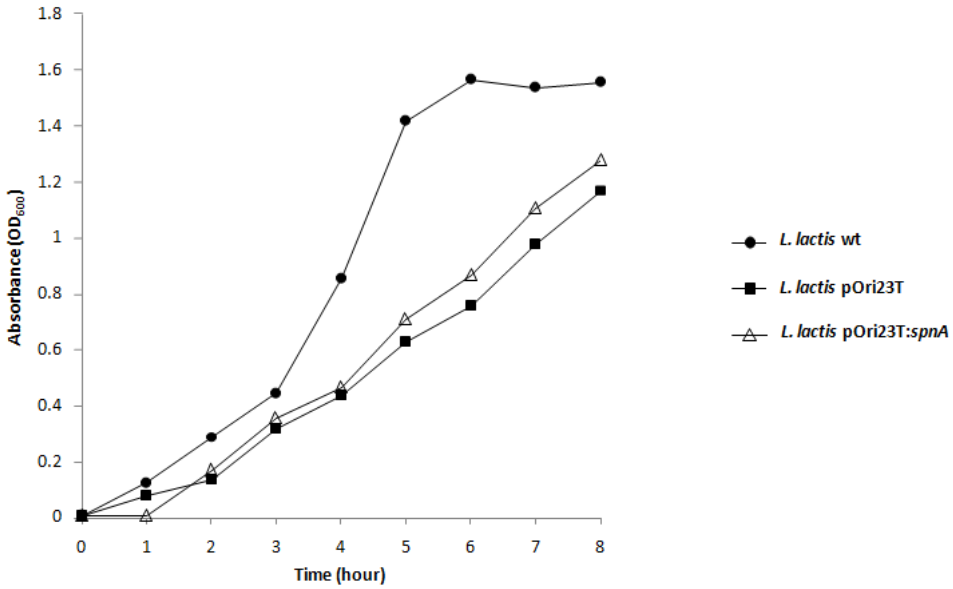

Figure 4.3 Growth of L. lactis pOri23T:spnA and L. lactis pOri23T empty vector control

Growth of *L. lactis* pOri23T:*spnA* was compared with the growth of *L. lactis* wildtype and pOri23T empty vector control. Growth rate of *L. lactis* pOri23T:*spnA* is comparable with the empty vector control, whereas the wildtype bacterium has the highest growth rate. Wildtype bacterium reached stationary phase after 6 hrs of incubation at 28°C, while *L. lactis* pOri23T:*spnA* and the empty vector control reached stationary phase after more than 8 hrs of incubation.

4.2.1.4 Nuclease activity test of SpnA expressed by *L. latctis* pOri23T:*spnA*

The nuclease activity of SpnA expressed by *L. lactis* gain-of-function mutant was analyzed in a methyl green-DNase activity assay. Methyl green is a triphenylmethane dye that produces a green colour when it intercalates between the bases of double-stranded DNA. The dye decolorizes as it dissociates from DNA when it is hydrolysed, and the decolorization can be quantified as a reduction in absorbance reading at 620 nm.

L. lactis pOri23T:*spnA* was subjected to methyl green-DNase activity assay to assess its nuclease activity in comparison to the *L. lactis* pOri23T empty vector control. Bacterial cells were grown to late exponential phase and washed before being incubated with methyl green conjugated salmon sperm DNA for 16 hours. The wells containing *L. lactis* pOri23T:*spnA* had a colour change from green to colourless, while the *L. lactis* pOri23T empty vector control and the negative control wells showed no obvious colour change (Figure 4.4 A). The decolorization event was quantified, showing *L. lactis* pOri23T:*spnA* had a 5-fold decrease in absorbance in comparison to *L. lactis* pOri23T empty vector and the negative control which had similar readings of 1.0 (Figure 4.4 B).

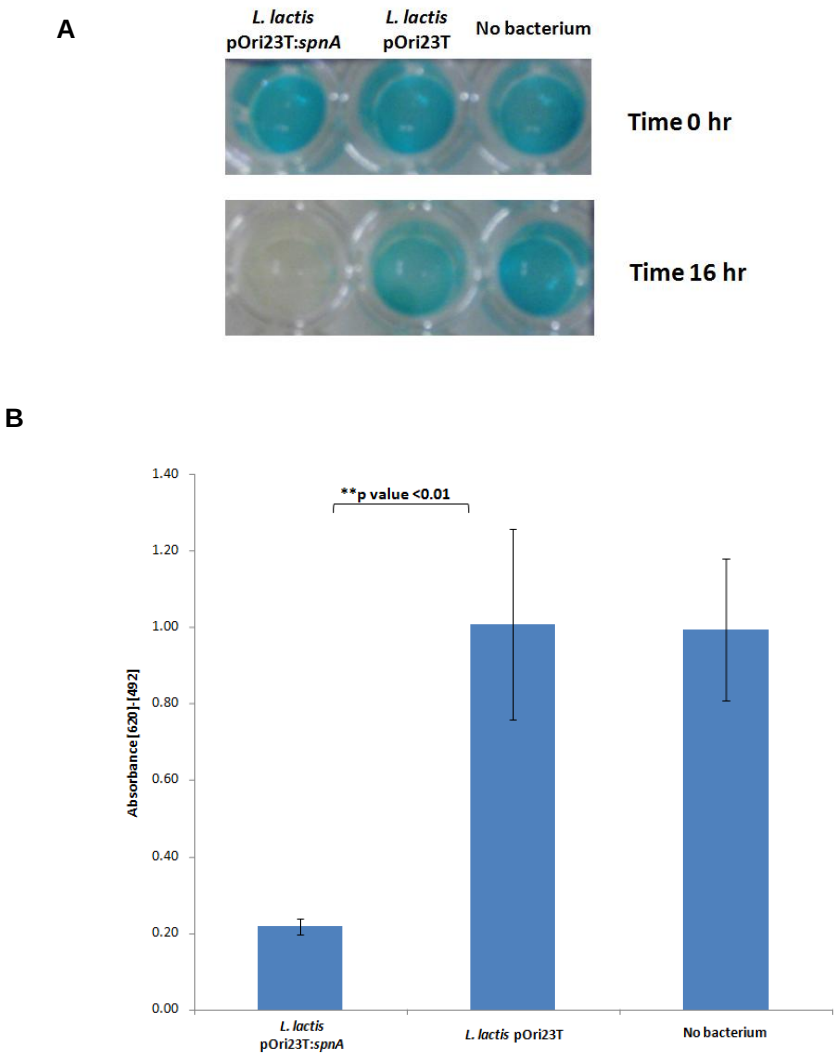

Figure 4.4 Nuclease activity analysis of L. lactis expressed SpnA

A. Methyl green when conjugated to double-stranded DNA produces a green colour. Decolorisation of methyl green was observed after incubation with *L. lactis* pOri23T:*spnA* for 16 hrs but not with the empty vector control. This indicates SpnA expressed by *L. lactis* has nuclease activity. The well that contained *L. lactis* pOri23T empty vector control appeared to have moderate decolorisation after 16 hrs in the picture; however, this was due to the accumulation of bacterial cells at the bottom of the well but not decolorisation of the reaction buffer.

B. The nuclease activity of *L. lactis* pOri23T:*spnA* was quantified by the absorbance reading at 620 nm (subtracting the basal reading at 492 nm). Gain-of-funciton mutant *L. lactis* pOri23T:*spnA* has 5-fold decrease in absorbance reading compared to the negative control, whereas the pOri23T empty vector control showed similar absorbance level to the negative control. The result is representative of three independent experiments, and error bars show the standard deviation of the three experiments

4.2.2 Generation of GAS *spnA*-knockout and complement strain

4.2.2.1 The construction of GAS *spnA*-knockout mutant

The deletion of *spnA* gene in GAS M1 SF370 strain was achieved through a double crossover process that replaces the target *spnA* gene with an antibiotic resistance gene for selection. An *E. coli – S. pyogenes* shuttle vector, pFW11, was employed for the task. This vector has a spectinomycin resistance gene, *aad9*, flanked by two multiple cloning sites. The vector only replicates in *E. coli* but not GAS; thus GAS cells would not survive in the presence of spectinomycin if the crossover event was absent (Figure 4.5). DNA sequences 1 kb upstream (namely F1, bp -1000 to -1) and 960 bp downstream (F2, bp 2181 to +407) of *spnA* gene in the GAS M1 SF370 genome were amplified through PCR and inserted into the multiple cloning sites of pFW11 vector respectively, flanking the *aad9* gene. The F2 fragment contained part of the *spnA* gene. The original plan was to employ the region immediately downstream of *spnA* gene (bp +1 to +1000) as F2. However, this DNA fragment appeared to be toxic to *E. coli* cells and could not be cloned. The pFW11 plasmid containing F1 and F2 fragments was eletroporated into GAS M1 SF370 and double-crossover events were identified by spectinomycin selection.

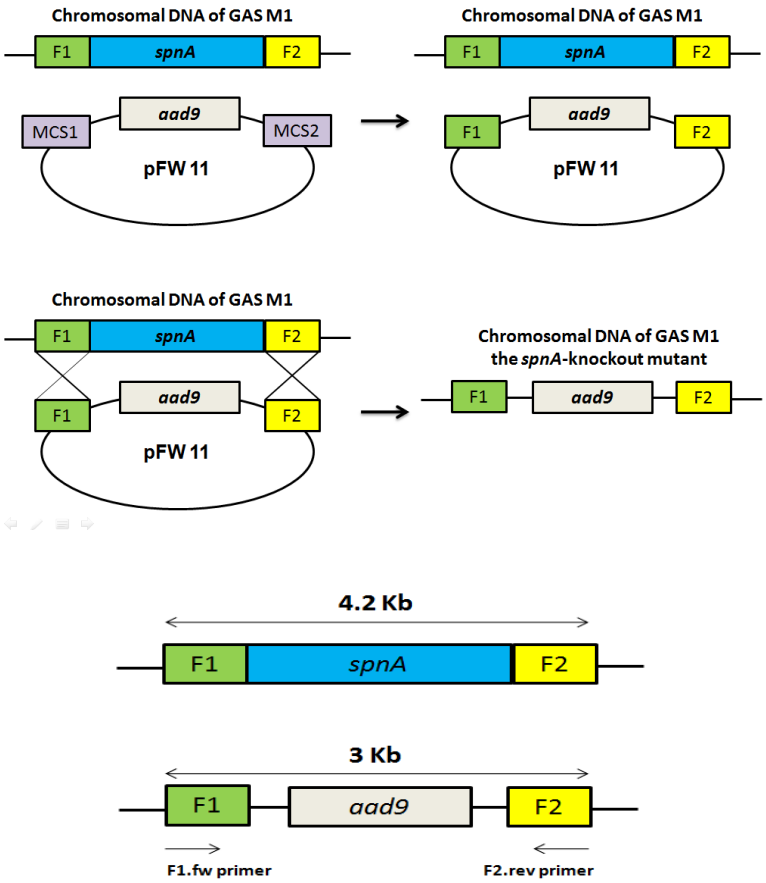

Figure 4.5 The gene replacement strategy for constructing GAS M1 spnA-knockout strain

The flanking regions of *spnA* gene in the GAS M1 SF370 genome were amplified and inserted into the multiple cloning sites (MCS1 and MCS2) of suicide vector pFW11, flanking the *aad9* gene. Double crossover event occurred when the plasmid was introduced into GAS M1, and *aad9* gene replaced *spnA* in the chromosome of GAS M1.

4.2.2.2 The construction of complement plasmid

The expression of SpnA was restored by reintroducing the *spnA* gene into the GAS M1 *spnA*-knockout strain through the vector pLZ12km2. The plasmid, pOri23T:*spnA*, was originally designed for the purpose of constructing the *L. lactis* gain-of-function mutant and the complementation in GAS M1 knockout strain. However, the plasmid was not taken up by GAS M1 *spnA*-knockout after several attempts for unknown reason; thus, pLZ12km2 vector was employed for such task.

The *spnA* gene and its ribosomal binding site were amplified from the genome of GAS M1 SF370, and inserted between *Xho*I – *Bam*HI sites in the multiple cloning site of vector pLZ12km2. The resultant plasmid was pLZ12km2:*spnA*. The vector carries a kanamycin resistance gene that allows antibiotic selection for bacteria that take up the plasmids successfully.

4.2.2.3 The growth rate of GAS M1 *spn*A-knock out and the complement strains

The growth rate of GAS M1 *spnA*-knockout and the complement strain, GAS M1::*spnA*, were compared with wildtype bacteria. Bacterial cells were grown in THY medium with appropriate antibiotics supplemented to *spnA*-knockout and complement strains. The *spnA*-knockout strain was observed to have moderate reduction in growth rate while the complement strain was further delayed in growth in comparison to the wildtype. This delayed growth observed in *spnA*-knock out and complement strain is possibly due to extra energy expenditure in antibiotic resistance and over expression of *spnA* gene in the complement strain (Figure 4.6).

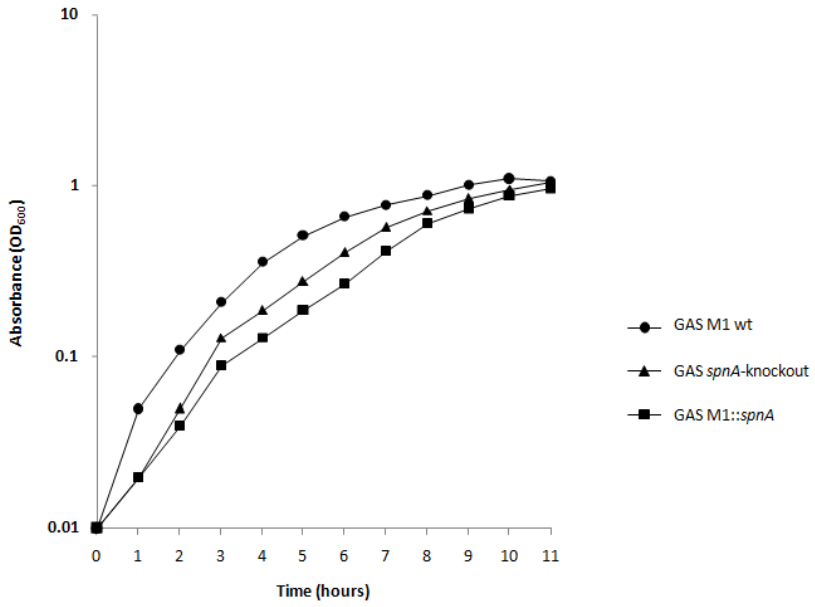

Figure 4.6 Growth of GAS M1 wildtype, spnA-knockout and the complement strain

The GAS M1 *spnA*-knockout strain displayed a moderately reduced growth rate comparing to wildtype, while the complement strain showed further delay in growth. The wildtype strain reached stationary phase 9 hrs after the inoculation.

4.2.2.4 Expression of SpnA in GAS M1 wildtype, *spnA*-knockout and the complement strain

Expression of SpnA on the surface of wildtype GAS M1 could be detected through flow cytometry analysis. Wildtype bacteria were collected at mid exponential (OD_{600} = 0.4-0.5), late exponential (OD600 = 0.7-0.8) and late stationary phase (OD600 = 1.2) of growth and labeled with rabbit multiclonal anti-SpnA antibodies followed by FITC-labeled anti-rabbit antibodies to analyse the expression of SpnA. Moderate expression of SpnA was found during the mid exponential phase and reached the highest level during late exponential phase. Bacteria collected at stationary phase displayed minimal level of SpnA on bacterial surface (Figure 4.7 A).

Furthermore, the absence of SpnA expression in *spnA*-knockout mutant and the subsequent restoration of expression on bacterial cell surface in GAS M1 complemented with the complete *spnA* gene (GAS M1::*spnA*) were also confirmed through flow cytometry analysis (Figure 4.7 B). Each bacterial strain was grown to late exponential phase in THY supplemented with appropriate antibiotics. The relative intensity of fluorescence of each bacterial strain revealed the complement strain expressed SpnA on cell surface in

similar quantity to the wildtype. The *spnA*-knockout had significantly lower fluorescence signal, which was close to basal reading, indicating the absence of SpnA expression.

Interestingly, trace amounts of SpnA were also discovered from the growth medium of GAS M1 wildtype and the complement strain. Growth medium of GAS M1 wildtype, *spnA*-knockout, and GAS M1::*spnA* were collected at late exponential phase and precipitated by TCA for Western Blot analysis. Multiple bands from growth media of the wildtype and complement strain were picked up by rabbit multiclonal anti-SpnA antibodies, this might be caused by protein degradation during sample preparation and precipitation. The result suggests the cell wall anchored SpnA might be cleaved off from bacterial surface during growth. There was no expression of SpnA found from the supernatant of *spnA*-knockout strain (Figure 4.7 C).

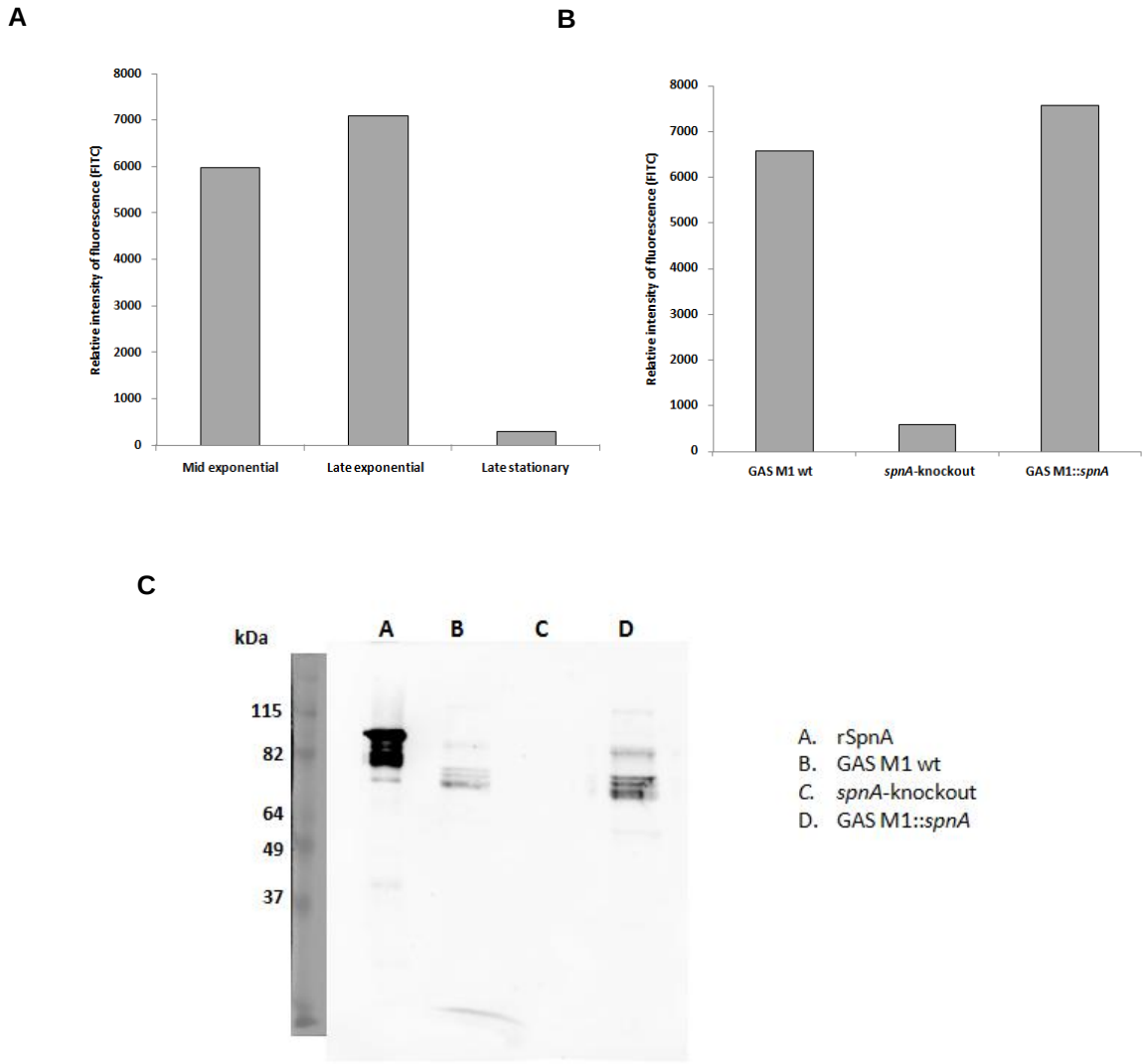

Figure 4.7 Expression of SpnA in GAS M1 wildtype, spnA-knockout and complement strain

A. Expression of SpnA on the surface of GAS M1 wildtype at different growth phase was analysed through flow cytometry analysis. SpnA expression occurred during mid exponential phase and reached peak levels during late exponential phase, whereas bacteria at stationary phase did not display SpnA on the cell surface.

B. The expression of SpnA in *spnA*-knockout and GAS M1::*spnA* were also detected through flow cytometry analysis. The knockout strain had basal level of signal for SpnA expression, while GAS M1::*spnA* had similar SpnA expression to the wildtype.

C. Western Blot of TCA precipitated (100x) growth supernatant from GAS M1 wildtype, *spnA*-knockout, and GAS M1::*spnA* showed that SpnA could be found from the supernatant of wildtype M1 and the complement GAS M1::*spnA* but not the *spnA*-knockout strain. Recombinant SpnA (10 ug) was used as the positive control.

4.2.2.5 Nuclease activity test for GAS *spnA*-knockout mutant in comparison to the parental strain

The nuclease activity of GAS *spnA*-knockout mutant was analysed in a methyl green-DNA nuclease activity assay and compared to GAS M1 wildtype. Bacterial cells were grown to late exponential phase and washed before being incubated with methyl green conjugated salmon sperm DNA for 16 hours. Both GAS *spnA*-knockout mutant and GAS M1 wildtype decolorized the methyl green-DNA reaction buffer after the incubation. The decolorization event was quantified, showing the *spnA*-knockout mutant had nuclease activity at a similar level to the parental strain as both of them reduced the absorbance of reaction buffer by about 10-fold in comparision to the negative control (Figure 4.8). This result suggests GAS M1 SF370 has more than one DNase, and the elimination of SpnA expression does not have great impact for the overall nuclease activity of the bacterium.

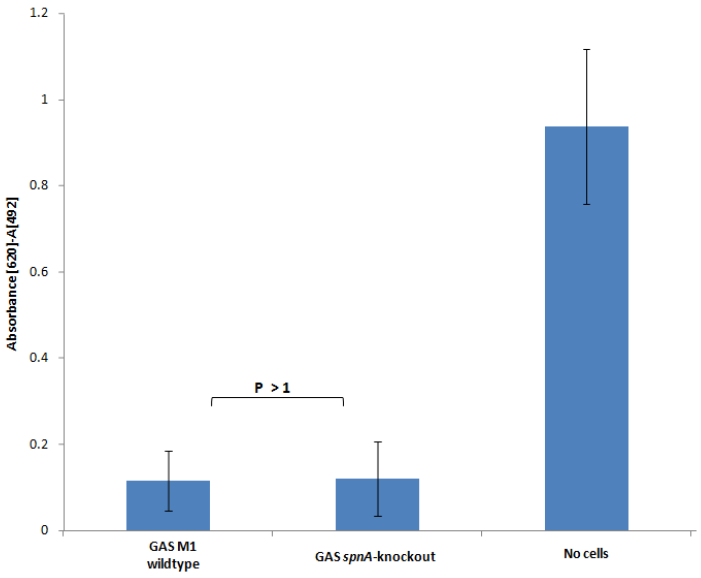

Figure 4.8 Nuclease activity analysis of GAS spnA-knockout mutant in comparison to GAS M1 wildtype

The nuclease activity of GAS *spnA*-knockout mutant and the M1 wildtype were quantified by the absorbance reading at 620 nm (subtracting the basal reading at 492 nm). The nuclease activity of *spnA*-knockout mutant was at similar level to GAS M1 wildtype. Both GAS *spn*A-knockout mutant and GAS M1 wildtype reduced the absorbance of reaction buffer by around 10-fold in comparision to the negative control. The result is representative of three independent experiments, and error bars show the standard deviation of the three experiments

4.3 Discussion

As GAS secretes four types of DNases that might have overlapping activities, the study of SpnA's effect on pathogenesis in GAS was made difficult if SpnA could not be separated from other streptococcal DNases. In order to examine the activities of SpnA in isolation, the gene was heterologously expressed in the non-pathogenic Gram-positive bacterium *L. lactis* which has a Sortase A-cell wall protein anchoring system similar to that in GAS (Dieye et al., 2010), and has no DNase expression. In the study by Kurupati *et al*, a *L. lactis* mutant that heterologously expresses the GAS cell wall-anchored chemokin-cleaving SpyCEP protein was able to cause dramatic systematic illness in mice within 24 hr in contrast to its avirulent parental strain (Kurupati et al., 2010). These results support *L. latics* as a suitable heterologous expression system for the study of SpnA's role in virulence.

The construction of a pOri23T plasmid containing *spnA* gene was described in this chapter. The lactococcal shuttle plasmid was designed to express cell wall-anchored SpnA that represents SpnA in its native status. SpnA is constitutively expressed in *L. lactis* under the control of P23 promoter in pOri23T vector (Que, Haefliger, Francioli, & Moreillon, 2000). Expression of SpnA was detected in the cell wall fraction of *L. lactis* pOri23T:*spnA* through Western Blotting analysis. The nuclease activity of *L. lactis* expressed cell wall-anchored SpnA was examined in a methyl green-DNase activity assay, in which lactococcal SpnA protein actively degraded DNA molecule and resulted in dissociation and decolorization of methyl green.

Hasegawa *et al* has previously shown that deleting *spnA* gene would result in reduction in overall virulence of GAS and the knockout mutant failed to cause substantial skin lesion in contrast to wildtype GAS. In this chapter, a GAS M1 *spnA* isogenic knockout mutant was also constructed in addition to the *L. lactis* gain-of-function mutants to study the role of SpnA in GAS virulence. The *spnA*-deletion mutant was constructed through allelic replacement method, replacing *spnA* gene with spectinomycin resistance gene *aad9* in a double crossover event, to minimize possible downstream polar effect. SpnA expression was restored through a plasmid, pLZ12Km2:*spnA*.

Expression of SpnA on the surface of wildtype GAS M1 was confirmed through flow cytometry analysis, with moderate expression level at mid exponential phase (OD_{600} = 0.4) and highest level during late exponential phase (OD_{600} = 0.8) while minimal level of SpnA was found during late stationary phase (OD600 = 1.2). The level of SpnA expressed on the surface of the complement strain was comparable to the wildtype as confirmed through flow cytometry analysis. Interestingly, the protein was also detected

from the growth medium of both wildtype and the *spnA*-complement strain. This phenomenon was also described in the report by Hasegawa *et al* (Hasegawa et al., 2010). The GAS and *L. lactis* mutants generated in this chapter could assist further understandings in the mechanisms of SpnA in contributing to virulence.

The evidence of Spy0747/SpnA expression in GAS strains was first reported by Reid *et al* (Reid et al., 2002), in which antibodies specifically bound to this protein were detected in 87 % convalescent sera collected from patients with GAS diseases (with 27 invasive and 4 non-invasive infections). The report included 19 representative M protein serotypes. This result implies this protein is produced by majority of GAS serotypes tested in this report during infection, suggesting SpnA might play a role during GAS infection. Transcription of *spnA* at various growth phases of GAS M1, M3 and M18 was also investigated through TaqMan analysis looking at the RNA level of *spnA*. Reid and colleagues found highest *spnA* transcription level during late exponential phase (OD_{600} = 0.8) in M1 and M3 serotypes, while M18 displayed highest *spnA* transcription during early exponential phase (OD_{600} = 0.4) (Reid et al., 2002). The TaqMan analysis of *spnA* in this report coincided with our findings as we have shown the expression of SpnA peaks during late exponential phase of bacterial growth. However, the study did not look into the function or the surface localisation of this protein.

The expression and surface-association of Spy0747/SpnA was later confirmed by the work of Rodriguez-Ortega *et al* and Severin *et al* (Rodriguez-Ortega et al., 2006; Severin et al., 2007). Whole GAS M1 SF370 cells were subjected to direct digestion by trypsin to release surface exposed proteins in these two reports, and the resultant protein peptides were analyzed through mass spectrometry to identify proteins. Peptides of SpnA were detected in both reports confirming the expression as well as the surface localisation of SpnA (Rodriguez-Ortega et al., 2006; Severin et al., 2007).

The recent work by Hasegawa and colleagues identified SpnA protein not only from the bacterial surface of GAS M1 SF370, but also from the growth supernatant of the bacterium through 2-dimentional gel electrophoresis and peptide mass mapping analysis (Hasegawa et al., 2010). This finding suggests SpnA might be expressed as a cell wall-anchored protein through its Gram-positive LPKTG sortase A recognition motif and later being cleaved off from surface by bacterial protease such as SpeB. Some streptococcal surface virulence factors, including C5a peptidase and M protein, undergo similar regulation process during the course of bacterial growth and infection (Nelson et al., 2011; Rasmussen & Bjorck, 2002). Accumulation of virulence factors in high concentrations on bacterial surface might provide the organism a

better chance to adhere to host cells through adhesins and to survive the host immune responses by inhibiting components from immune system at the beginning of a streptococcal infection. At later stages of infection, degradation or release of these bacterial surface-associated proteins might allow bacterial dissemination from sites of infection and could neutralise immune effectors at a distance from the bacterium.

Chapter 5
Functional Analysis of SpnA in Evading Host Innate Immune System

5.1 Introduction

The interesting finding of nuclease activity in recombinant SpnA protein and its destructive effect on the innate immune antimicrobial mechanism, by destruction of NETs, leads to the speculation that SpnA might contribute to the virulence of GAS by mediating evasion of host immune defense. In order to investigate the importance of SpnA to the virulence of GAS and the mechanisms it employs to achieve so, a GAS M1 isogenic *spnA*-knockout mutant and a *spnA*-complement strain was constructed. The *spnA* gene was also introduced into and expressed in non-pathogenic Gram-positive bacterium *L. lactis* to investigate the contribution of SpnA to virulence in isolation from other virulence factors and DNases.

Neutrophils have long been recognized for their crucial role in the immediate immune defense response against microbial invasion through phagocytosis and the subsequent intracellular killing of microbes. It has recently been discovered that neutrophils have extracellular defense mechanism via the production of NETs (Brinkmann et al., 2004). The nuclear DNA composed fibrous structure of NETs traps microbes and prevents bacterial dissemination from initial infected regions, while the antimicrobial proteins attached to the DNA backbone kill or inhibit microbes (Brinkmann et al., 2004). The efficiency of NET's antimicrobial activities is highly dependent on its structure to immobilize microbes and to create an environment with high concentrations of antimicrobial components that have direct access to trapped microbes. Bacteria, which includes *S. aureus*, *S. pneumoniae* and GAS, expressing DNases that degrade the DNA network of NETs are evidently more potent to establish infections in host than their isogenic DNase-knockout mutants (Beiter et al., 2006; Berends et al., 2010; Buchanan et al., 2006; Sumby et al., 2005). This chapter outlines the functional analysis of SpnA through *in vitro* killing assays to investigate if expression of SpnA could promote bacterial survival.

To extend the understanding in how the expression of SpnA could influence the virulence of GAS and the course of infection *in vivo*, a streptococcus-zebrafish embryo infection model was established. Zebrebrafish has become the interest of research for studies on host-pathogen interactions and the development of immune system in recent years (Allen & Neely, 2010; Meijer & Spaink, 2011). The

well-developed immune system of zebrafish has many commonalities with the human immune system (Meijer & Spaink, 2011). This, together with its small size and rapid generation time, made zebrafish an attractive tool to study pathogen virulence. This chapter outlines the survival assay of zebrafish embryos infected with GAS and *L. lactis* strains expressing SpnA in comparison to the strains without SpnA expression to analyse the effect of SpnA in bacterial virulence during the course of infection.

5.2 Result

5.2.1 SpnA expression promotes bacterial survival in *in vitro* killing assays

The ability of SpnA in promoting bacterial survival was investigated in *in vitro* killing assays. GAS and *L. lactis* strains expressing SpnA were incubated with human whole blood or NETs produced by PMA-induced human neutrophils to assess their survival rates in comparison to the strains without SpnA expression.

5.2.1.1 SpnA expression promotes bacterial survival in human whole blood

GAS M1 *spnA*-knockout mutant was subjected to a whole blood killing assay to assess its survival in comparison to the parental GAS strain. Approximately 1000 cfu of each bacterial strain was mixed with heparinized human whole blood. Samples were taken at specific time points and plated for enumeration and calculation of survival rate.

Almost half of the GAS M1 wildtype bacteria were killed during the first 30 min of incubation. However the *spnA*-knockout mutant showed a significantly lower survival rate, 9.63 %, compared to the wildtype ($P <$ 0001) (Figure 5.1 A). The growth of GAS M1 wildtype subsequently recovered during the second 30 min time interval that the survival rate had increased to around 85 % from 50 %, while at the end of the 2 hr assay the total cfu of the wildtype strain had a 6.5-fold increase compared to the initial bacterial count. In contrast, the number of bacteria in the *spnA*-knockout strain was not restored from the initial decrease and the survival rate was constantly below 10 % throughout the assay (Figure 5.1 A).

To further demonstrate that the enhanced survival rate in blood was due to SpnA expression, the survival rate of *L. lactis* gain-of-function mutant expressing SpnA was also examined in this assay together with *L. lactis* pOri23T as the negative control. Both the gain-of-function mutant and the negative control were mostly killed during the 2 hr assay, yet the pOri23T empty vector control was killed more efficiently than the mutant *L. lactis* pOri23T:*spnA*. Without SpnA expression, the *L. lactis* pOri23T empty vector control

showed about 10 % survival after 90 min and < 5 % after 2 hr incubation with blood, compared to *L. lactis* pOri23T:*spnA*, which showed survival rate of > 40 % after 90 min and about 20 % after 2 hr ($P < 0.001$) (Figure 5.1 B).

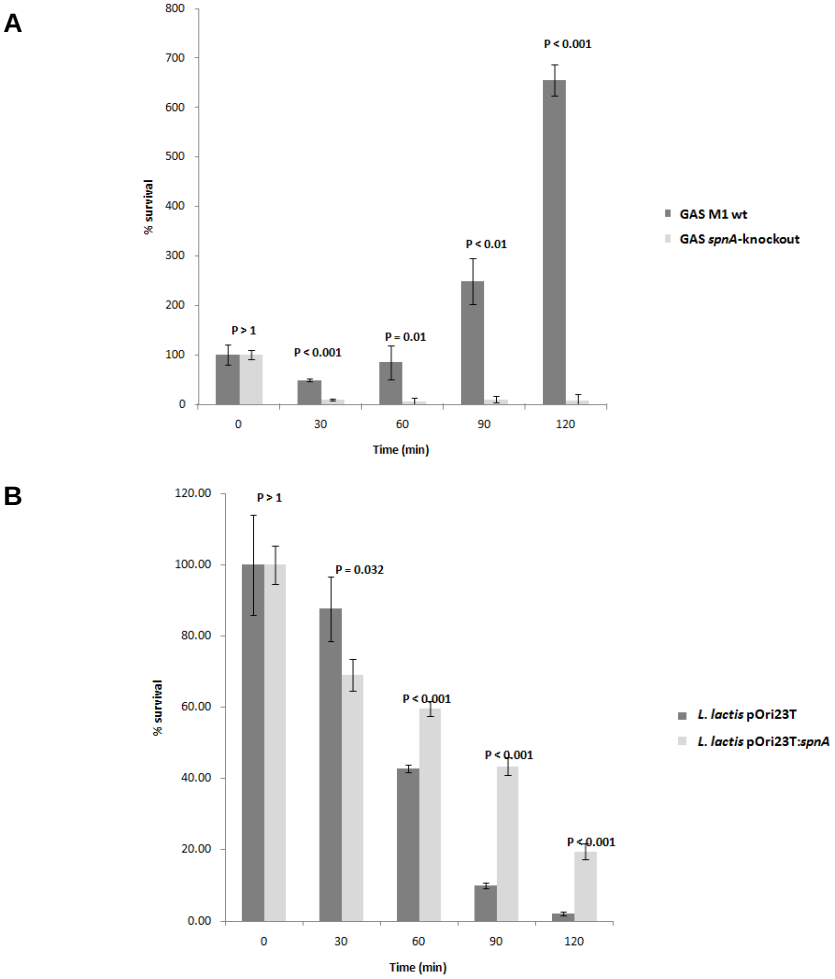

Figure 5.1 SpnA promotes bacterial survival in human whole blood

A. Human whole blood killing assay with GAS, where 1 mL of blood was inoculated with 1000 cfu of bacteria in each group. The *spnA*-knockout mutant exhibited a significantly reduced survival rate comparing to GAS wildtype. Survival rate of the knockout strain remained below 10 % throughout the 2 hr experiment, while parental wildtype GAS had a 6.5-fold increase in growth.

B. Human whole blood killing assay with *L. lactis,* where 1 mL of blood was inoculated with 1000 cfu of bacteria in each group. *L. lactis* pOri23T:*spnA* presented an enhanced ability in resisting killing by whole blood comparing to the *L. lactis* pOri23T empty vector control. While majority of both bacterial strains were killed over the 2 hr incubation with whole blood, the killing of *L. lactis* pOri23T:*spnA* was less efficient than the negative control. Survival rate of *L. lactis* pOri23T:*spnA*, at around 20 %, was significantly higher than the negative control, at less than 5 %.

The result is representative of three independent experiments, and error bars show the standard deviation of the three experiments. No antibiotics were used in these assays.

5.2.1.2 SpnA expression promotes bacterial survival in NET killing assay

An *in vitro* NET killing assay was set up to investigate if SpnA expression promotes bacterial survival. Freshly isolated human neutrophils were treated with PMA to induce NET production. GAS M1 wildtype and *spnA*-knockout mutant were incubated with PMA-stimulated neutrophils for 1 hr in the presence of cytochalacin-D which blocked phagocytosis. Bacterial samples were diluted and plated for calculating the survival rate. The parental GAS M1 strain was found significantly more resistant to NET killing than the isogenic *spnA*-knockout mutant. GAS M1 wildtype strain had a 150 % growth during the 1 hr incubation, whereas only about 30 % of *spnA*-knockout survived the assay ($P < 0.001$) (Figure 5.2 A)

Similarly, the *spnA*-expressing *L. lactis* mutant showed an enhance survival rate compared to the pOri23T empty vector control when both strains were subjected to this assay. Almost 100 % of *L. lactis* pOri23T:*spnA* survived the 1 hr incubation with PMA-induced NETs, while the *L. lactis* pOri23T empty vector control had a less than 30 % survival rate ($P = 0.01$) (Figure 5.2 B).

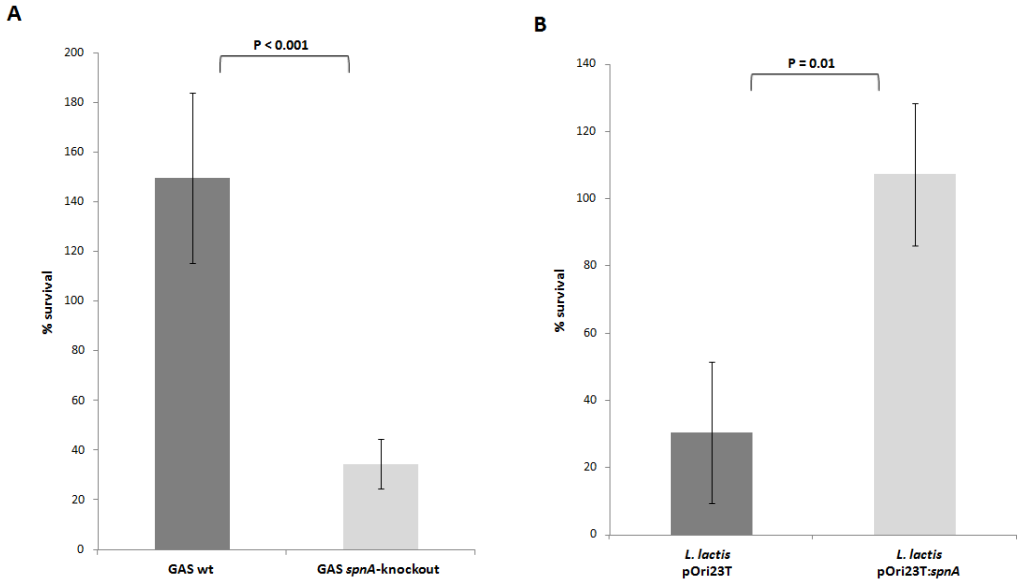

Figure 5.2 SpnA expression promotes bacterial survival against killing by NETs

A. NET killing assay with GAS wildtype and *spnA*-knockout (MOI = 2). GAS wildtype and *spnA*-knockout mutant were incubated with NETs produced by PMA-induced human neutrophils for 1 hr. The knockout mutant displayed a significantly lower survival rate at around 30 % than the wildtype, which had a 150 % increase in growth.

B. NET killing assay with *L. lactis* pOri23T:*spnA* and pOri23T empty vector (MOI = 2). The *L. lactis* gain-of-function mutant was resistant to NET killing with the additional expression of SpnA than the pOri23T empty vector control. Almost 100 % of *L. lactis* pOri23T:*spnA* mutant survived the assay, while survival rate of the negative control was around 30 %.

The result is representative of three independent experiments, and error bars show the standard deviation of the three experiments. No antibiotics were used in these assays.

5.2.1.3 The enhanced bacterial survival rate with SpnA expression was directly related to NET destruction

An *in vitro* NETs destruction assay was designed to confirm the enhanced bacterial survival rate was due to the destruction of the extracellular structure NETs. Bacterial strains were incubated for 1 hr with NETs produced by PMA-induced human neutrophils in the presence of cytochalacin-D, which inhibits phagocytosis. Sytox orange, a membrane non-permeable DNA dye, was added after the 1 hr incubation to stain for extracellular DNA, which could be quantified by measuring the fluorescence at Ex/Em, 530/590 nm.

Addition of PMA to human neutrophils stimulated the production of NETs, thus an increase from around

1400 FU to about 2000 FU (P < 0.001) was observed (Figure 5.3). Although addition of bacteria to PMA-stimulated neutrophils resulted in a further increase in fluorescence reading, the amount of extracellular DNA was significantly lower with GAS wildtype, around 2800 FU, compared with the GAS *spnA*-knockout mutant, around 3700 FU (P < 0.0001) (Figure 5.3). Similarly, incubation with SpnA-expression *L. lactis* pOri23T:*spnA* mutant resulted in a large drop of extracellular DNA, around 2500 FU, compared with the pOri23T empty vector control, around 3300 FU (Figure 5.3). These results suggest SpnA mediates NET destruction and possibly promotes bacterial survival through such mechanism.

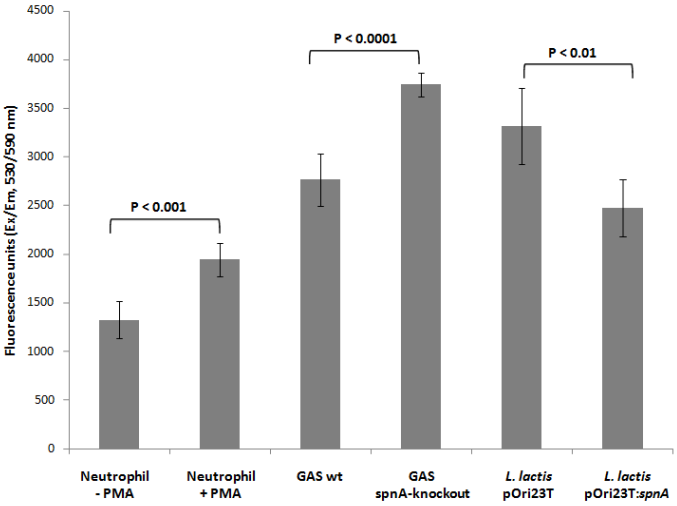

Figure 5.3 SpnA expression is correlated with NET destruction

The extracellular DNA was quantified by Sytox orange stain. NET destruction correlates with the expression of SpnA and an increased survival rate in the neutrophil killing assay. Addition of PMA to neutrophils significantly increased the fluorescence level, indicating the production of NETs. Addition of bacterial cells to PMA-induced neutrophils further promoted the production of extracellular DNA, resulted in an additional increase in fluorescence. The amount of extracellular DNA detected in the wells containing GAS wildtype was significantly less compared to the *spnA*-knockout mutant. The amount of extracellular DNA detected in the wells containing *L. lactis* pOri23T:*spnA* was significantly less than the *L. lactis* pOri23T empty vector control. These results indicated that SpnA degrades NETs and such degradation correlated with enhanced bacterial survival. The error bars represented the standard deviation of three independent experiments.

5.2.2 Zebrafish embryo as an infection model for analysing the effect of SpnA in virulence

A zebrafish embryo infection model was developed to investigate the role of SpnA in immune evasion *in vivo*. The survival rate of zebrafish embryo were analysed after being infected with GAS and *L. lactis* strains expressing SpnA in comparison to the strains without SpnA expression.

5.2.2.1 Establishment of sufficient GAS dose to initiate infection in zebrafish embryo

To determine the optimal dose of GAS required to induce a moderate infection in zebrafish embryos, GAS wildtype was titrated and injected into the hindbrain region of the embryo to initiate a local infection (n = 30 for each dose) (Figure 5.4 A).

The majority of embryos (63 %) injected with 1 cfu GAS wildtype did not develop infection leading to mortality 4 days post infection (Figure 5.4 B). The group infected with 10 cfu GAS wildtype developed moderate infections and the survival of embryo declined gradually over the 4-day experimental period, with about 60 % surviving 1 day post infection and gradually reducing to 12 % at the end of the experiment (Figure 5.4 B). The wildtype GAS at 100 cfu and 1000 cfu had similar effect on embryos and around 80 % of embryos were killed 24 hrs post infection (Figure 5.4 B). Therefore, the optimal dose was determined to be 10 cfu and was used for subsequent experiments.

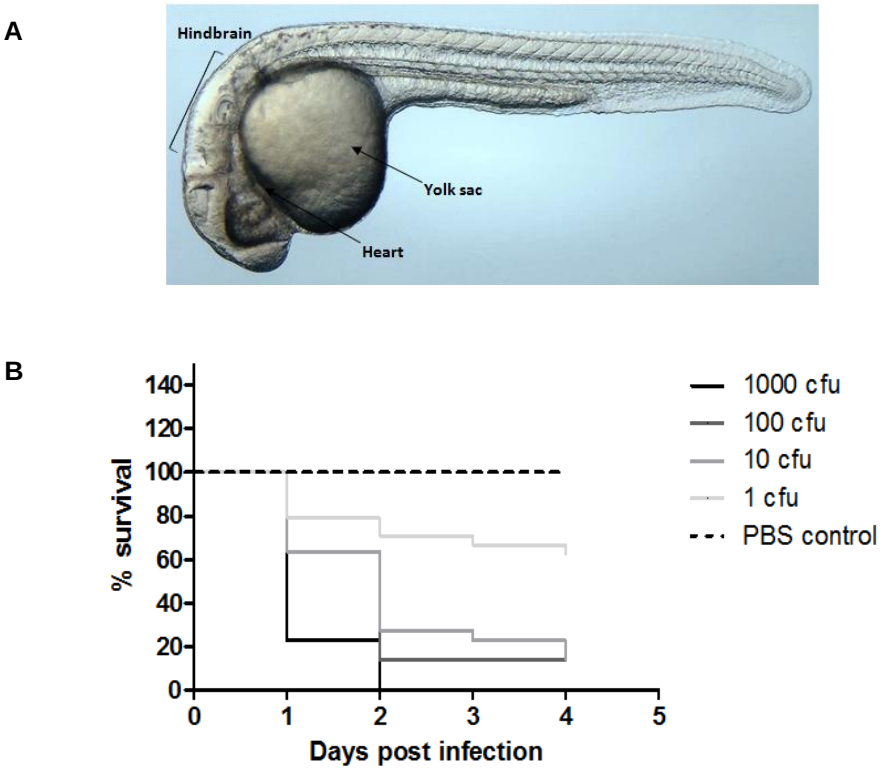

Figure 5.4 Establishment of a streptococcus-zebrafish embryo infection model

A. The histology of zebrafish embryo at 2 dpf. Zebrafish embryos were injected with GAS wildtype and mutant strains through the hindbrain region to generate a local infection.

B. A bacterial dose titration of GAS wildtype in zebrafish embryo (n = 30 for each dose). At >100 cfu, embryos were overwhelmed by GAS and acute lethality was observed 1 day post infection. Embryos infected with 10 cfu GAS wildtype generated infection that had moderate progression.

5.2.2.2 Analysis of SpnA's effect on GAS virulence in zebrafish embryo infection models

To investigate how the expression of SpnA promotes GAS survival in host through mediating immune evasion, thus allowing establishment of lethal infection, zebrafish embryos (n = 30 for each bacterial strain) were injected with 10 cfu of either GAS wildtype, the isogenic *spnA*-knockout mutant or the *spnA*-complemented strain. The survival of embryos was recorded over the 4-day experimental period.

The survival rate of the embryos injected with 10 cfu GAS wildtype was similar to the group injected with the *spnA*-knockout mutant, at around 70 %, 24 hr after the injection (Figure 5.5). However, the group infected with wildtype GAS developed a higher mortality rate than the group infected with *spnA*-knockout mutant 2 days post infection and for the remaining days of the experiment. The survival rate of embryos infected with GAS wildtype declined to around 35 % 2 days after infection and further reduced to around 20 % at the end of the observation period; whereas the knockout mutant infected embryos had about 50 %

survival rate 2 days post infection and around 45 % survived at the end of the experiment (Figure 5.5). The Log-rank test showed a *P*-value of 0.023 between the two groups, suggesting there is a moderate difference between the survival rates of the two groups. The *spnA*-complemented strain showed a slightly delayed onset of infection, about 52 % of embryos were alive 2 days after infection (Figure 5.5). Yet, the mortality rate of the embryos infected with the *spnA*-complemented strain had a drop 3 days post infection, from 52 % to 30 %, and further declined to 25 % at the end of the observation period, which was similar to the survival rate of embryos infected with GAS wildtype (Figure 5.5). The Log-rank test showed no significant difference between the group infected with GAS wildtype and the group with *spnA*-complement strain. The result is representative for two independent experiments.

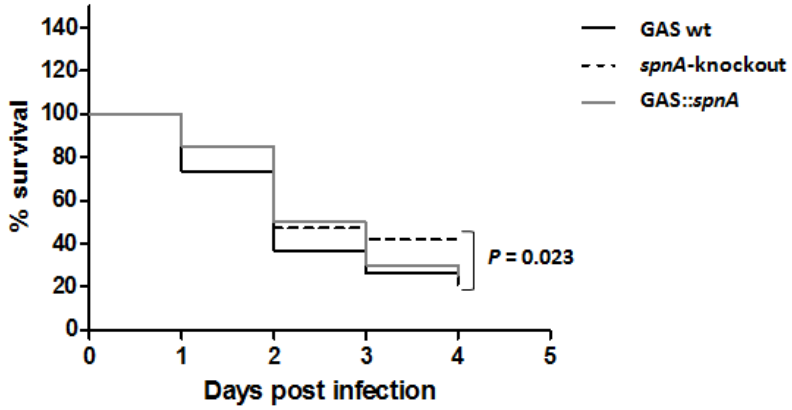

Figure 5.5 Zebrafish embryo survival assay with GAS wildtype and mutants

GAS wildtype and *spnA*-knockout were injected into two groups of embryos respectively and the survival of embryos was monitored over 4 days (n = 30 for each bacterial strain). The pattern of survival curve for both groups appeared similar in the first two days, but the group infected with *spnA*-knockout strain had a slightly higher survival rate at around 45 % than the GAS wildtype group at 20 %.

5.2.2.3 Establishment of sufficient *L. lactis* pOri23T:*spnA* dose to initiate infection in zebrafish embryo

A zebrafish embryo – *L. lactis* infection model was established to investigate if the expression of SpnA could promote the survival of non-pathogenic *L. lactis* in the host and lead to mortality in embryos. The *L.lactis* gain-of-function mutant displayed an enhanced survival ability in human blood and in presence of NETs, therefore the survival rate of zebrafish embryos infected with *L. lactis* pOri23T:*spnA* would be used as the baseline in comparison to the group infected with pOri23T empty vector control to analyse the effect of SpnA. Three doses of *L. lactis* pOri23T:*spnA* were given to zebrafish embryos through the hindbrain region (n = 30 for each dose) to determine the minimal dose required for infection in zebrafish embryos that produces a gradual decrease in survival rate over the 6-day observation period.

The three bacterial doses tested gave similar effect on the survival rate of zebrafish embryos. There was no mortality observed in the first 2 days of infection, and less than 10 % of embryos were killed 3 days post infection (Figure 5.6). The survival rate declined gradually between day 4 and day 6, and about 40 % of embryos survived at the end of the experiment in all three groups (Figure 5.6). As all three bacterial doses a produced similar effect on the survival rate of zebrafish embryo, the lowest bacterial dose, 15 cfu, was selected for further experiment in the *L. lactis* – zebrafish embryo infection model.

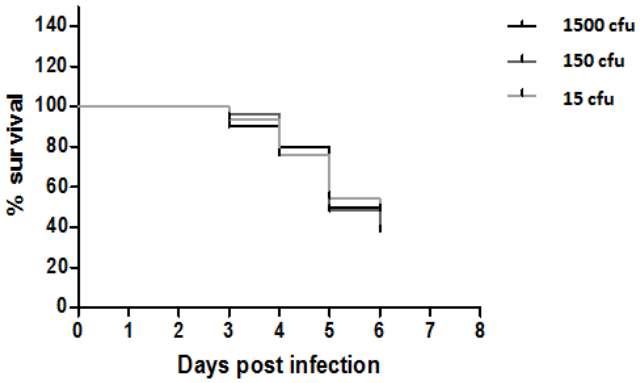

Figure 5.6 A titration of L. lactis pOri23T:spnA in zebrafish embryo infection model

Three bacterial doses were tested to determine the optimal dose for the establishment of lethal infection in zebrafish embryos (n = 30 for each dose). All three doses, 1500, 150 and 15 cfu of *L. lactis* pOri23T:*spnA* gave similar effect on the survival rate of embryos. No mortality was observed during the first 2 days of infection, with more than 90 % survived the first 3 days. Gradual decline in survival was observed between day 4 and day 6 post infection that the survival rate decreased from around 80 % to 40 %.

5.2.2.4 Analysis of SpnA's effect on *L. lactis* virulence in zebrafish embryo infection model

Zebrafish embryos (n = 30 for each bacterial strain) were infected with 15 cfu of either *L. lactis* pOri23T:*spnA* gain-of-function mutant or the *L.lactis* pOri23T empty vector control through the hindbrain region and monitored for survival over 6 days.

There was no difference in the survival patterns observed between the two groups (Figure 5.7). Both group showed the first decrease in survival rate 3 days post infection, and had about 63 % of infected embryos were alive on the 6th day. The Log-rank test showed there was no statistically significant difference between the survival rate of these two groups (P = 0.52).

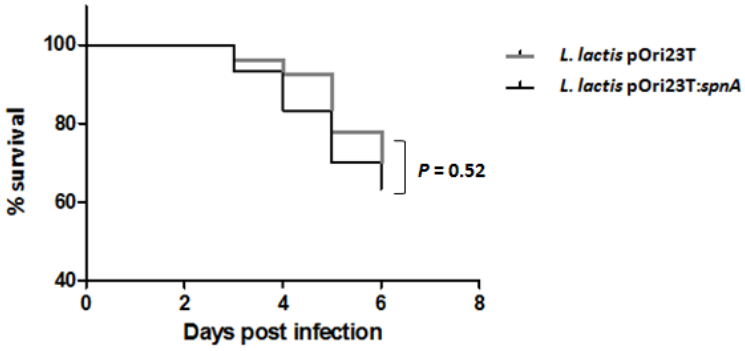

Figure 5.7 Zebrafish embryo survival assay with L. lactis pOri23T:spnA and pOri23T empty vector control

Zebrafish embryos were infected with *L. lactis* pOri23T:*spnA* or *L. lactis* pOri23T empty vector control respectively at 15 cfu and monitored for 6 days for embryo survival (n = 30 for each bacterial strain). The two groups had a similar pattern in the survival curve, with no statistically significant difference between the two. The result is representative for two independent experiments.

5.3 Discussion

In this chapter, the effect of SpnA on bacterial survival *in vitro* was investigated and a streptococcus-zebrafish embryo infection model was established to extend the investigation of SpnA's contribution to virulence *in vivo*. The findings of recombinant SpnA's ability in cleaving DNA fibrous network of NETs suggest the protein might have a role in evasion of host immune response which promotes bacterial survival in the host. Using a combination of GAS isogenic *spnA*-knockout mutant and a *L. lactis* gain-of-function mutant expressing SpnA, it was demonstrated that expression of SpnA promptly enhanced bacterial survival in human whole blood for both GAS and *L. lactis*. Similarly, the expression of SpnA in *L. lactis* pOri23T:*spnA* significantly delayed bacterial killing by whole blood when compared to the pOri23T empty vector control. These results indicate SpnA does play an important role in promoting bacterial survival in blood.

There are several factors that could contribute to the killing of bacteria in whole blood, including complement activation, antimicrobial peptides, phagocytosis and the release of reactive oxygen species (Segal, 2005). Several recent reports demonstrated a role of other bacterial DNases in destruction of NETs, including EndA of *S. pneumonia* (Beiter et al., 2006) and Sda1 of the hypervirulent GAS M1T1 strain (Buchanan et al., 2006). Animal models infected with the DNase-expressing bacteria in these studies tend to have poorer outcomes compared to the group infected with DNase-knockout mutants, suggesting antimicrobial activity of NETs is a crucial factor for limiting bacterial invasion. In the *in vitro* NET killing assay, it is evident that expression of SpnA significantly increases survival rate of bacteria when incubated with NET-producing neutrophils. The neutrophils were pretreated with cytochalasin D to prevent phagocytosis, thus bacterial killing observed was limited to extracellular mechanisms. SpnA expression and bacterial survival also correlated with destruction of extracellular DNA, which suggests that degradation of NETs might play a role in GAS immune evasion.

Interestingly, there was no significant difference between the overall nuclease activity of the GAS isogenic *spnA*-knockout mutant and the parental GAS strain, indicating the expression of other DNases. However, the enhanced bacterial survival rates in blood and NET killing assays were distinctively due to activities of SpnA suggesting SpnA's effect is non-redundant with other DNases. It is possible that GAS DNases are differentially expressed that an individual DNase only expresses at a certain growth phase or in a particular environment. Musser and colleagues analysed the complete transcriptome of GAS M1 strain MGAS5005 and found transcription of *spy0747* (*spnA*) had more than 3500-fold upregulation during first 30 min growth in human blood. The transcription level of *spnA* ranked at 404th among the GAS genes when the

bacterium was cultured in growth medium. The ranking of *spnA* transcription was elevated greatly to the 42nd place after 30 min of incubation in blood (Graham et al., 2005). In contrary, transcripts for the secreted DNases Sda1 and Spd3 were downregulated during that time by > 2000-fold and > 1000-fold respectively. This observation might suggest that SpnA has a role in interacting with host components as its expression is highly upregulated once the bacterium encounters blood.

A zebrafish embryo infection model for GAS and *L. lactis* was described in this chapter. Zebrafish has become the interest of research as infection model for studying host-pathogen interaction in recent years for its short reproduction time, small size, well-characterised genome sequence and the immune system which has much in common with human immune system. Adult zebrafish have fully developed adaptive and innate immune systems, whereas zebrafish embryos have only the innate immunity (Meijer & Spaink, 2011). The pathways of inducing transcriptional regulators and immune effectors are highly conserved between zebrafish and the human system as demonstrated by microarray and deep sequencing technology (Meijer & Spaink, 2011). As for innate immune system in zebrafish embryos, the central signaling pathways are developed and functional during infection in 1 dpf embryos (Aggad et al., 2010; Stockhammer, Zakrzewska, Hegedus, Spaink, & Meijer, 2009).

Neely and colleagues reported the first streptococcus-zebrafish infection model. The study focused on the pathogenesis of GAS and demonstrated the use of the adult zebrafish infection model for identification of GAS mutants with attenuated virulence (Neely, Pfeifer, & Caparon, 2002). The adult zebrafish infection model has since been employed in the identification of novel virulence determinants of GAS (Kizy & Neely, 2009) and in studies of other GAS virulence factors, including cytolytic toxin streptolysin S (Lin, Loughman, Zinselmeyer, Miller, & Caparon, 2009) and iron uptake transporter Siu (Montanez, Neely, & Eichenbaum, 2005). NETs production was previously observed in zebrafish neutrophils isolated from kidney, thus making zebrafish a possible infection model to investigate the effect of SpnA on bacterial virulence through destruction of NETs (Palic, Andreasen, Ostojic, Tell, & Roth, 2007).

Due to constrained facility in housing pathogen infected adult zebrafish, zebrafish embryos at 2 dpf were adopted as infection model in this project. Zebrafish embryos were injected with GAS or *L. lactis* mutant strains expressing SpnA for the investigation of SpnA's contribution in bacterial virulence in comparison to strains without SpnA expression. The *L. lactis*-zebrafish infection model did not present a clear difference between the virulence of *L. lactis* pOri23T:*spnA* and the empty vector control. It is not surprising to find such result as *L. lactis* is non-pathogenic and lacks virulence factors that promote bacterial invasion. With

the expression of SpnA, the *L. lactis* gain-of-function mutant might be able to resist the initial entrapment by NETs, but the organism has limited ability in causing further destructive damage.

A bacterial dose titration of GAS M1 wiltype in embryos revealed that at 10 cfu GAS per embryo could induce infection with moderate progression, allowing the observation of potential effects of SpnA in virulence during the course of infection. The survival of embryos infected with GAS *spnA*-knockout mutant shared a similar declining pattern with embryos infected with wildtype GAS in the first two days of infection. However, the embryos infected with *spnA*-knockout mutant exhibited a slightly higher survival rate than the positive control group, at 45 % and 20 % respectively, indicating the loss of SpnA expression correlated with attenuated virulence and ability to cause mortality in zebrafish embryos. The difference in survival rate between groups infected with *spnA*-knockout mutant and GAS wildtype strain indicates SpnA plays a role in virulence of GAS that promotes bacterial lethality in zebrafish embryos.

A similar but more prominent result was observed by Hasegawa and colleagues, GAS *spnA*-knockout mutant caused 10 % mortality rate in subcutaneously infected mice while the parental GAS strain killed 80 % of infected mice (Hasegawa et al., 2010). The zebrafish embryo infection model appeared to be less sensitive in detecting and presenting the attenuated virulence of the GAS *spnA*-knockout strain than the mouse subcutaneous infection model. This may be explained by the fact that zebrafish embryos lack mature adaptive immune system; thus the host is more susceptible to be overwhelmed by GAS, which is well-equipped with virulence factors specialized in evading immune responses and invading the host, than the murine infection model that has a matured innate and adaptive immune system. Effects of SpnA in virulence of GAS might be observed more prominently in adult zebrafish as the model provides a host immune defense system that resembles the human system more closely, and a wider range of infection routes are available for the study of SpnA activities in local and systematic infections.

Streptococcus iniae, could be used as an alternative pathogen to study the effect of SpnA in zebrafish embryos. *S. iniae* is a fish pathogen and it is a close relative to GAS. It is capable of infecting humans and cause illnesses that resemble GAS induced soft tissue infections (M. Weinstein et al., 1996; M. R. Weinstein et al., 1997). The genome of *S. iniae* was recently published and revealed the bacterium has a homolog of *spnA* gene with high similarity in the amino acid sequences (69.8 %, sequence alignment in Appendix I). The effect of SpnA could be further investigated in zebrafish embryo model through the infectious agent *S. iniae* and its SpnA homolog.

Chapter 6

The Structural and Mutational Analysis of SpnA

6.1 Introduction

The conserved Gram-positive cell wall sorting motif, LPKTG, and the predicted cell wall anchorage domain encoded by spy0747/spn hinted the gene might encode for a surface associated protein. The cell wall localisation renders the encoded protein an advantage in interacting with host components in close proximity. The predicted cell wall localisation of SpnA was the first indication for its possible role in GA*S* virulence. SpnA was later confirmed for its cell wall localisation (Rodriguez-Ortega et al., 2006) (Severin et al., 2007) and nuclease activity (Chang et al., 2011; Hasegawa et al., 2010), making it the only surface-associated nuclease indentified in GAS thus far. The contribution of SpnA in enhancing bacterial survival was evident in the *in vitro* killing assays by whole blood and NETs, as well as in the *in vivo* zebrafish embryo infection model (chapter 5). The cell surface localisation of SpnA allows accumulation of the protein at high concentrations on the surface for a joint activity. However, trace amounts of SpnA had also been recovered from the culture medium of GAS (Chapter 4, section 4.2.1.4), suggesting the protein might undergo modification or regulation by bacterial proteases, such as SpeB, after being covalently linked to the bacterial cell wall. Some cell wall linked virulence factors were able to function at a distance from bacterial cells after being cleaved off. The major virulence factors M protein, C5a peptidase and SpyCEP are examples of the phenomenon (Berge & Bjorck, 1995; Chiappini et al., 2012; Edwards et al., 2005; Wexler & Cleary, 1985). This chapter outlines the construction of a L. lactis gain-of-function mutant and a GAS complement strain that express secreted SpnA to investigate if the protein could promote bacterial survival in its secreted form.

The previous chapter demonstrated that GAS *spnA*-knockout mutant displayed a phenotype which was extremely susceptible to killing by blood and NETs *in vitro* compared to the parental strain. The work by Hasegawa and colleagues also provided similar finding in the murine infection model (Hasegawa et al., 2010). GAS is a potent pathogen that survives and causes life-threatening infections in host through the combined force from a large arsenal of virulence factors. Many virulence factors have overlapping functions that compensate each other. The observation of extensively reduced virulence in a strain lacking one single gene, *spnA*, led to the speculation that SpnA had more than one mechanism in contributing to virulence. Solving the structure of SpnA would allow identification of possible mechanisms of reaction, and further understanding in how SpnA contributes in virulence. This chapter outlines the computational analysis on the structure of SpnA.

6.2 Results

6.2.1 Construction of *L. lactis* mutant expressing secreted SpnA

6.2.1.1 Primer design and plasmid construction

A *L. lactis* mutant expressing secreted SpnA was constructed through the shuttle vector pOri23T in the method similar to the construction of *L. lactis* pOri23T:*spnA* mutant (chapter 4, section 4.2.1.1). Instead of introducing the entire *spnA* gene into pOri23T, the DNA fragment was truncated to exclude the region encoding for the LPKTG motif and the cell wall anchorage domain. The reverse primer, SpnAsec_LL.rev, was designed to bind to bp 2612 to 2628 of the gene, which is immediately prior to the region encoding for the LPKTG motif, and followed by an introduced stop codon, TAG (Figure 6.1). The DNA fragment was amplified from GAS M1 SF370 genome by PCR through the primer pair, SpnA_LL.fw and SpnAsec_LL.rev, and inserted between the *Bam*HI and *Xho*I site in the pOri23T vector. The resultant plasmid was named pOri23T:*spnA_sec.*

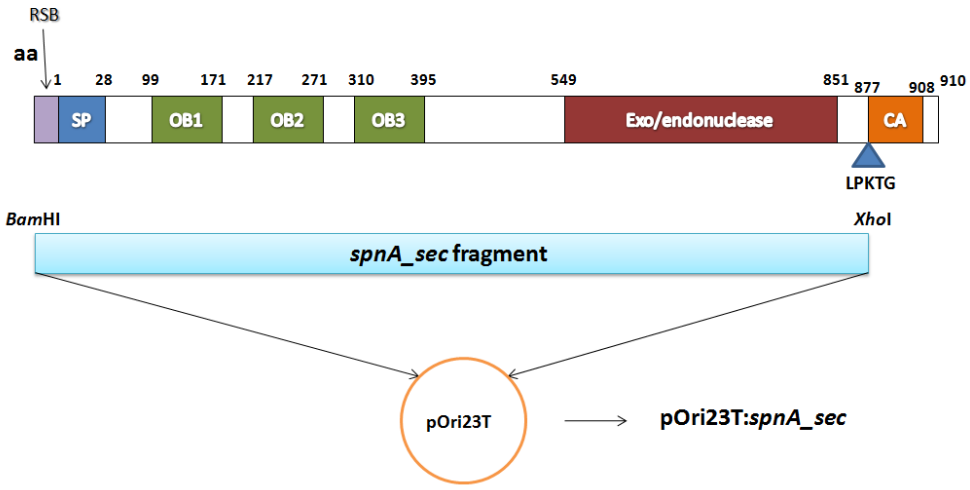

Figure 6.1 The construction of pOri23T:spnA_sec plasmid

A truncated DNA fragment was amplified from the *spnA* gene. The DNA fragment contains the RSB of *spnA* and ends immediately before the LPKTG cell wall anchoring motif with an introduced stop codon, TAG. The DNA fragment was named *spnA*_sec, and inserted into the pOri23T vector via *Bam*HI and *Xho*I sites in the MCS of the vector. The resultant plasmid is pOri23T:*spnA_sec*.

6.2.1.2 Analysis of expression and nuclease activity of secreted SpnA expressed by *L. lactis* pOri23T:*spnA_sec*

The expression of secreted SpnA by *L. lactis* pOri23T:*spnA_sec* mutant was first analysed in Western Blot. The growth medium of *L. lactis* pOri23T empty vector control and *L. lactis* pOri23T:*spnA_sec* were collected at late exponential phase (OD_{600} = 0.8 - 1.0), and precipitated by TCA. Expression of secreted SpnA in *L. lactis* pOri23T:*spnA_sec* mutant was detected through binding of polyclonal rabbit anti-SpnA antibodies, but no trace of SpnA was found in the medium of *L. lactis* empty vector control (Figure 6.2 A).

The nuclease activity of *L. lactis* pOri23T:*spnA_sec* was then analysed using the methyl green-DNase activity assay and compared to *L. lactis* empty vector control and *L. lactis* pOri23T:*spnA.* Each bacterial strain was grown to late exponential phase and collected for the reaction. The *L. lactis* pori23T:*spnA_sec* decolourized the methyl green-DNA substrate at similar levels to *L. lactis* pOri23T:*spnA*, indicating that the secreted SpnA in *L. lactis* pOri23T:*spnA_sec* had nuclease activity, while no nuclease activity was observed in *L. lactis* empty vector control (Figure 6.2 B).

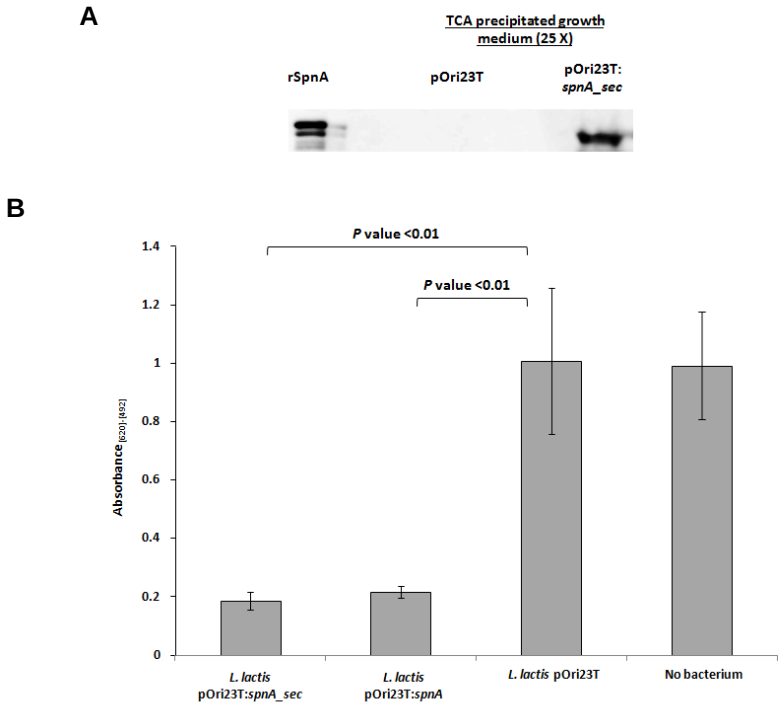

Figure 6.2 Analysis of the expression and nuclease activity of secreted SpnA in L. lactis pOri23T:spnA_sec

A. Western Blot of TCA precipitated culture medium of *L. lactis* pOri23T:*spnA_sec* for detection of secreted SpnA. Expression of secreted SpnA was detected in the TCA precipitated growth medium of *L. lactis* pOri23T:*spnA_sec* mutant through Western Blot analysis. No trace of SpnA was observed from the growth medium of the empty vector control. Recombinant full-length SpnA (0.5 ug) was used as positive control

B. The methyl green-DNase activity assay. Bacterial strains were incubated with methyl green-DNA substrate for 24 hrs. A reduction in absorbance indicated the presence of DNase activity. The secreted SpnA from *L. lactis* pOri23T:*spnA_sec* was nuclease active and decolourized the methyl green-DNA substrate at similar level to the cell wall anchored SpnA of *L. lactis* pOri23T:*spnA*. The *L. lactis* pOri23T empty vector control had no nuclease activity.

6.2.2 Construction of GAS M1 complement strain expressing secreted SpnA

6.2.2.1 The construction of pLZ12km2:*spnA_sec* plasmid

Expression of a secreted form of SpnA was constructed by introducing the a truncated version of *spnA* gene into GAS M1 *spnA*-knockout mutant via the pLZ12km2 expression system. A DNA fragment encoding for SpnA protein without the cell wall anchorage domain was amplified from the genomic DNA of GAS M1 and inserted between the *Xho*I and *Bam*HI sites in the pLZ12km2 vector. The resultant plasmid, pLZ12km2:*spnA_sec*, was employed for the making of the complement strain GAS M1::*spnA_sec*.

6.2.2.2 Expression of secreted SpnA was detected in the growth medium of GAS M1::*spnA_sec*

Growth medium of GAS M1 wildtype, *spnA*-knockout, GAS M1::*spnA* and GAS M1::*spnA*_sec were collected at late exponential phase and precipitated by TCA for Western Blot analysis. Multiple bands from the growth media of the wildtype strain and the two complement strains were detected by rabbit polyclonal anti-SpnA antibodies. The result suggested a secreted form of SpnA was expressed by GAS M1::*spnA_sec* (Figure 6.3).

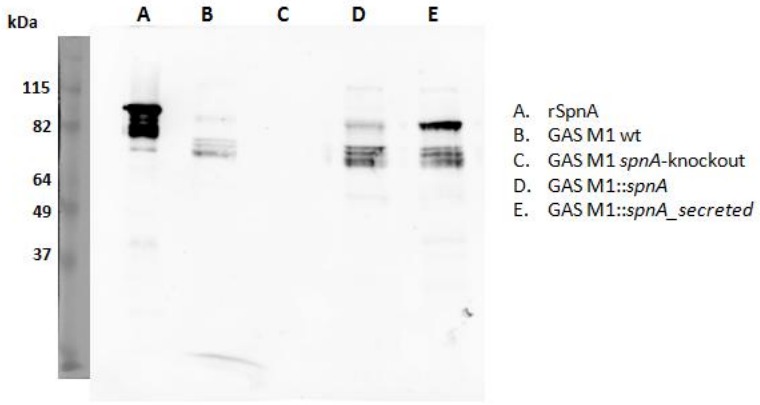

Figure 6.3 Western Blot analysis of the growth medium of GAS M1 wildtype, spnA-knockout and the two complement strains for SpnA expression

Western Blot of TCA precipitated (100x) growth supernatant from GAS M1 wildtype, *spnA*-knockout, GAS M1::*spnA* and GAS M1::*spnA_sec* showed that SpnA could be found from the growth medium of wildtype M1 and the two complement strains but not the *spnA*-knockout strain. Recombinant full-length SpnA (10 ug) protein was used as a positive control.

6.2.3 Expression of secreted SpnA promotes bacterial survival in human whole blood

The GAS M1::*spnA_sec* complemented strain was subjected to a whole blood killing assay to evaluate if the cell wall localisation of SpnA was crucial for promoting bacterial survival in blood. Approximately 1000 cfu of each GAS wildtype and mutant strains were mixed with human blood, with samples being taken and plated after 2 hrs for enumeration.

The parental GAS wildtype strain was not killed in human blood over the 2 hr incubation as observed previously, and there was a 5.2-fold increase compared to the initial bacterial count. In contrast, no *spnA*-knockout mutant survived the assay (Figure 6.4 A). The reintroduction of SpnA to the knockout mutant, in either cell wall anchored or secreted forms, was able to restore the bacterial resistance to killing by whole blood. The GAS M1::*spnA* and GAS M1::*spnA_sec* strains had a 1.2-fold and 1.7-fold increase in growth respectively (Figure 6.4 A). The result confirmed the previous finding that SpnA enhances bacterial survival in blood, yet the cell wall localisation of SpnA is not essential for such effect.

A similar experiment was performed using the *L. lactis* constructs. The exogenous expression of secreted SpnA in *L. lactis* was shown to promote bacterial survival in blood with the same effectiveness as cell wall anchored SpnA to *L. lactis* (Figure 6.4 B). Approximately 1500 cfu of each *L. lactis* mutant strains were incubated with human blood for 2 hrs and were plated for enumeration. Both *L. lactis* pOri23T:*spnA* and *L. lactis* pOri23T:*spnA_sec* mutant displayed enhanced resistance to blood killing in comparison to the *L. lactis* empty vector control, which had no resistance to the killing and was almost completely eliminated (Figure 6.4 B). Both *L. lactis* pOri23T:*spnA* and *L. lactis* pOri23T:*spnA_sec* mutant had a 50 % survival rate 2 hrs after incubation (Figure 6.4 B), suggesting the cell wall localisation is not essential for the protective effect of SpnA on bacteria.

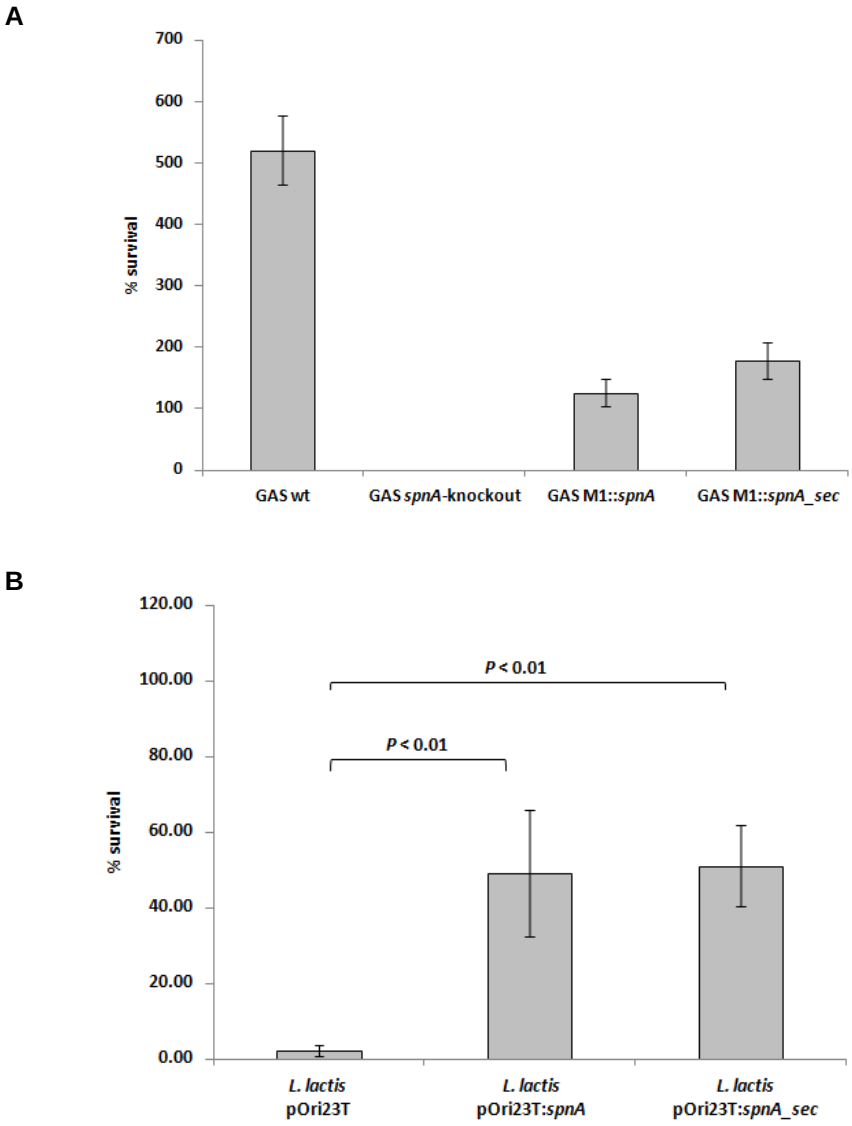

Figure 6.4 Secreted SpnA promotes bacterial survival in blood

A. Human whole blood killing assay with GAS wildtype and mutants, where 1 mL of blood was inoculated with 1000 cfu of bacteria in each group. The wildtype strain was resistant to killing by blood, and exhibited a 5.2-fold growth in 2 hrs. No *spnA*-knockout survived the assay, while GAS M1::*spnA* and GAS M1::*spnA_sec* complement strains had 1.2-fold and 1.7-fold increase in growth.

B. Human whole blood killing assay with *L. lactis* mutants, where 1 mL of blood was inoculated with 1000 cfu of bacteria in each group. The *L. lactis* pOri23T empty vector control was almost completely killed. However, the survival rate of the *L. lactis* pOri23T:*spnA* and *L. lactis* pOri23T:*spnA_sec* mutants were significantly higher than the negative control. Both *L. lactis* gain-of-function mutant had a survival rate at around 50 % after being incubated with blood for 3 hrs.

The result is representative of three independent experiments, and error bars show the standard deviation of the three experiments. No antibiotics were used in these assays.

6.2.4 The structural analysis of SpnA

The survival rate of GAS *spnA*-knockout mutant was found to be greatly reduced in comparison to the parental strain in the *in vitro* blood-mediated and NET-mediated killing assays. These results indicated SpnA might have functions in addition to being a nuclease since the effect was so dramatic. Since the activity of a protein is largely dependent on its structure, solving the 3-D structure of SpnA could reveal possible mechanisms of action and further extend the understanding in how the protein operates. Recombinant SpnA was purified and concentrated to 2 mg/mL in Tris pH 7.4 buffer with 1 mM $CaCl_2$ before being subjected to DNase treatment to remove the *E. coli* DNA molecules attached to the protein. However, the purified rSpnA protein precipitated at 4°C after long storage time, and the crystallography of rSpnA was not accomplished during the time period of this project (personal communication with Ms. Heather Baker, University of Auckland). Computer software was therefore employed to model the structure of SpnA based on its amino acid sequence in search for distinctive domains for binding or catalyzing reactions.

6.2.4.1 The prediction on disordered regions in SpnA

The amino acid sequence of SpnA was analysed by the XtalPred server for the prediction of its structure. The analysis revealed several predicted disordered regions in SpnA that might account for the failure in crystallizing rSpnA (Figure 6.5). Two short disordered regions were predicted between aa 42 – 49 and 90 – 93, which were located between the predicted signal peptide and the first OB-fold domain. The second longest disordered region was between aa 533 – 549, immediately before the predicted exo/endonuclease domain (extended from 549 – 851). The longest predicted disordered region, aa 855 – 881, was located between the exo/endonuclease domain and the cell wall anchorage motif.

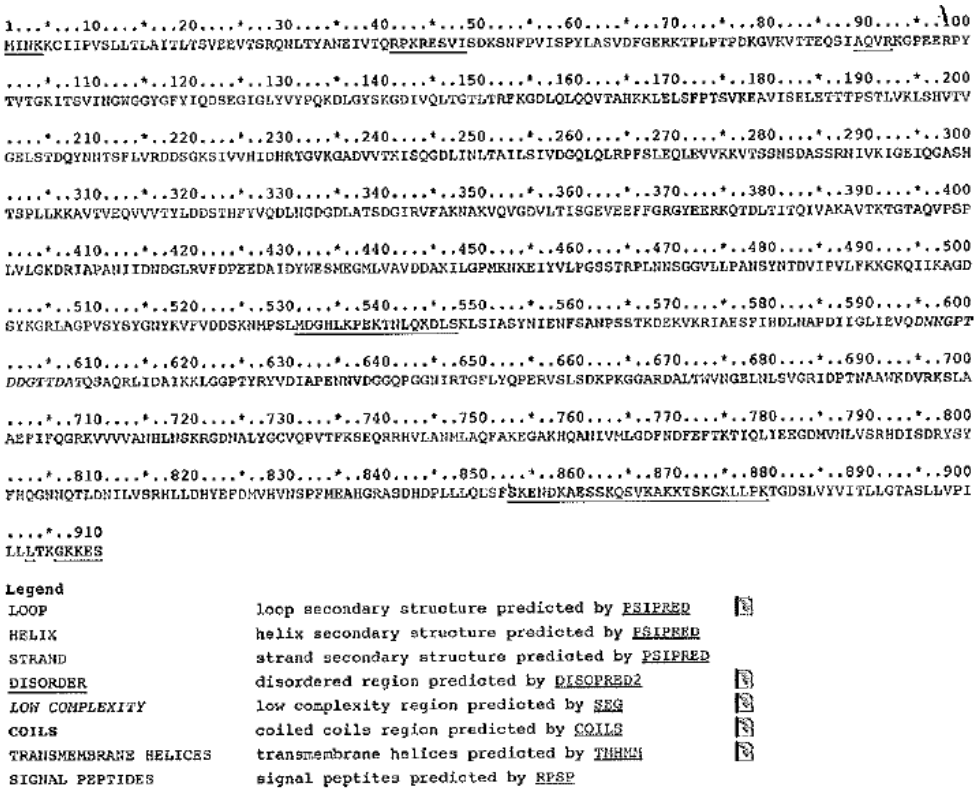

Figure 6.5 The predicted disordered regions in SpnA by XtalPred server

The underlined regions represented the predicted disordered regions. Two short disordered regions, aa42 – 49 and90 – 93, were predicted to be between the signal peptide and the OB1-domain. A longer disordered region, aa 533 – 549, located immediately before the C-terminal exo/endonuclease domain. The longest disordered region was between the nuclease domain and the cell wall anchorage motif, aa 855 – 881.

6.2.4.2 The 3-D structural model of SpnA nuclease domain

There was no suitable template in the protein database to generate a structural model for the complete mature SpnA. However, a structural model of SpnA C-terminal nuclease domain (SpnA_ND), position 549 - 851, could be created based on the structure of BP DNase 1 (PBD ID 1 atn, chain D), which was the only suitable template found in the protein structure database (Swiss Model server with automated template search). The amino acid sequence identity between SpnA_ND and BP DNase I was low (17.2%), yet the model showed that regions around the catalytic site were conserved (Figure 6.6).

The structure of BP DNase I consists of two six-stranded β-pleated sheets packed against each other to form a sandwich core structure, with several α-helices flanking the two central sheets (Suck, Oefner, & Kabsch, 1984). The model shows SpnA_ND has conserved the central six-stranded β-pleated sheet-structure, with the characteristic feature of having both the N-terminus and C-terminus aligned with each other within one of the two β-sheets. The structural model of SpnA_ND possesses two additional

putative β-hairpin structures compared to BP DNase I that extend from the region flanking one of the two core sheets.

The catalytic sites and Mg^{2+} binding sites are well conserved in the two structures. Studies showed residues His-134, Asp-168, Asp-212 and His-252 are crucial for the catalytic activity of BP DNase I (Jones, Worrall, & Connolly, 1996), and these residues superimpose well with SpnA_ND residues His-716, Asp-767, Asp-810 and His-843 in the predicted structure (Figure 6.6 C). Residues Glu-39 and Asp-251 of BP DNase I are the Mg^{2+} binding sites (Jones et al., 1996), which superimpose well with Glu-592 and Asp-842 in the SpnA_ND structure model (Figure 6.6 D).

The substrate binding sites of the two protein models appear to be less conserved in contrast. The residues Arg-9, Arg-41, Tyr-76, Arg-111, Asn-170, Thr-207 and Tyr-211 in BP DNase I have been proven to be important for substrate binding through site-directed mutagenesis studies (Doherty, Worrall, & Connolly, 1991; Evans, Shipstone, Maughan, & Connolly, 1999; Liao, Ho, & Abe, 1991). The SpnA_ND model showed that only two of the substrate binding sites are conserved, Arg-111 (BP DNase I) superimposes with Arg-696 (SpnA_ND) and Asn-170 (BP DNase I) correlates to Asn-769 in SpnA_ND.

The Ca^{2+} binding site of BP DNase I located on a flexible loop region which cannot be resolved completely; hence, a homologous region in SpnA_ND could not be superimposed. Another major difference between the two protein structure models is the presence of disulphide bond. There are three disulphide bonds found in BP DNase I, and they are important for the thermal stability and protease resistance of the protein (W. J. Chen, Lee, Chen, & Liao, 2004). In contrast, the SpnA_ND structure has no disulphide bonds, and contains a single cysteine residue, Cys-729, located on the loop of one of the two predicted additional β-hairpins.

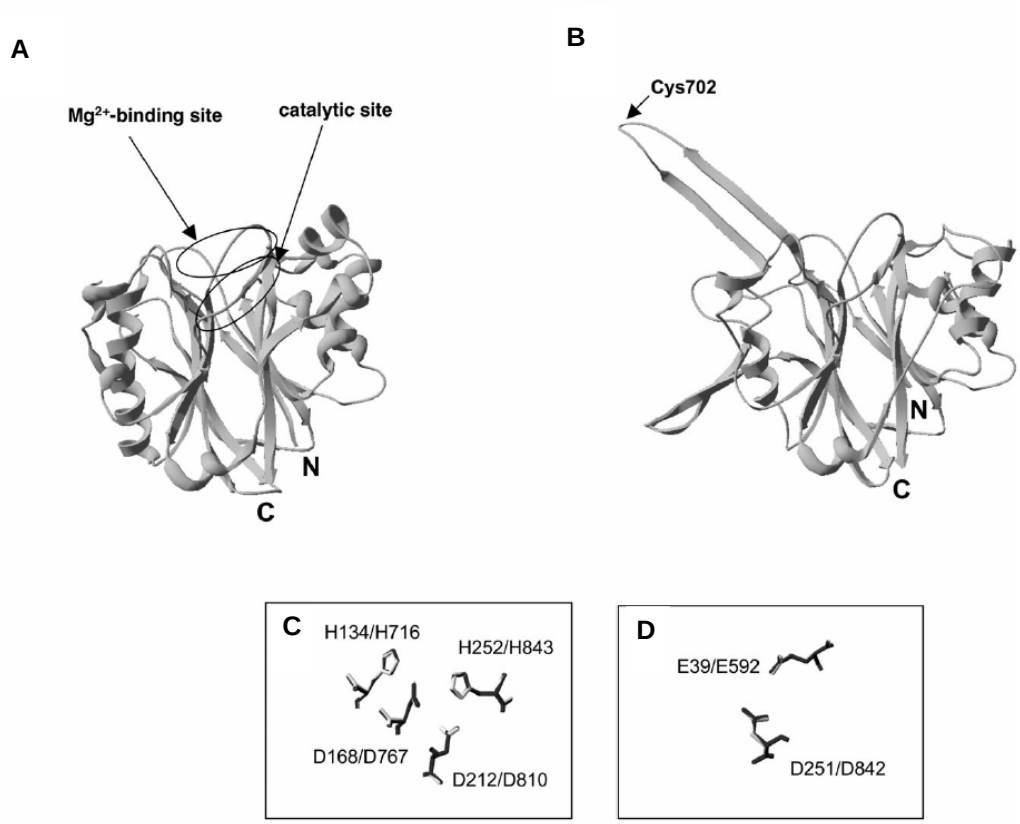

Firuge 6.6 Structural modeling of the SpnA nuclease domain (SpnA_ND)

A. The structure of BP DNase I (PBD ID 1 atn, chain D). BP DNase I has a sandwich-like core structure consisting of two six-stranded β-pleated sheets packed against each other. The two central β-pleated sheets are flanked by several α-helices. The catalytic site is located between the central sheets of the protein and comprises two histidines and two aspartic acids. The Mg^{2+} binding site is positioned on one of the two central sheets and comprises an aspartic acid and a glutamic acid.

B. The predicted structure of SpnA_ND, based on the structure of BP DNase I. The SpnA_ND model shows significant structural conservation with two additional β-hairpins extending from the structure forming a loop region.

C. Conserved catalytic site residues (BP DNase I residues are shown in grey and SpnA_ND residues are shown in black) in BP DNase I and SpnA_ND.

D. Conserved Mg^{2+} binding site residues in BP DNase I and SpnA_ND.

6.2.4.3 SpnA stability analysis with trypsin digestion

A report by Chen et al (W. J. Chen et al., 2004) found BP DNase I was more resistant to trypsin digestion in presence of 10 mM $CaCl_2$. Although no Ca^{2+} binding sites were identified in the predicted structural model of SpnA_ND, the requirement of Ca^{2+} ions for SpnA nuclease activity suggested the presence of such a site. Therefore, the role of Ca^{2+} in the structural integrity of SpnA was analysed. In the presence of 1 mM $CaCl_2$, rSpnA was significantly more resistant to trypsin degradation compared to trypsin digestion in absence of Ca^{2+} (Figure 6.7).

Significant SpnA degradation was observed after 10 min of trypsin treatment in absence of Ca^{2+}, and complete degradation occurred after 40 min of incubation at 37°C. The enhanced protease resistance was not a result of trypsin inhibition by Ca^{2+} ions, as when BSA was treated with trypsin in presence of 1 mM Ca^{2+} the trypsin activity was increased (Figure 6.7, right).

Notably, a stable product at approximately 21 kDa was observed after 60 min of trypsin treatment (Figure 6.7, left, circled). This stable fragment of rSpnA was still present after being treated with trypsin for 2 hrs. Mass spectral analysis of this 21 kDa stable product revealed a fragment with a molecular mass of 21246.199 that correspond to position 97-291 (Appendix II) in the N-terminal region encompassing the first two predicted OB-fold domains (OB1 and OB2).

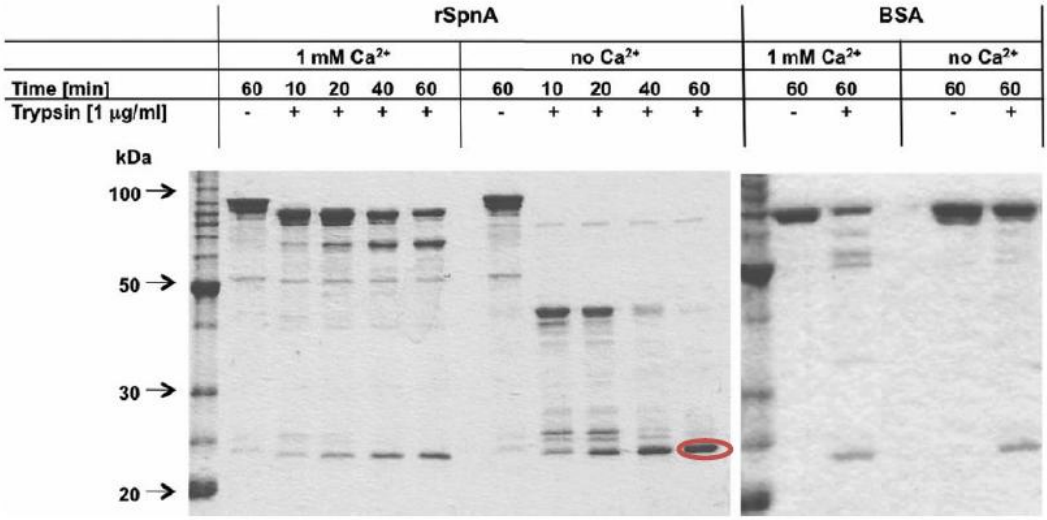

Figure 6.7 The presence of Ca^{2+} enhances rSpnA resistance to trypsin digestion

Recombinant SpnA was digested by 0.3 ug/mL trypsin at different time intervals in the presence or absence of Ca^{2+}. The absence of Ca^{2+} significantly increased the sensitivity of rSpnA to trypsin digestion. Most of the recombinant protein was digested after 10 min incubation with trypsin, and a fragment at around 42 kDa accumulated. After 60 min of digestion, the 42 kDa was further degraded and a fragment at about 21 kDa accumulated (circled in red). Mass spectral analysis of this 21 kDa tryptic fragment revealed it corresponded to position 97 – 219 in SpnA.

In a control experiment, BSA was digested by trypsin showing that addition of 1 mM $CaCl_2$ did not inhibit trypsin activity.

6.2.5 Mutational analysis on the nuclease activity of rSpnA

Based on the predicted 3-D structure of SpnA_ND, the possible sites for catalytic activity, Mg^{2+} binding and substrate binding were identified (Figure 6.6, Table 6.1). Alanine mutations were introduced at these sites to assess their role in the nuclease activity of SpnA.

Table 6.1 The predicted sites for substrate binding, catalytic activity and Mg^{2+} binding in SpnA

Residue in SpnA	Corresponding residue in BP DNase I	Predicted function
R696	R111	Substrate binding
N796	N170	Substrate binding
H716	H134	Catalytic activity
D767	D168	Catalytic activity
D810	D212	Catalytic activity
E592	E39	Mg^{2+} binding
D842	D251	Mg^{2+} binding

6.2.5.1 Analysis of the nuclease activity of the rSpnA mutants

Alanine mutations at the predicted substrate binding, catalysis and Mg^{2+} binding sites were achieved through overlap PCR. The mutants were expressed in *E. coli* BL21 and purified as soluble proteins through the method described in Chapter 3. The level of expression was the same as the wildtype rSpnA. Nuclease activity of these mutants were quantified and compared to wildtype rSpnA in a methyl green-DNase activity assay. An equimolar amount of each mutant was mixed with methyl green-DNA substrate and incubated for 24 hrs. The decolourization of methyl green-DNA substrate and the reduction in absorbance was used as the index of nuclease activity.

The alanine mutagenesis in all the recombinant mutants inactivated the nuclease activity completely, except for the mutation at the predicted Mg^{2+} binding site D842 (Figure 6.8). The D842A mutant had a 3-fold decrease in nuclease activity compared to wildtype rSpnA. This result indicated these predicted functional residues of SpnA were crucial for the nuclease activity of the protein, while D842 had relative less significance in the nuclease activity of SpnA.

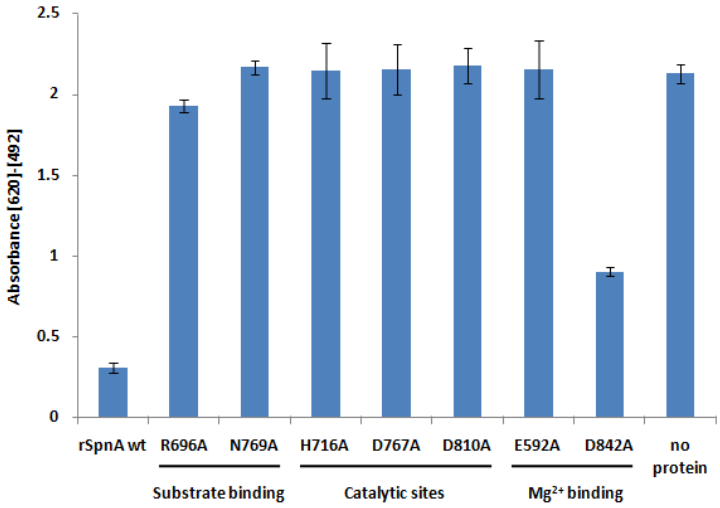

Figure 6.8 Analysis on the nuclease activity of recombinant SpnA mutants

Wildtype rSpnA and mutant proteins were incubated with methyl green-DNA substrate. A reduction in the absorbance indicated the presence of nuclease activity. The nuclease activity of all the mutants generated in this chapter was completely inactivated by the alanine mutagenesis, except for D842A mutant. The D842A mutant exhibited moderate nuclease activity comparing to the wildtype, it was 3-fold less active than wildtype rSpnA. The error bars represented the standard deviation of three independent experiments.

6.2.6 Functional analysis of rSpnA_H716A

SpnA expression in GAS and *L. lactis* promotes bacterial survival in blood and in attack by NETs. Such protective effect of SpnA on bacterial survival was hypothesized to link to its nuclease activity and its capability in disrupting the killing by NETs. The nuclease-inactive SpnA mutant H716A was subjected to a whole blood killing assay *in vitro* to examine its ability in inhibiting blood-mediated bacterial killing compared to wildtype SpnA.

6.2.6.1 Construction of *L. lactis* pOri23T:*spnA_H716A*

The construction of pOri23T:*spnA_H716A* plasmid for the expression of a cell wall anchored and nuclease inactive SpnA in *L. lactis* was unsuccessful after several attempts. The pOri23T:*spnA_H716A* plasmid underwent recombination in *E. coli* during the cloning process, and insertional mutation of the *spnA_H716A* DNA fragment was observed. The original size of *spnA_H716A* fragment was 2.7 Kb, however almost all the *E. coli* colonies screened possessed fragment at around 4 Kb (Figure 6.9). Colony 10 in Figure 6.9 was the only colony presented an insert with the correct size. However, no SpnA expression was found in *L. lactis* transformed with plasmid purified from clone 10.

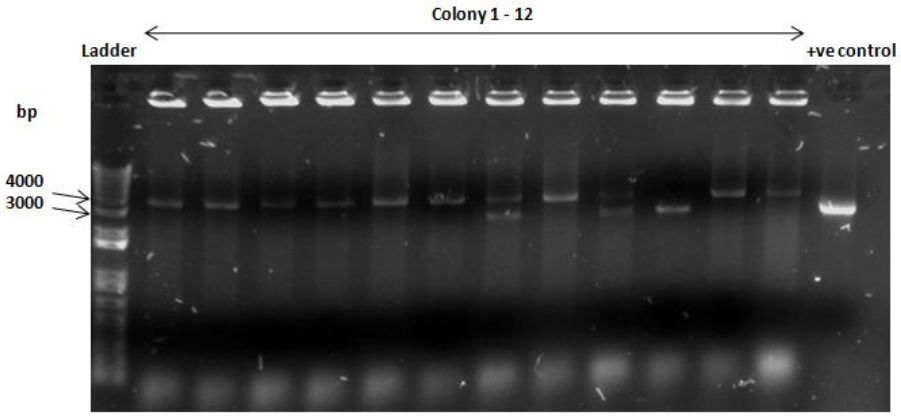

Figure 6.9 Single colony PCR on E. coli pOri23T:spnA_H716 colonies revealed recombination event in spnA_H716A DNA fragment

The correct size of the *spnA_H716A* DNA fragment was 2.7 Kb, however almost all the colonies screened possessed *spnA_H716A* fragment at around 4 Kb. Colony 10 appeared to have an insert with correct size, however no expression of SpnA was found in the transformed *L. lactis* bacterium.

6.2.6.2 Functional analysis of rSpnA_H716A mutant in promoting bacterial survival in human whole blood

An alternative approach was employed to investigate if the nuclease-inactive H716A mutant could promote bacterial survival in blood through other mechanisms than nuclease activity. A titration of recombinant H716A was added to the blood-*L. lactis* (wildtype) mix as an alternative. The concentration of H716A ranged from 2 uM to 0.01 uM. At 2 uM H716A, the bacterial survival rate was around 87 % after 3 hrs of incubation with blood. In contrast, only 32 % of bacteria survived the assay when PBS was added as a negative control (Figure 6.10). This result indicated that SpnA may have functions other than nuclease activity that promote bacterial survival in blood. Unfortunately, due to inconsistent results when trying to generate a standard curve with wildtype rSpnA, these results remain inconclusive.

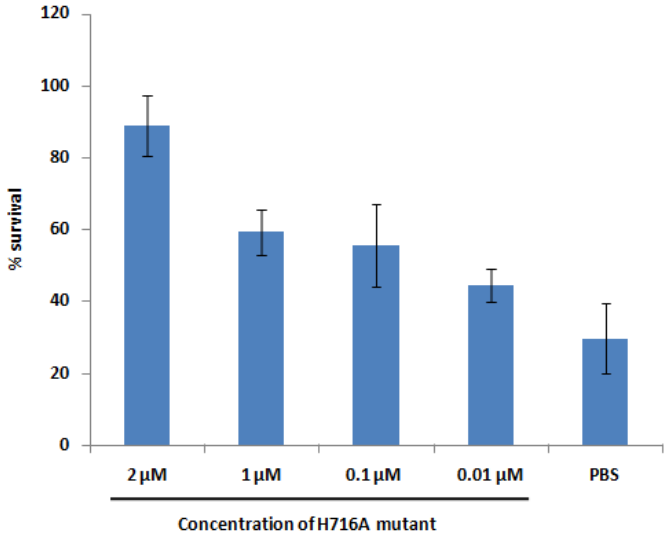

Figure 6.10 Recombinant H716A inhibits bacterial killing by blood in a dose-dependent manner

A titration of recombinant H716A ranging from 2 uM to 0.01 uM was added to a blood-*L. lactis* mix, and samples were plated after 3 hr incubation. A dose-dependent inhibition of killing was observed. At 2 uM of H716A, the bacterial survival rate was around 87 %, while the survival rate of the group with no H716A protein was around 32 %. The result is representative of three independent experiments, and error bars show the standard deviation of three experiments.

6.3 Discussion

Although SpnA is a surface-associated protein, trace amounts of SpnA have been detected in the growth supernatant of GAS M1 wildtype and the GAS M1::*spnA* complement strain, indicating the protein might be cleaved off from cell surface by bacterial proteases during growth and infection. It was therefore speculated that SpnA could retain its protective effect on bacterial cells after being cleaved off from cell wall. The cystine protease SpeB is a potent protein modifier of GAS. Many cell wall anchored proteins of GAS are substrates of SpeB, including major virulence factors: adhesins, M protein, C5a peptidase and Fba (Nelson et al., 2011), and SpnA might be one of them. Some virulence factors, such as DNase Sda1, lose their activities after being processed by SpeB (Walker et al., 2007); while others, including M protein, C5a peptidase and Fba , retain the activities and function at a distance from bacterial cells. The functional ability of a secreted form of SpnA was confirmed by using the GAS M1::*spnA_sec* complemented strain. Resistance to killing by blood was restored when compared to the *spnA*_knockout mutant. Furthermore, the strength of secreted SpnA in promoting bacterial survival appeared to be the same as when the protein was cell surface-associated. However, the two complemented GAS strains exhibited a much lower survival rate (around 120 % and 170 %) compared to the wildtype GAS M1 strain (520 %) (Figure 6.4 A). A delayed growth rate of the complemented strain was observed previously compared to wildtype (Chapter 4, section 4.1.2.3). The delayed growth rate of the complemented strains might be the cause for this lower survival compared to the wildtype, as they required longer time to expend in number. Furthermroe, it is known that SpnA expression in GAS M1 wildtype through its native regulatory system is highly upregulated in blood (Graham et al., 2005). It is possible that the plasmid-based expression of SpnA in complement strains was not comparatable to the elevated SpnA expression found in GAS M1 wildtype to achieve the enhanced growth rate observed in the parental strain. However, the result did support the hypothesis that SpnA possessed protective effect on bacterial cells against blood-mediated killing in both cell wall-anchored and secreted forms.

The delayed bacterial killing in blood was observed with the *L. lactis* pOri23T:*spnA_sec* mutant further confirmed this phenomenon. The expression of cell wall anchored SpnA, by *L. lactis* pOri23T:*spnA*, and secreted SpnA, by *L. lactis* pOri23T:*spnA_sec*, both rescued around 50 % of bacteria from killing by blood; while almost all *L. lactis* pOri23T empty vector control were killed during the incubation. The results from blood killing assay of GAS complement strains and *L. lactis* gain-of-function mutants coincided with each other, and indicated SpnA could protect the bacterium from a distance as well as when it was associated to the cell wall.

An extensively reduced survival rate was observed in the GAS *spnA*-knockout mutant in the *in vitro* killing assays by the loss of a single gene. Surprisingly, the loss of one gene could result in major defects in survival of GAS in blood and NETs even though the bacterium had multiple mechanisms in supporting bacterial survival and evading host immune defenses other than the nuclease activity of SpnA. SpnA was therefore hypothesized to have multiple functions to assist GAS in survival in addition to nuclease activity.

Solving the structure of SpnA would be advantageous to understand how the protein functions, as activities of a protein are largely dependent on its structure. Residues that are crucial for enzymatic activities can also be identified by matching the protein structure with a database of known functional domains. The crystallography of SpnA was not completed in the time period of this project, thus computer softwares were employed to predict the structure of SpnA.

Structural analysis of SpnA through the XtalPred server, based on the protein's amino acid sequence, revealed several disordered regions in the protein. These disordered regions, with no defined structures, are often linkages between activity domains. Thus the presence of these regions interferes with the formation of protein crystals. Despite their interference in protein crystallization, identifying the positions of these disordered regions gave a clearer understanding in how the secondary structure of the protein was arranged. The four major disordered regions were predicted to locate at the positions corresponding to the stretch between the signal peptide and the first OB-fold domain, the linkage between the third OB-fold domain in the N-terminus and the nuclease domain, and the region between the nuclease domain and the cell wall anchorage domain.

There is no suitable protein structure template found in the database for the full-length mature SpnA protein. However, BP DNase I was detected as suitable template when the C-terminus of SpnA (SpnA_ND) was entered into the Swiss Model search engine. The computer-predicted structure of SpnA_ND shows some striking similarities to BP DNase I. Both DNases possess a highly conserved sandwich-like core region with a well-conserved catalytic site and Mg^{2+} binding site residues.

Although no Ca^{2+} binding site was identified in this predicted structure of SpnA, the absolute dependency on Ca^{2+} ions for its nuclease activity suggests the presence of such site. It is in line with the classic two-metal ion choreography found in most enzymes that cleave DNA and in many enzymes that cut RNA (Strater, Lipscomb, Klabunde, & Krebs, 1996). Interestingly, Ca^{2+} not only plays a role in the nuclease activity of SpnA, but also participates in maintaining the integrity of the SpnA structure. The results show

that addition of 1 mM $CaCl_2$ can significantly lower the sensitivity of rSpnA to trypsin digestion. Such protective effect of Ca^{2+} on protein structure against trypsin proteolysis was also observed in BP DNase I. Reports have showed that BP DNase I can be completely inactivated after trypsin digestion, and the presence of 10 mM $CaCl_2$ effectively protected the protein from trypsin inactivation (W. J. Chen et al., 2004; Poulos & Price, 1972).

Despite the strong structural similarity with BP DNase I, it was surprising to find that the SpnA C-terminus domain completely lacks nuclease activity. It is possible that SpnA shares a conserved structure with BP DNase I, but has adapted a different substrate-binding site. This is also in line with the low degree of conservation of predicted substrate binding residues. Indeed, there is a difference in the substrate specificity of the two proteins. BP DNase I shows a strong preference for double-stranded DNA (Suck et al., 1984), whereas rSpnA has been demonstrated to cleave both single and double-stranded DNA and RNA (Chang et al., 2011).

In order to investigate the roles of the conserved residues between SpnA_ND and BP DNase I in the nuclease activity of SpnA, recombinant SpnA mutants with site directed mutations at the conserved Mg^{2+} binding sites, E592 and D842, and catalytic sites, H716, D767 and D810, were constructed through overlap PCR. The positions corresponding to the substrate binding sites, R696 and N796, in SpnA based on the model were also mutated for investigation. Nuclease activity assay using methyl green conjugated DNA revealed all the sites examined were involved with nuclease activity of SpnA. Complete inhibition of nuclease activity was observed with alanine mutations of all mutated residues except D842A, which exhibited moderate reduction in nuclease activity.

To test the hypothesis that SpnA mediates bacterial survival in host via more than one mechanism in addition to its nuclease activity, it was planned to construct a *L. lactis* mutant expressing the nuclease inactive SpnA_H716A on the bacterial surface and evaluate its ability to resist killing by blood. Unfotunately, due to a consistent recombination event occurring during the construction of pOri23T:*spnA_H716A* plasmid, this was unable to be used. One of the colonies appeared to habour the fragment with correct size (colony 10 in Figure 6.9). However, no expression of SpnA was found in *L. lactis* transformed with the plasmid extracted from this clone. It is possible that small recombination event has occurred in this clone that disrupts the expression of SpnA, but the event is undetectable through PCR. Recombination events have been observed during cloning of other streptococcal genes into pOri23T vector (personal communication with Dr. Jacelyn Loh, Univeristy of Auckland, New Zealand). Some DNA

fragments/genes appeared to be more susceptible to such events, for a reason that remains unclear.

An alternative method was employed to investigate the possibility of additional mechanisms of action of SpnA. Recombinant wildtype SpnA and SpnA_H716A proteins were added to the mixture of blood and wildtype *L. lactis* to assess their ability in inhibiting bacterial killing. Unfortunately, failure in generating a standard curve with wildtype rSpnA meant that a suitable control was unavailable. However, rSpnA_H716A mutant did appear to promote bacterial survival in blood in a dose-dependent trend, despite its lack of nuclease activity. This suggests SpnA may possess activities other than digesting DNA and may facilitate the virulence of GAS through multiple mechanisms.

It is recently found the C-terminus of SpnA binds to human monocytes and granulocytes, while the N-terminus binds monocytes only (personal communication with Ms. Angela Chang, University of Auckland, New Zealand). It is possible that SpnA exerts other activities and promotes bacterial survival through its interaction with monocytes and granulocytes. Further studies are required to explore the additional functions of SpnA.

Upon the completion of this thesis, a new protein structural template for SpnA_ND has been detected by the Swiss Model server through automated template search. It is an exo/endonuclease (3g6sA) from the Gram-negative bacterium *Bacteroides vulgates* (structure prediction of SpnA_ND based on the structure of exo/endonuclease 3g6sA in Appendix III). Further studies in this new predicted structure of SpnA_ND may provide more information in how the protein functions.

Chapter 7

Summary and Future Directions

7.1 Introduction

GAS is a major human pathogen that causes great medical and financial burdens globally. The interaction between GAS and its human host is complex, and involves a vast number of host and bacterial components. A more advanced understanding in the GAS-host interaction and the mechanisms of individual virulence factors might provide the opportunity for developing novel therapeutic methods against GAS infections.

The human immune system has evolved to efficiently eradicate pathogens from the host through an interactive network of molecular and cellular effectors. GAS, therefore, produces a large arsenal of virulence factors that facilitate the evasion of host immune responses and assist the pathogen in invading the host. This study characterises the contribution of a cell wall-associated protein SpnA to GAS virulence. The *spnA* gene is well conserved among all M serotypes of GAS. The structural prediction of SpnA based on its amino acid sequence suggests it is a cell wall-anchored nuclease. The 910 amino acid-protein is predicted to have a exo/endonuclease domain in the C-terminus, followed by a conserved Gram-positive sortase cell wall anchoring motif, LPKTG, and a cell wall anchorage domain. The structural prediction on SpnA suggests the protein is a cell wall-anchored nuclease. Functional studies on recombinant mature full-length SpnA confirmed the protein is a nuclease, with Ca^{2+} and Mg^{2+}-dependent nucleolytic activity on DNA and RNA substrates (Chang et al., 2011).

Bacterial nucleases have been considered as spreading factors that facilitate bacterial dissemination from the site of infection by liquefying purulent material. Nucleases may also be involved in bacterial nutrient uptake by supplying digested DNA and RNA molecules as nutrient source (J. D. Chen & Morrison, 1987; Lacks et al., 1975). Some bacterial nucleases have recently been recognized for their destructive activities on NETs, enhancing bacterial survival in the host (Beiter et al., 2006; Buchanan et al., 2006). A report by Hasegawa and colleagues have characterised SpnA as a cell wall-associated nuclease, confirming our finding and prediction on the protein (Hasegawa et al., 2010). A GAS isogenic *spnA*-knockout mutant displayed a phenotype of significantly weakened virulence in a murine infection model compared to its parental strain (Hasegawa et al., 2010). However, there was no investigation into the exact role of SpnA in GAS pathogenesis and virulence.

The aim of this protect was to further functionally characterise the contribution of SpnA in promoting bacterial survival in the host, and to determine if such effect was a result of NETs destruction by the nuclease activity of SpnA. Furthermore, it was examined if the ability of SpnA in promoting bacterial survival could be transferred and presented in a zebrafish embryo infection model.

7.2 SpnA and NETs

In this study, SpnA was hypothesised to facilitate evasion of host immune defense by degrading the DNA backbone of NETs. Destruction of NETs would allow bacteria to escape from killing by the bactericidal granule proteins attached to the framework. Recombinant full-length SpnA protein has been shown to be capable in degrading NETs in this study. This study has also shown that the heterologous expression of cell wall-anchored SpnA in non-pathogenic *L. lactis* confers the bacterium an elevated resistance to bacterial killing in whole blood and in NETs when compared to the *L. lactis* pOri23T empty vector control. The enhanced bacterial survival of *L. lactis* pOri23T:*spnA* mutant was indeed the direct result of SpnA expression and its destructive nucleolytic activity on NETs. A similar result was observed in *in vitro* killing assays with GAS M1 wildtype and GAS M1 *spnA*-knockout

7.3 The cell wall localisation of SpnA

GAS produces four antigenically different secreted DNases, and SpnA is the first cell wall-associated DNase identified in the bacterium. The expression of SpnA on the surface of GAS was detected through flow cytometry analysis in this study. The cell wall-localisation of SpnA allows it to accumulate at a high concentration on the bacterial surface. However, trace amounts of SpnA were also discovered in the culture medium of GAS M1 wildtype and GAS M1::*spnA* in this study, suggesting that the protein might be cleaved off from surface by bacterial proteases after being anchored to cell wall. In this study, the *L. lactis* pOri23T:*spnA_sec* mutant that expresses secreted SpnA has an enhanced resistance to bacterial killing in blood comparable to the *L. lactis* pOri23T:*spnA* mutant. This result indicates that SpnA is active in both cell wall-anchored and secreted forms.

7.4The structure and activity of SpnA

Our preliminary study showed the N-terminal OB-fold domains were essential for the nucleolytic activity of SpnA (Chang et al., 2011). Results from this project indicate the N-terminal OB-fold domains of SpnA mediate substrate-binding for the protein, as a large amount of DNA was found bound to the N-terminus ($rSpnA_{99-395}$) during protein purification. Further studies revealed that SpnA requires at least two of the

three OB-fold domains (OB2 and OB3) for its nuclease activity.

Prediction of SpnA's structure revealed four major disordered regions between domains of the proteins, thus might interfere with SpnA crystallisation. The 3-D protein structure of the C-terminal nuclease domain of SpnA (SpnA_ND) could be modeled onto the D chain of BP DNase I. The two domains share limited sequence similarity (17.2 %), but conservation in structure and reactive residues were observed. A six-stranded β-pleated sheet-structure is conserved in BP DNase I and SpnA_ND, with the characteristic feature of having both the N-terminus and C-terminus aligned to each other within one of the two β-sheets. The catalytic sites and Mg^{2+} binding sites are also well conserved between the two models, while the substrate binding sites between BP DNase I and SpnA are less conserved. Although the positions of Ca^{2+} binding sites were not conserved between PB DNase I and SpnA, the absolute dependency on Ca^{2+} ions for SpnA's nuclease activity and the protective effect of Ca^{2+} ions on SpnA integrity against trypsin digestion suggest the presence of such site in SpnA.

Site directed alanine mutations at the predicted Mg^{2+} binding/substrate binding/catalytic activity residues demolished the nuclease activity of SpnA completely, except for the predicted Mg^{2+} binding residue D842. Alanine mutation at D842 only moderately decreases the protein's nuclease activity. The result indicates, these predicted sites are all essential for the nuclease activity of SpnA, while D842 residues has less significance in such activity.

7.5 The contribution of SpnA's nuclease activity to GAS virulence

A significantly reduced virulence was observed in the GAS *spnA*-knockout mutant. No survival of the knockout mutant was observed in the *in vitro* killing assays. It is a surprise to find the loss of one gene resulted in this extensive reduction in virulence of GAS. GAS produces other secreted DNases and the loss of SpnA could be compensated through the redundant nucleolytic activities of other DNases. SpnA was thus speculated to have other functions than being a nuclease alone. The speculation was indirectly proven in this project when the nuclease-inactive SpnA_H716A mutant protein prevented blood mediated bacterial killing significantly. The result suggests SpnA possesses other activities that may assist the pathogen in survival, and the contribution of SpnA to the virulence of GAS is not exclusively through its ability in destroying NETs.

7.6 Zebrafish embryos as an infection model for studying SpnA activity

Zebrafish embryos were employed as animal infection model for the study of SpnA's contribution in bacterial virulence. Zebrafish embryos were selected as an infection model for this study for its rapid turnover time, small size and the presence of a mature innate immune system. However, there was no

previous example of employing zebrafish embryos as an infection model for GAS. The difference in virulence observed between the GAS M1 wildtype and GAS *spnA*-knockout in zebrafish embryos was statistically significant but less prominent compared to the difference observed in the murine infection model (Hasegawa et al., 2010). It was speculated that innate immune system of the embryos was not sufficient to defend the organism from GAS attack, thus the organism could not present the difference in the virulence between wildtype and *spnA*-knockout strain before being killed.

7.7 Future directions

SpnA promotes bacterial survival partially through its destructive nucleolytic activities on NETs. The nuclease inactive SpnA_H716A mutant displayed the ability of inhibiting blood-mediated bacterial killing, suggesting SpnA employs multiple mechanisms that facilitate the survival of GAS in host. The N-terminus of SpnA was recently found to bind to human monocytes, while the C-terminus binds to both monocytes and granulocytes (personal communication with Ms. Angela Chang, University of Auckland, New Zealand). SpnA might promote bacterial survival through its interaction with monocytes and granulocytes. Further investigation is required to identify the specific receptors for SpnA on the surfaces of monocytes and granulocytes. Identification of these surface receptors might help with the understanding in how SpnA interacts with the immune cells and the mechanisms it employs to promote bacterial survival.

The zebrafish embryo-GAS infection model in this project provided some promising results in presenting the contribution of SpnA to GAS virulence. However, the use of a fish pathogen instead of a human pathogen in this system might provide a more prominent result. The fish pathogen *S. iniae* is a close relative of GAS and habours a SpnA homologue. The use of *S. iniae* and its SpnA homologue in the zebrafish embryo model may better represent how SpnA functions. Alternatively, adult zebrafish may be employed as an animal infection model if the facilities in housing GAS-infected adult zebrafish were available. Adult zebrafish possesses both adaptive and innate immune systems and may provide an infection model that has more resemblance to human immune system.

A refined prediction on the 3-D structure of SpnA_ND can be achieved as another homolog, exo/endonuclease (3g6sA) of *Bacteroides vulgate*, of SpnA_ND has been found in the database. The refined prediction on SpnA's structure allows the identification of more important residues and activity sites in the protein, and may grant us more information in how SpnA achieves its protective effect on bacterial cells.

GAS is a major human pathogen that causes medical and financial burdens globally. Treatment with antibiotics can efficiently eliminate GAS infections; however, there are concerns with the emergence of antibiotic-resistant GAS strains. Although our knowledge in the virulence factors of GAS has been greatly expanded since the revelation of the pathogen's genome, it has also highlighted the complex interaction between the pathogen and the host. It is therefore vital to gain a more advanced understanding of GAS for the development of alternative therapeutic methods and identification of vaccine targets against this pathogen.

Appendix I

Sequence Alignment of SpnA and the Homolog in *Streptococcus iniae*

```
CLUSTAL 2.1 Multiple Sequence Alignments
Sequence type explicitly set to Protein
Sequence format is Pearson
Sequence 1: SpnA              910 aa
Sequence 2: S.iniaeAGM99047   871 aa
Start of Pairwise alignments
Aligning...
Sequences (1:2) Aligned. Score:  64
Guide tree file created:   [clustalw.dnd]
There are 1 groups
Start of Multiple Alignment
Aligning...
Group 1: Sequences:   2      Score:12484
Alignment Score 3437
CLUSTAL-Alignment file created  [clustalw.aln]
```

```
clustalw.aln
CLUSTAL 2.1 multiple sequence alignment
SpnA                MINKKCIIPVSLLTLAITLTSVEEVTSRQNLTYANEIVTQRPKRES----------VIS
S.iniaeAGM99047     MLNKKFFTYASLLALVAVSPVIEESFDQHNSVYAEEIIGPKTEPIVNTTAESLEPLNTLV
                    *:*** :  .***:*. . . :**  .::* .**:**:  ::              .:

SpnA                DKSNFPVISPYLASVDFGERKTPLPTPDKGVKVTTEQSIAQVRKGPEERPYTVTGKITSV
S.iniaeAGM99047     TKDTREKNSTERPLEERAAVETLTVSPEVLADANGSKPIAEVKASPQNQTYTVTGKIISA
                     *..    *.  .  : .  :*   :*:  .... .:.**:*: .*:::.******* *.

SpnA                INGWGGYGFYIQDSEGIGLYVYPQKDLGYSKGDIVQLTGTLTRFKGDLQLQQVTAHKKLE
S.iniaeAGM99047     VDGWGGNGFYMQDSKGTGIYVYPGQSLGYVSGDLIQITGQLTNFNGELQLKTISDHHKIQ
                    ::**** ***:***:* *:**** :.*** .**::*:** **.*:*:***: :: *:*::
```

```
SpnA                LSFPTSVKEAVISELETTTPSTLVKLSHVTVGELSTDQYNNTSFLVRDDSGKSIVVHIDH
S.iniaeAGM99047     GQLPTTVLEKTIPQLTDESLSTLVKVSEVTVGKITSEKSETSNFEVKDKFGNTIAVRVDS
                     .:**:* * .*.:*   : *****:*.****:::::: :.:.* *:*. *::*.*::*

SpnA                RTGVKGADVVTKISQGDLINLTAILSIVDGQLQLRPFSLEQLEVVKKVTSSN--SDASSR
S.iniaeAGM99047     RTGIKTSDLLLKINEGDVINLTAIHSIFKTKFQLKPFNLDQFEVVKKAIRKEEASPEPLS
                    ***:* :*:: **.:**:****** **.. ::**:**.*:*:*****.  .:  *  .

SpnA                NIVKIGEIQGASHTSPLLKKAVTVEQVVVTYLDDSTHFYVQDLNGDGDLATSDGIRVFAK
S.iniaeAGM99047     QLLKIGQIQGTSHQSPYDKKNVTVEQVVVTYIDDSTHFYVQDIQGDANIATSDGIRIFTQ
                    :::***:***:** **  ** **********:**********::**.::*******:*::

SpnA                NAK--VQVGDVLTISGEVEEFFGRGYEERKQTDLTITQIVAKAVTKTGTAQVPSPLVLGK
S.iniaeAGM99047     NLKPQVKVGDVLTISGLVEEYFGRGYQDLKKTDLTMTQIKAKSILKTGETSVPAPLVLGK
                    * *  *:********* ***:*****:: *:****:*** **:: *** :.**:******

SpnA                DRIAPANIIDNDGLRVFDPEEDAIDYWESMEGMLVAVDDAKILGPMKNKEIYVLPGSSTR
S.iniaeAGM99047     DRKAPVDIIDNDGLKQFDPQEDAIDYWESMEGMLVAVDNAKIVGPSKNSEIYVLPGDTTR
                    ** **.:*******: ***:******************:***:** **.*******.:**

SpnA                PLNNSGGVLLPANSYNTDVIPVLFKKGKQIIKAGDSYKGRLAGPVSYSYGNYKVFVDDSK
S.iniaeAGM99047     TLNNSGGVSLRPTAYNTDLIPILFKKGKQIIKAGDFYTGRLTGPVSYSYGNYKVVVDGIK
                    .******* * ..:****:**:************ *.***:***********.**. *

SpnA                NMPSLMDGHLKPEKTNLQKDLSKLSIASYNIENFSANPSSTKDEKVKRIAESFIHDLNAP
S.iniaeAGM99047     GMPTLNDGQLKPEKTHLPKDPSKLSIASYNIENFSANPKSTKNEKVNRIAESFINDLNSP
                    .**:* **:******:* ** ****************.***:***:*******:***:*

SpnA                DIIGLIEVQDNNGPTDDGTTDATQSAQRLIDAIKKLGGPTYRYVDIAPENNVDGGQPGGN
S.iniaeAGM99047     DIIGLIEVQDNNGPTNDGTTDASQSAQRLIDAIKALGGPIYRYVDIAPENNADGGEPGGN
                    ***************:******:********** **** **********.***:****

SpnA                IRTGFLYQPERVSLSDKPKGGARDALTWVNGELNLSVGRIDPTNAAWKDVRKSLAAEFIF
S.iniaeAGM99047     IRTGFLYQPDRVSLSEKAKGGANDAVSWENGGLNFSVGRIDPTNAIWKDVRKSLAAEFIF
                    *********:*****:*.****.**:* ** **:********** **************
```

```
SpnA                QGRKVVVVANHLNSKRGDNALYGCVQPVTFKSEQRRHVLANMLAQFAKEGAKHQANIVML
S.iniaeAGM99047     QGNKVVVVANHLNSKRGDNALYGRIQPVTFKSEERRHELAKVLAQFAKEGSRQQANIVML
                    **.******************** :********:*** **::********:::*******

SpnA                GDFNDFEFTKTIQLIEEGDMVNLVSRHDISDRYSYFHQGNNQTLDNILVSRHLLDHYEFD
S.iniaeAGM99047     GDYNDFEFTKTIQLIEEGEMANLVSRHDWSDRYSYFYQGNNQSLDNMLVSTNLLGRYAFD
                    **:***************:*.******* *******:*****:***:*** :**.:* **

SpnA                MVHVNSPFMEAHGRASDHDPLLLQLSFSKENDKAESSKQSVKAKKTSKGKLLPKTGDSLV
S.iniaeAGM99047     MVHVNSPFMEAHGRASDHDPLVATIGISKKG----------------------------
                    ********************:  :.:**:.

SpnA                YVITLLGTASLLVPILLLTKGKKES
S.iniaeAGM99047     -------------------------
```

Appendix II

Mass Spectrometry Result for the Tryptic Fragment

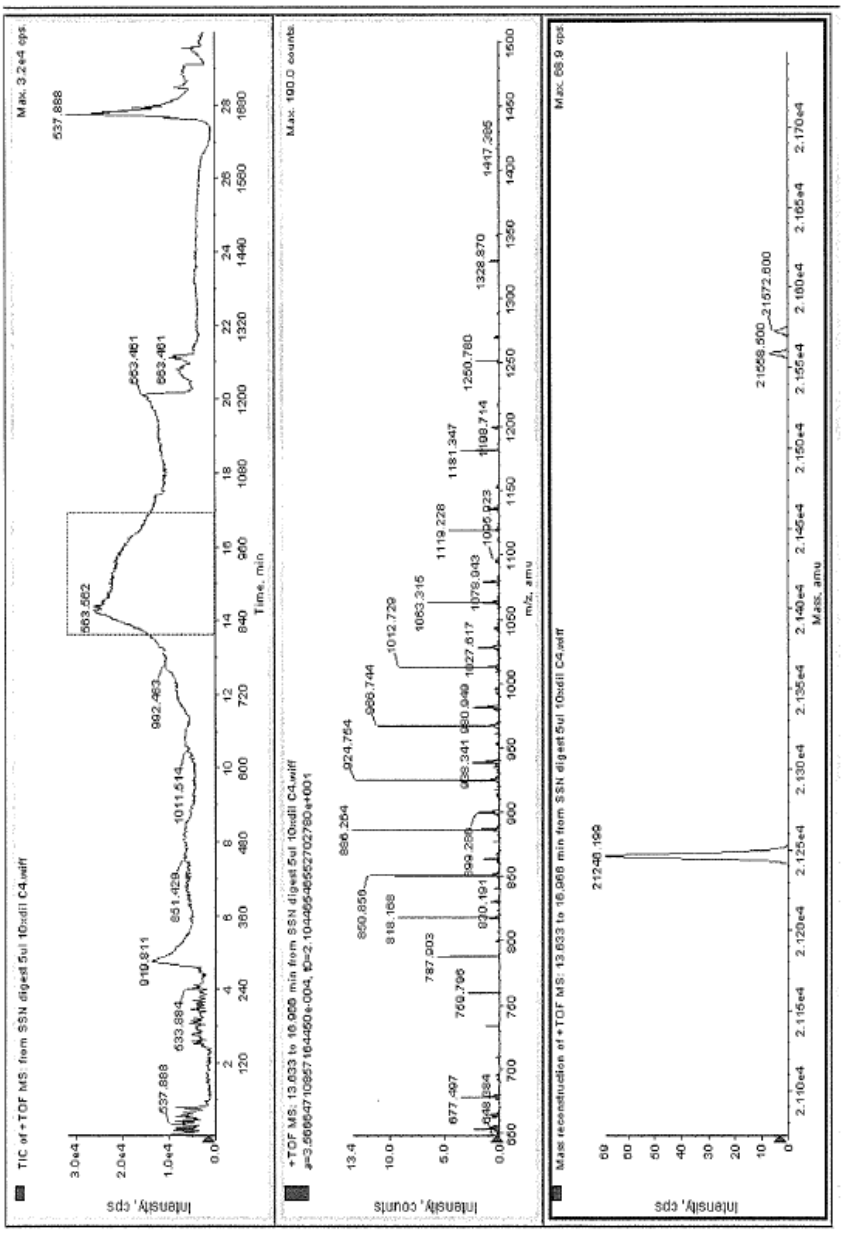

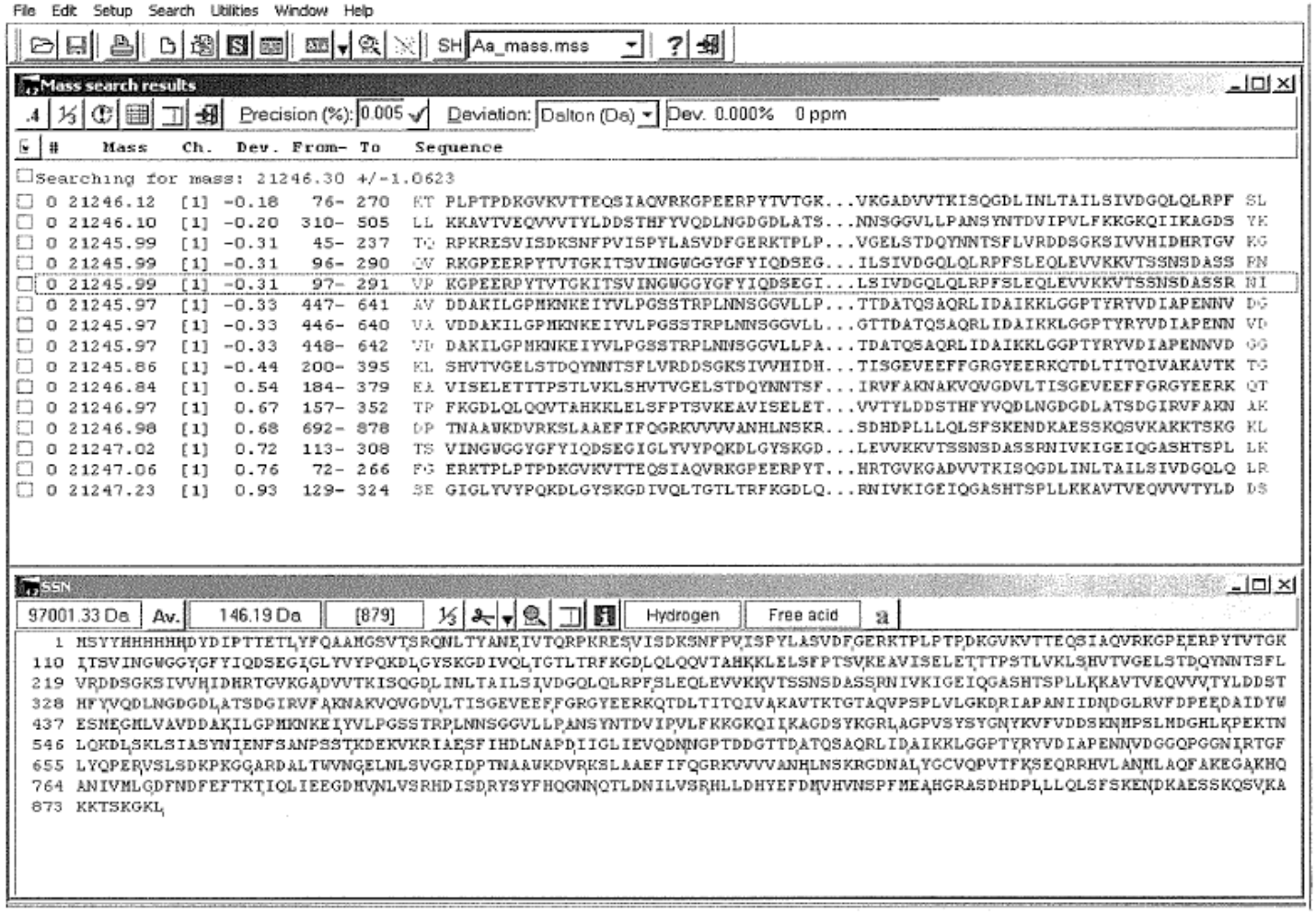
File Edit Setup Search Utilities Window Help
SH Aa_mass.mss
Mass search results
Precision (%): 0.005
Deviation: Dalton (Da)
Dev. 0.000% 0 ppm
Mass Ch. Dev. From- To Sequence
Searching for mass: 21246.30 +/-1.0623
0 21246.12 [1] -0.18 76- 270 KT PLPTPDKGVKVTTEQSIAQVRKGPEERPYTVTGK...VKGADVVTKISQGDLINLTAILSIVDGQLQLRPF SL
0 21246.10 [1] -0.20 310- 505 LL KKAVTVEQVVVTYLDDSTHFYVQDLNGDGDLATS...NNSGGVLLPANSYNTDVIPVLFKKGKQIIKAGDS YK
0 21245.99 [1] -0.31 45- 237 TQ RPKRESVISDKSNFPVISPYLASVDFGERKTPLP...VGELSTDQYNNTSFLVRDDSGKSIVVHIDHRTGV KG
0 21245.99 [1] -0.31 96- 290 QV RKGPEERPYTVTGKITSVINGWGGYGFYIQDSEG...ILSIVDGQLQLRPFSLEQLEVVKKVTSSNSDASS FN
0 21245.99 [1] -0.31 97- 291 VP KGPEERPYTVTGKITSVINGWGGYGFYIQDSEGI...LSIVDGQLQLRPFSLEQLEVVKKVTSSNSDASSR NI
0 21245.97 [1] -0.33 447- 641 AV DDAKILGPMKNKEIYVLPGSSTRPLNNSGGVLLP...TTDATQSAQRLIDAIKKLGGPTYRYVDIAPENNV DG
0 21245.97 [1] -0.33 446- 640 VA VDDAKILGPMKNKEIYVLPGSSTRPLNNSGGVLL...GTTDATQSAQRLIDAIKKLGGPTYRYVDIAPENN VD
0 21245.97 [1] -0.33 448- 642 VD DAKILGPMKNKEIYVLPGSSTRPLNNSGGVLLPA...TDATQSAQRLIDAIKKLGGPTYRYVDIAPENNVD GG
0 21245.86 [1] -0.44 200- 395 KL SHVTVGELSTDQYNNTSFLVRDDSGKSIVVHIDH...TISGEVEEFFGRGYEERKQTDLTITQIVAKAVTK TG
0 21246.84 [1] 0.54 184- 379 EA VISELETTTPSTLVKLSHVTVGELSTDQYNNTSF...IRVFAKNAKVQVGDVLTISGEVEEFFGRGYEERK QT
0 21246.97 [1] 0.67 157- 352 TP FKGDLQLQQVTAHKKLELSFPTSVKEAVISELET...VVTYLDDSTHFYVQDLNGDGDLATSDGIRVFAKN AK
0 21246.98 [1] 0.68 692- 878 DP TNAAVKDVRKSLAAEFIFQGRKVVVVANHLNSKR...SDHDPLLLQLSFSKENDKAESSKQSVKAKKTSKG KL
0 21247.02 [1] 0.72 113- 308 TS VINGWGGYGFYIQDSEGIGLYVYPQKDLGYSKGD...LEVVKKVTSSNSDASSRNIVKIGEIQGASHTSPL LK
0 21247.06 [1] 0.76 72- 266 FG ERKTPLPTPDKGVKVTTEQSIAQVRKGPEERPYT...HRTGVKGADVVTKISQGDLINLTAILSIVDGQLQ LR
0 21247.23 [1] 0.93 129- 324 SE GIGLYVYPQKDLGYSKGDIVQLTGTLTRFKGDLQ...RNIVKIGEIQGASHTSPLLKKAVTVEQVVVTYLD DS
SSN
97001.33 Da Av. 146.19 Da [879] Hydrogen Free acid
1 MSYYHHHHHHDYDIPTTETLYFQAAMGSVTSRQNLTYANEIVTQRPKRESVISDKSNFPVISPYLASVDFGERKTPLPTPDKGVKVTTEQSIAQVRKGPEERPYTVTGK
110 ITSVINGWGGYGFYIQDSEGIGLYVYPQKDLGYSKGDIVQLTGTLTRFKGDLQLQQVTAHKKLELSFPTSVKEAVISELETTTPSTLVKLSHVTVGELSTDQYNNTSFL
219 VRDDSGKSIVVHIDHRTGVKGADVVTKISQGDLINLTAILSIVDGQLQLRPFSLEQLEVVKKVTSSNSDASSRNIVKIGEIQGASHTSPLLKKAVTVEQVVVTYLDDST
328 HFYVQDLNGDGDLATSDGIRVFAKNAKVQVGDVLTISGEVEEFFGRGYEERKQTDLTITQIVAKAVTKTGTAQVPSPLVLGKDRIAPANIIDNDGLRVFDPEEDAIDYW
437 ESNEGHLVAVDDAKILGPMKNKEIYVLPGSSTRPLNNSGGVLLPANSYNTDVIPVLFKKGKQIIKAGDSYKGRLAGPVSYSYGNYKVFVDDSKNNPSLMDGHLKPEKTN
546 LQKDLSKLSIASYNIENFSANPSSTKDEKVKRIAESFIHDLNAPDIIGLIEVQDNNGPTDDGTTDATQSAQRLIDAIKKLGGPTYRYVDIAPENNVDGGQPGGNIRTGF
655 LYQPERVSLSDKPKGGARDALTWVNGELNLSVGRIDPTNAAVKDVRKSLAAEFIFQGRKVVVVANHLNSKRGDNALYGCVQPVTFKSEQRRHVLANMLAQFAKEGAKHQ
764 ANIVMLGDFNDFEFTKTIQLIEEGDHVNLVSRHDISDRYSYFHQGNNQTLDNILVSRHLLDHYEFDMVHVNSPFMEAHGRASDHDPLLLQLSFSKENDKAESSKQSVKA
873 KKTSKGKL

Appendix III

SpnA_ND Structural Prediction Based on a Homolog in *Bacteroides vulgate*

SWISS-MODEL Workspace

Workunit: P000029 Title:SpnA

1 856

Model Summary:

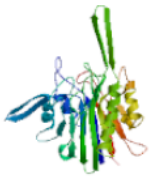

Model information:

Modelled residue range:	523 to 829
Based on template:	3g6sA (2.50 A)
Sequence Identity [%]:	15.047
Evalue:	1.2E-22

Quality information:
QMEAN Z-Score: -6.02

Quaternary structure information:
Template (3g6s): MONOMER
Model built: SINGLE CHAIN

Ligand information:
Ligands in the template: none.
Ligands in the model: none.

Global Model Quality Estimation:

QMEAN4 global scores:

QMEANscore4: 0.386

Estimated absolute model quality:

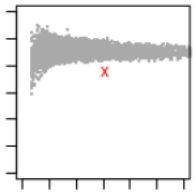

Z-Score: -6.02

Score components:

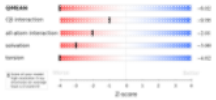

Local scores:

Coloring by residue error:

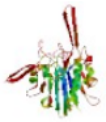

Residue error plot:

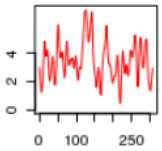

QMEAN4 global scores:

The QMEAN4 score is a composite score consisting of a linear combination of 4 statistical potential terms (estimated model reliability between 0-1). The pseudo-energies of the contributing terms are given below together with their Z-scores with respect to scores obtained for high-resolution experimental structures of similar size solved by X-ray crystallography:

Scoring function term	Raw score	Z-score
C_beta interaction energy	-90.31	-0.98
All-atom pairwise energy	-4612.20	-2.01
Solvation energy	-0.70	-3.00
Torsion angle energy	3.14	-4.62
QMEAN4 score	0.386	-6.02

If you publish results from QMEAN, please cite the following paper:
Benkert P, Biasini M, Schwede T. (2011). "Toward the estimation of the absolute quality of individual protein structure models." Bioinformatics, 27(3):343-50.

Local Model Quality Estimation:

1

Bibliography

Aggad, D., Stein, C., Sieger, D., Mazel, M., Boudinot, P., Herbomel, P., . . . Leptin, M. (2010). *In vivo* analysis of Ifn-gamma1 and Ifn-gamma2 signaling in zebrafish. *J Immunol, 185*(11), 6774-6782. doi: 10.4049/jimmunol.1000549

Alberti, S., Ashbaugh, C. D., & Wessels, M. R. (1998). Structure of the has operon promoter and regulation of hyaluronic acid capsule expression in group A Streptococcus. *Molecular microbiology, 28*(2), 343-353.

Allen, J. P., & Neely, M. N. (2010). Trolling for the ideal model host: zebrafish take the bait. *Future Microbiology, 5*(4), 563-569.

Amulic, B., Cazalet, C., Hayes, G. L., Metzler, K. D., & Zychlinsky, A. (2012). Neutrophil function: from mechanisms to disease. *Annu Rev Immunol, 30*, 459-489. doi: 10.1146/annurev-immunol-020711-074942

Aziz, R. K., Edwards, R. A., Taylor, W. W., Low, D. E., McGeer, A., & Kotb, M. (2005). Mosaic prophages with horizontally acquired genes account for the emergence and diversification of the globally disseminated M1T1 clone of Streptococcus pyogenes. *Journal of Bacteriology, 187*(10), 3311-3318.

Aziz, R. K., Ismail, S. A., Park, H., & Kotb, M. (2004). Post-proteomic identification of a novel phage-encoded streptodornase, Sda1, in invasive M1T1 Streptococcus pyogenes. *Molecular microbiology, 54*(1), 184-197.

Aziz, R. K., & Kotb, M. (2008). Rise and persistence of global M1T1 clone of Streptococcus pyogenes. *Emerging Infectious Diseases, 14*(10), 1511-1517.

Aziz, R. K., Pabst, M. J., Jeng, A., Kansal, R., Low, D. E., Nizet, V., & Kotb, M. (2004). Invasive M1T1 group A Streptococcus undergoes a phase-shift *in vivo* to prevent proteolytic degradation of multiple virulence factors by SpeB. *Molecular Microbiology, 51*(1), 123-134.

Baker, V. S., Imade, G. E., Molta, N. B., Tawde, P., Pam, S. D., Obadofin, M. O., . . . Keller, T. Cs, 3rd. (2008). Cytokine-associated neutrophil extracellular traps and antinuclear antibodies in Plasmodium falciparum infected children under six years of age. *Malaria Journal, 7*, 41.

Barkulis, S. S., Boltralik, J. J., Hankin, H., & Heymann, H. (1967). Biosynthesis of streptococcal cell walls: N-acetyl-D-muramic acid. *Journal of Bacteriology, 94*(4), 963-965.

Beiter, K., Wartha, F., Albiger, B., Normark, S., Zychlinsky, A., & Henriques-Normark, B. (2006). An endonuclease allows Streptococcus pneumoniae to escape from neutrophil extracellular traps. *Current Biology, 16*(4), 401-407.

Berends, E. T. M., Horswill, A. R., Haste, N. M., Monestier, M., Nizet, V., & von Kockritz-Blickwede, M. (2010). Nuclease expression by Staphylococcus aureus facilitates escape from neutrophil

extracellular traps. *Journal of Innate Immunity, 2*(6), 576-586.

Berge, A., & Bjorck, L. (1995). Streptococcal Cysteine Proteinase Releases Biologically-Active Fragments of Streptococcal Surface-Proteins. *Journal of Biological Chemistry, 270*(17), 9862-9867.

Billington, S. J., Jost, B. H., & Songer, J. G. (2000). Thiol-activated cytolysins: structure, function and role in pathogenesis. *FEMS Microbiology Letters, 182*(2), 197-205.

Bisno, A. L., Brito, M. O., & Collins, C. M. (2003). Molecular basis of group A streptococcal virulence. *Lancet Infectious Diseases, 3*(4), 191-200.

Brinkmann, V., Reichard, U., Goosmann, C., Fauler, B., Uhlemann, Y., Weiss, D. S., . . . Zychlinsky, A. (2004). Neutrophil extracellular traps kill bacteria. *Science, 303*(5663), 1532-1535.

Brinkmann, V., & Zychlinsky, A. (2007). Beneficial suicide: why neutrophils die to make NETs. *Nature Reviews Microbiology, 5*(8), 577-582. doi: Doi 10.1038/Nrmicro1710

Bruns, S., Kniemeyer, O., Hasenberg, M., Aimanianda, V., Nietzsche, S., Thywissen, A., . . . Gunzer, M. (2010). Production of extracellular traps against Aspergillus fumigatus *in vitro* and in infected lung tissue is dependent on invading neutrophils and influenced by hydrophobin RodA. *PLoS Pathogens, 6*(4), e1000873.

Buchanan, J. T., Simpson, A. J., Aziz, R. K., Liu, G. Y., Kristian, S. A., Kotb, M., . . . Nizet, V. (2006). DNase expression allows the pathogen group A streptococcus to escape killing in neutrophil extracellular traps. *Current Biology, 16*(4), 396-400.

Carapetis, J. R., Steer, A. C., Mulholland, E. K., & Weber, M. (2005). The global burden of group A streptococcal diseases. *Lancet Infectious Diseases, 5*(11), 685-694.

Carlsson, F., Berggard, K., Stalhammar-Carlemalm, M., & Lindahl, G. (2003). Evasion of phagocytosis through cooperation between two ligand-binding regions in Streptococcus pyogenes M protein. *Journal of Experimental Medicine, 198*(7), 1057-1068.

Chang, A. (2007). *Cloning, expression and functional characterisation of a putative novel cell surface anchored deoxyribonuclease of Streptococcus pyogenes.* (Master Master thesis), University of Auckland.

Chang, A., Khemlani, A., Kang, H., & Proft, T. (2011). Functional analysis of Streptococcus pyogenes nuclease A (SpnA), a novel group A streptococcal virulence factor. *Mol Microbiol, 79*(6), 1629-1642.

Chen, J. D., & Morrison, D. A. (1987). Modulation of competence for genetic transformation in Streptococcus pneumoniae. *J Gen Microbiol, 133*(7), 1959-1967.

Chen, W. J., Lee, I. S., Chen, C. Y., & Liao, T. H. (2004). Biological functions of the disulfides in bovine pancreatic deoxyribonuclease. *Protein Science, 13*(4), 875-883.

Chiang-Ni, C., & Wu, J. (2008). Effects of streptococcal pyrogenic exotoxin B on pathogenesis of Streptococcus pyogenes. *Journal of the Formosan Medical Association, 107*(9), 677-685.

Chiappini, N., Seubert, A., Telford, J. L., Grandi, G., Serruto, D., Margarit, I., & Janulczyk, R. (2012). Streptococcus pyogenes SpyCEP influences host-pathogen interactions during infection in a murine air pouch model. *PLoS One, 7*(7), e40411.

Cleary, P. P., Kaplan, E. L., Handley, J. P., Wlazlo, A., Kim, M. H., Hauser, A. R., & Schlievert, P. M. (1992). Clonal basis for resurgence of serious Streptococcus pyogenes disease in the 1980s. *Lancet, 339*(8792), 518-521.

Cleary, P. P., LaPenta, D., Vessela, R., Lam, H., & Cue, D. (1998). A globally disseminated M1 subclone of group A streptococci differs from other subclones by 70 kilobases of prophage DNA and capacity for high-frequency intracellular invasion. *Infection & Immunity, 66*(11), 5592-5597.

Cleary, P. P., Prahbu, U., Dale, J. B., Wexler, D. E., & Handley, J. (1992). Streptococcal C5a peptidase is a highly specific endopeptidase. *Infection & Immunity, 60*(12), 5219-5223.

Cole, J. N., Pence, M. A., von Kockritz-Blickwede, M., Hollands, A., Gallo, R. L., Walker, M. J., & Nizet, V. (2010). M protein and hyaluronic acid capsule are essential for *in vivo* selection of covRS mutations characteristic of invasive serotype M1T1 group A Streptococcus. *mBio, 1*(4).

Collin, M., & Olsen, A. (2001). Effect of SpeB and EndoS from Streptococcus pyogenes on human immunoglobulins. *Infection & Immunity, 69*(11), 7187-7189.

Collin, M., Svensson, M. D., Sjoholm, A. G., Jensenius, J. C., Sjobring, U., & Olsen, A. (2002). EndoS and SpeB from Streptococcus pyogenes inhibit immunoglobulin-mediated opsonophagocytosis. *Infection & Immunity, 70*(12), 6646-6651.

Courtney, H. S., Hasty, D. L., & Dale, J. B. (2002). Molecular mechanisms of adhesion, colonization, and invasion of group A streptococci. *Annals of Medicine, 34*(2), 77-87.

Cowburn, A. S., Condliffe, A. M., Farahi, N., Summers, C., & Chilvers, E. R. (2008). Advances in neutrophil biology: clinical implications. *Chest, 134*(3), 606-612.

Cue, D., Dombek, P. E., Lam, H., & Cleary, P. P. (1998). Streptococcus pyogenes serotype M1 encodes multiple pathways for entry into human epithelial cells. *Infection & Immunity, 66*(10), 4593-4601.

Cunningham, M. W. (2008). Pathogenesis of group A streptococcal infections and their sequelae. *Hot Topics in Infection and Immunity in Children Iv, 609*, 29-42.

Cywes, C., & Wessels, M. R. (2001). Group A Streptococcus tissue invasion by CD44-mediated cell signalling. *Nature, 414*(6864), 648-652.

Dieye, Y., Oxaran, V., Ledue-Clier, F., Alkhalaf, W., Buist, G., Juillard, V., . . . Piard, J. C. (2010). Functionality of sortase A in Lactococcus lactis. *Applied & Environmental Microbiology, 76*(21), 7332-7337.

Doherty, A. J., Worrall, A. F., & Connolly, B. A. (1991). Mutagenesis of the DNA-Binding Residues in Bovine Pancreatic Dnase-1 - an Investigation into the Mechanism of Sequence Discrimination by a Sequence Selective Nuclease. *Nucleic Acids Research, 19*(22), 6129-6132.

Edwards, R. J., Taylor, G. W., Ferguson, M., Murray, S., Rendell, N., Wrigley, A., . . . Sriskandan, S. (2005). Specific C-terminal cleavage and inactivation of interleukin-8 by invasive disease isolates of Streptococcus pyogenes. *J Infect Dis, 192*(5), 783-790.

Egesten, A., Olin, A. I., Linge, H. M., Yadav, M., Morgelin, M., Karlsson, A., & Collin, M. (2009). SpeB of Streptococcus pyogenes differentially modulates antibacterial and receptor activating properties of human chemokines. *PLoS ONE [Electronic Resource], 4*(3), e4769.

Ellen, R. P., & Gibbons, R. J. (1972). M protein-associated adherence of Streptococcus pyogenes to epithelial surfaces: prerequisite for virulence. *Infection & Immunity, 5*(5), 826-830.

Eriksson, A., Eriksson, B., Holm, S. E., & Norgren, M. (1999). Streptococcal DNase B is immunologically identical to superantigen SpeF but involves separate domains. *Clinical & Diagnostic Laboratory Immunology, 6*(1), 133-136.

Evans, S. J., Shipstone, E. J., Maughan, W. N., & Connolly, B. A. (1999). Site-directed mutagenesis of phosphate-contacting amino acids of bovine pancreatic deoxyribonuclease I. *Biochemistry, 38*(13), 3902-3909.

Facklam, R. F., Martin, D. R., Lovgren, M., Johnson, D. R., Efstratiou, A., Thompson, T. A., . . . Beall, B. (2002). Extension of the Lancefield classification for group A streptococci by addition of 22 new M protein gene sequence types from clinical isolates: emm103 to emm124. *Clinical Infectious Diseases, 34*(1), 28-38.

Feito, M. J., Sanchez, A., Oliver, M. A., Perez-Caballero, D., Rodriguez de Cordoba, S., Alberti, S., & Rojo, J. M. (2007). Membrane cofactor protein (MCP, CD46) binding to clinical isolates of Streptococcus pyogenes: binding to M type 18 strains is independent of Emm or Enn proteins. *Molecular Immunology, 44*(14), 3571-3579.

Ferretti, J. J., McShan, W. M., Ajdic, D., Savic, D. J., Savic, G., Lyon, K., . . . McLaughlin, R. (2001). Complete genome sequence of an M1 strain of Streptococcus pyogenes. *Proceedings of the National Academy of Sciences of the United States of America, 98*(8), 4658-4663.

Fraser, J. D., & Proft, T. (2008). The bacterial superantigen and superantigen-like proteins. *Immunological Reviews, 225*, 226-243.

Frick, I., Schmidtchen, A., & Sjobring, U. (2003). Interactions between M proteins of Streptococcus pyogenes and glycosaminoglycans promote bacterial adhesion to host cells. *European Journal of Biochemistry, 270*(10), 2303-2311.

Fuchs, T. A., Abed, U., Goosmann, C., Hurwitz, R., Schulze, I., Wahn, V., . . . Zychlinsky, A. (2007). Novel cell death program leads to neutrophil extracellular traps. *Journal of Cell Biology, 176*(2), 231-241.

Georgousakis, M. M., McMillan, D. J., Batzloff, M. R., & Sriprakash, K. S. (2009). Moving forward: a mucosal vaccine against group A streptococcus. *Expert Review of Vaccines, 8*(6), 747-760.

Gerlach, D., Reichardt, W., Fleischer, B., & Schmidt, K. H. (1994). Separation of mitogenic and pyrogenic activities from so-called erythrogenic toxin type B (Streptococcal proteinase). *Zentralblatt fur Bakteriologie, 280*(4), 507-514.

Graham, M. R., Virtaneva, K., Porcella, S. F., Barry, W. T., Gowen, B. B., Johnson, C. R., . . . Musser, J. M. (2005). Group A Streptococcus transcriptome dynamics during growth in human blood reveals bacterial adaptive and survival strategies. *American Journal of Pathology, 166*(2), 455-465.

Guimaraes-Costa, A. B., Nascimento, M. T. C., Froment, G. S., Soares, R. P. P., Morgado, F. N., Conceicao-Silva, F., & Saraiva, E. M. (2009). Leishmania amazonensis promastigotes induce and are killed by neutrophil extracellular traps. *Proceedings of the National Academy of Sciences of the United States of America, 106*(16), 6748-6753.

Hasegawa, T., Minami, M., Okamoto, A., Tatsuno, I., Isaka, M., & Ohta, M. (2010). Characterization of a virulence-associated and cell-wall-located DNase of Streptococcus pyogenes. *Microbiology (Reading, England), 156*(Pt 1), 184-190.

Hemmi, H., Takeuchi, O., Kawai, T., Kaisho, T., Sato, S., Sanjo, H., . . . Akira, S. (2000). A Toll-like receptor recognizes bacterial DNA.[Erratum appears in Nature 2001 Feb 1;409(6820):646]. *Nature, 408*(6813), 740-745.

Horstmann, R. D., Sievertsen, H. J., Leippe, M., & Fischetti, V. A. (1992). Role of fibrinogen in complement inhibition by streptococcal M protein. *Infection & Immunity, 60*(12), 5036-5041.

Hryniewicz, W., & Pryjma, J. (1977). Effect of streptolysin S on human and mouse T and B lymphocytes. *Infection & Immunity, 16*(3), 730-733.

Johnson, D. R., Wotton, J. T., Shet, A., & Kaplan, E. L. (2002). A comparison of group A streptococci from invasive and uncomplicated infections: are virulent clones responsible for serious streptococcal infections? *Journal of Infectious Diseases, 185*(11), 1586-1595.

Jones, S. J., Worrall, A. F., & Connolly, B. A. (1996). Site-directed mutagenesis of the catalytic residues of bovine pancreatic deoxyribonuclease I. *Journal of Molecular Biology, 264*(5), 1154-1163.

Kapur, V., Topouzis, S., Majesky, M. W., Li, L. L., Hamrick, M. R., Hamill, R. J., . . . Musser, J. M. (1993). A conserved Streptococcus pyogenes extracellular cysteine protease cleaves human fibronectin and degrades vitronectin. *Microbial Pathogenesis, 15*(5), 327-346.

Keiser, H., Weissmann, G., & Bernheimer, A. W. (1964). Studies on Lysosomes. Iv. Solubilization of Enzymes during Mitochondrial Swelling and Disruption of Lysosomes by Streptolysin S and Other Hemolytic Agents. *Journal of Cell Biology, 22*, 101-113.

Kizy, A. E., & Neely, M. N. (2009). First Streptococcus pyogenes signature-tagged mutagenesis screen identifies novel virulence determinants. *Infection & Immunity, 77*(5), 1854-1865.

Kolb, W. P., & Muller-Eberhard, H. J. (1975). Neoantigens of the membrane attack complex of human complement. *Proc Natl Acad Sci U S A, 72*(5), 1687-1689.

Kosciuczuk, E. M., Lisowski, P., Jarczak, J., Strzalkowska, N., Jozwik, A., Horbanczuk, J., . . . Bagnicka, E. (2012). Cathelicidins: family of antimicrobial peptides. A review. *Molecular Biology Reports, 39*(12), 10957-10970.

Kuo, C., Lin, Y., Chuang, W., Wu, J., & Tsao, N. (2008). Degradation of complement 3 by streptococcal pyrogenic exotoxin B inhibits complement activation and neutrophil opsonophagocytosis. *Infection & Immunity, 76*(3), 1163-1169.

Kurupati, P., Turner, C. E., Tziona, I., Lawrenson, R. A., Alam, F. M., Nohadani, M., . . . Sriskandan, S. (2010). Chemokine-cleaving Streptococcus pyogenes protease SpyCEP is necessary and sufficient for bacterial dissemination within soft tissues and the respiratory tract. *Molecular Microbiology, 76*(6), 1387-1397.

Lacks, S., Greenberg, B., & Neuberger, M. (1975). Identification of a deoxyribonuclease implicated in genetic transformation of Diplococcus pneumoniae. *Journal of Bacteriology, 123*(1), 222-232.

Lancefield, R. C. (1928). The Antigenic Complex of Streptococcus Haemolyticus : I. Demonstration of a

Type-Specific Substance in Extracts of Streptococcus Haemolyticus. *Journal of Experimental Medicine, 47*(1), 91-103.

Lancefield, R. C. (1933). A Serological Differentiation of Human and Other Groups of Hemolytic Streptococci. *Journal of Experimental Medicine, 57*(4), 571-595.

Le Loir, Y., Azevedo, V., Oliveira, S. C., Freitas, D. A., Miyoshi, A., Bermudez-Humaran, L. G., . . . Langella, P. (2005). Protein secretion in Lactococcus lactis : an efficient way to increase the overall heterologous protein production. *Microb Cell Fact, 4*(1), 2.

Liao, T. H., Ho, H. C., & Abe, A. (1991). Chemical Modification of Bovine Pancreatic Deoxyribonuclease with Phenylglyoxal - the Involvement of Arg-9 and Arg-41 in Substrate Binding. *Biochimica Et Biophysica Acta, 1079*(3), 335-342.

Lin, A., Loughman, J. A., Zinselmeyer, B. H., Miller, M. J., & Caparon, M. G. (2009). Streptolysin S inhibits neutrophil recruitment during the early stages of Streptococcus pyogenes infection. *Infection & Immunity, 77*(11), 5190-5201.

Magassa, N., Chandrasekaran, S., & Caparon, M. G. (2010). Streptococcus pyogenes cytolysin-mediated translocation does not require pore formation by streptolysin O. *EMBO Reports, 11*(5), 400-405.

Manthey, H. D., Woodruff, T. M., Taylor, S. M., & Monk, P. N. (2009). Complement component 5a (C5a). *Int J Biochem Cell Biol, 41*(11), 2114-2117.

McCarty, M. (1948). The occurrence of nucleases in culture filtrates of group A hemolytic streptococci. *Journal of Experimental Medicine, 88*(2), 181-188.

McCormick, J. K., Yarwood, J. M., & Schlievert, P. M. (2001). Toxic shock syndrome and bacterial superantigens: an update. *Annual Review of Microbiology, 55*, 77-104.

Meehl, M. A., & Caparon, M. G. (2004). Specificity of streptolysin O in cytolysin-mediated translocation. *Molecular microbiology, 52*(6), 1665-1676.

Meijer, A. H., & Spaink, H. P. (2011). Host-pathogen interactions made transparent with the zebrafish model. *Current Drug Targets, 12*(7), 1000-1017.

Mejean, V., & Claverys, J. P. (1993). DNA processing during entry in transformation of Streptococcus pneumoniae. *Journal of Biological Chemistry, 268*(8), 5594-5599.

Michod, R. E., Bernstein, H., & Nedelcu, A. M. (2008). Adaptive value of sex in microbial pathogens. *Infection, Genetics & Evolution, 8*(3), 267-285.

Montanez, G. E., Neely, M. N., & Eichenbaum, Z. (2005). The streptococcal iron uptake (Siu) transporter is required for iron uptake and virulence in a zebrafish infection model. *Microbiology, 151*(Pt 11), 3749-3757.

Mora, M., Bensi, G., Capo, S., Falugi, F., Zingaretti, C., Manetti, A. G. O., . . . Telford, J. L. (2005). Group A Streptococcus produce pilus-like structures containing protective antigens and Lancefield T antigens. *Proceedings of the National Academy of Sciences of the United States of America, 102*(43), 15641-15646.

Moses, A. E., Wessels, M. R., Zalcman, K., Alberti, S., Natanson-Yaron, S., Menes, T., & Hanski, E. (1997). Relative contributions of hyaluronic acid capsule and M protein to virulence in a mucoid strain of

the group A Streptococcus. *Infection & Immunity, 65*(1), 64-71.

Muotiala, A., Seppala, H., Huovinen, P., & Vuopio-Varkila, J. (1997). Molecular comparison of group A streptococci of T1M1 serotype from invasive and noninvasive infections in Finland. *Journal of Infectious Diseases, 175*(2), 392-399.

Musser, J. M., & Shelburne, S. A., 3rd. (2009). A decade of molecular pathogenomic analysis of group A Streptococcus. *Journal of Clinical Investigation, 119*(9), 2455-2463.

Neely, M. N., Pfeifer, J. D., & Caparon, M. (2002). Streptococcus-zebrafish model of bacterial pathogenesis. *Infect Immun, 70*(7), 3904-3914.

Nelson, D. C., Garbe, J., & Collin, M. (2011). Cysteine proteinase SpeB from Streptococcus pyogenes - a potent modifier of immunologically important host and bacterial proteins. *Biological Chemistry, 392*(12), 1077-1088.

Nizet, V. (2007). Understanding how leading bacterial pathogens subvert innate immunity to reveal novel therapeutic targets. *Journal of Allergy & Clinical Immunology, 120*(1), 13-22.

Oehmcke, S., Shannon, O., Morgelin, M., & Herwald, H. (2010). Streptococcal M proteins and their role as virulence determinants. *Clinica Chimica Acta, 411*(17-18), 1172-1180.

Oliferenko, S., Kaverina, I., Small, J. V., & Huber, L. A. (2000). Hyaluronic acid (HA) binding to CD44 activates Rac1 and induces lamellipodia outgrowth.[Erratum appears in J Cell Biol 2000 Apr 3;149(1):following 236]. *Journal of Cell Biology, 148*(6), 1159-1164.

Palic, D., Andreasen, C. B., Ostojic, J., Tell, R. M., & Roth, J. A. (2007). Zebrafish (Danio rerio) whole kidney assays to measure neutrophil extracellular trap release and degranulation of primary granules. *J Immunol Methods, 319*(1-2), 87-97.

Pangburn, M. K., & Muller-Eberhard, H. J. (1986). The C3 convertase of the alternative pathway of human complement. Enzymic properties of the bimolecular proteinase. *Biochem J, 235*(3), 723-730.

Patti, J. M., Allen, B. L., Mcgavin, M. J., & Hook, M. (1994). Mscramm-Mediated Adherence of Microorganisms to Host Tissues. *Annual Review of Microbiology, 48*, 585-617.

Poulos, T. L., & Price, P. A. (1972). Some effects of calcium ions on the structure of bovine pancreatic deoxyribonuclease A. *Journal of Biological Chemistry, 247*(9), 2900-2904.

Proft, T., & Fraser, J. D. (2007). Streptococcal superantigens. *Chemical Immunology & Allergy, 93*, 1-23.

Que, Y. A., Haefliger, J. A., Francioli, P., & Moreillon, P. (2000). Expression of Staphylococcus aureus clumping factor A in Lactococcus lactis subsp cremoris using a new shuttle vector. *Infection and immunity, 68*(6), 3516-3522.

Rasmussen, M., & Bjorck, L. (2002). Proteolysis and its regulation at the surface of Streptococcus pyogenes. *Molecular microbiology, 43*(3), 537-544.

Reid, S. D., Green, N. M., Sylva, G. L., Voyich, J. M., Stenseth, E. T., DeLeo, F. R., . . . Musser, J. M. (2002). Postgenomic analysis of four novel antigens of group A Streptococcus: Growth phase-dependent gene transcription and human serologic response. *Journal of Bacteriology, 184*(22), 6316-6324.

Rodriguez-Ortega, M. J., Norais, N.., Bensi, G., Liberatori, S., Capo, S., Mora, M., . . . Grandi, G. (2006).

Characterization and identification of vaccine candidate proteins through analysis of the group A Streptococcus surface proteome. *Nature Biotechnology, 24*(2), 191-197.

Sahu, A., & Lambris, J. D. (2001). Structure and biology of complement protein C3, a connecting link between innate and acquired immunity. *Immunol Rev, 180*, 35-48.

Segal, A. W. (2005). How neutrophils kill microbes. *Annual Review of Immunology, 23*, 197-223.

Severin, A., Nickbarg, E., Wooters, J., Quazi, S. A., Matsuka, Y. V., Murphy, E., . . . Olmsted, S. B. (2007). Proteomic analysis and identification of Streptococcus pyogenes surface-associated proteins. *Journal of Bacteriology, 189*(5), 1514-1522.

Sinicropi, D., Baker, D. L., Prince, W. S., Shiffer, K., & Shak, S. (1994). Colorimetric determination of DNase I activity with a DNA-methyl green substrate. *Anal Biochem, 222*(2), 351-358.

Sriskandan, S., Faulkner, L., & Hopkins, P. (2007). Streptococcus pyogenes: Insight into the function of the streptococcal superantigens. *International Journal of Biochemistry & Cell Biology, 39*(1), 12-19.

Stockhammer, O. W., Zakrzewska, A., Hegedus, Z., Spaink, H. P., & Meijer, A. H. (2009). Transcriptome profiling and functional analyses of the zebrafish embryonic innate immune response to Salmonella infection. *Journal of Immunology, 182*(9), 5641-5653.

Strater, N., Lipscomb, W. N., Klabunde, T., & Krebs, B. (1996). Two-metal ion catalysis in enzymatic acyl- and phosphoryl-transfer reactions. *Angewandte Chemie-International Edition in English, 35*(18), 2024-2055.

Suck, D., Oefner, C., & Kabsch, W. (1984). Three-dimensional structure of bovine pancreatic DNase I at 2.5 A resolution. *EMBO Journal, 3*(10), 2423-2430.

Sumby, P., Barbian, K. D., Gardner, D. J., Whitney, A. R., Welty, D. M., Long, R. D., . . . Musser, J. M. (2005). Extracellular deoxyribonuclease made by group A Streptococcus assists pathogenesis by enhancing evasion of the innate immune response. *Proceedings of the National Academy of Sciences of the United States of America, 102*(5), 1679-1684.

Sumby, P., Whitney, A. R., Graviss, E. A., DeLeo, F. R., & Musser, J. M. (2006). Genome-wide analysis of group a streptococci reveals a mutation that modulates global phenotype and disease specificity. *PLoS Pathogens, 2*(1), e5.

Sumby, P., Zhang, S., Whitney, A. R., Falugi, F., Grandi, G., Graviss, E. A., . . . Musser, J. M. (2008). A chemokine-degrading extracellular protease made by group A Streptococcus alters pathogenesis by enhancing evasion of the innate immune response. *Infect Immun, 76*(3), 978-985.

Sumitomo, T., Nakata, M., Higashino, M., Jin, Y., Terao, Y., Fujinaga, Y., & Kawabata, S. (2011). Streptolysin S contributes to group A streptococcal translocation across an epithelial barrier. *Journal of Biological Chemistry, 286*(4), 2750-2761.

Tamura, F., Nakagawa, R., Akuta, T., Okamoto, S.i, Hamada, S., Maeda, H., . . . Akaike, T. (2004). Proapoptotic effect of proteolytic activation of matrix metalloproteinases by Streptococcus pyogenes thiol proteinase (Streptococcus pyrogenic exotoxin B). *Infection & Immunity, 72*(8), 4836-4847.

Tart, A. H., Walker, M. J., & Musser, J. M. (2007). New understanding of the group A Streptococcus

pathogenesis cycle. *Trends in Microbiology, 15*(7), 318-325.

Tillett, W. S., Sherry, S., & Christensen, L. R. (1948). Streptococcal desoxyribonuclease; significance in lysis of purulent exudates and production by strains of hemolytic streptococci. *Proc Soc Exp Biol Med, 68*(1), 184-188.

Timmer, A. M., Timmer, J. C., Pence, M. A., Hsu, L., Ghochani, M., Frey, T. G., . . . Nizet, V. (2009). Streptolysin O promotes group A Streptococcus immune evasion by accelerated macrophage apoptosis. *Journal of Biological Chemistry, 284*(2), 862-871.

Uchiyama, S., Andreoni, F., Schuepbach, R. A., Nizet, V., & Zinkernagel, A. S. (2012). DNase Sda1 allows invasive M1T1 Group A Streptococcus to prevent TLR9-dependent recognition. *PLoS Pathogens, 8*(6), e1002736.

Urban, C. F., Reichard, U., Brinkmann, V., & Zychlinsky, A. (2006). Neutrophil extracellular traps capture and kill Candida albicans yeast and hyphal forms. *Cellular Microbiology, 8*(4), 668-676.

von Kockritz-Blickwede, M., Goldmann, O., Thulin, P., Heinemann, K., Norrby-Teglund, A., Rohde, M., & Medina, E. (2008). Phagocytosis-independent antimicrobial activity of mast cells by means of extracellular trap formation. *Blood, 111*(6), 3070-3080.

Walker, M. J., Hollands, A., Sanderson-Smith, M. L., Cole, J. N., Kirk, J. K., Henningham, A.a, . . . Nizet, V. (2007). DNase Sda1 provides selection pressure for a switch to invasive group A streptococcal infection. *Nature Medicine, 13*(8), 981-985.

Walport, M. J. (2001). Complement. First of two parts. *N Engl J Med, 344*(14), 1058-1066.

Wannamaker, L. W. (1958). The differentiation of three distinct desoxyrlbonucleases of group A Streptococci. *Journal of Experimental Medicine, 107*(6), 797-812.

Wannamaker, L. W., Hayes, B., & Yasmineh, W. (1967). Streptococcal nucleases. II. Characterization of DNAse D. *Journal of Experimental Medicine, 126*(3), 497-508.

Wartha, F., Beiter, K., Normark, S., & Henriques-Normark, B. (2007). Neutrophil extracellular traps: casting the NET over pathogenesis. *Current Opinion in Microbiology, 10*(1), 52-56.

Weinstein, M., Low, D., McGeer, A., Willey, B., Rose, D., Coulter, M., . . . Facklam, R. (1996). Invasive infection due to Streptococcus iniae: a new or previously unrecognized disease--Ontario, 1995-1996. *Can Commun Dis Rep, 22*(15), 129-131; discussion 131-122.

Weinstein, M. R., Litt, M., Kertesz, D. A., Wyper, P., Rose, D., Coulter, M., . . . Low, D. E. (1997). Invasive infections due to a fish pathogen, Streptococcus iniae. S. iniae Study Group. *N Engl J Med, 337*(9), 589-594.

Wessels, M. R., Moses, A. E., Goldberg, J. B., & DiCesare, T. J. (1991). Hyaluronic acid capsule is a virulence factor for mucoid group A streptococci. *Proceedings of the National Academy of Sciences of the United States of America, 88*(19), 8317-8321.

Wexler, D. E., & Cleary, P. P. (1985). Purification and characteristics of the streptococcal chemotactic factor inactivator. *Infect Immun, 50*(3), 757-764.

Zeleznick, L. D., Boltralik, J. J., Barkulis, S. S., Smith, C., & Heymann, H. (1963). Biosynthesis of streptococcal cell walls: A rhamnose polysaccharide. *Science, 140*, 400-401.

Zhu, L., Kuang, Z., Wilson, B. A., & Lau, G. W. (2013). Competence-independent activity of pneumococcal enda mediates degradation of extracellular DNA and nets and is important for virulence. *PLoS One, 8*(7), e70363.

Zinkernagel, A. S., Hruz, P., Uchiyama, S., von Kockritz-Blickwede, M., Schuepbach, R. A., Hayashi, T., . . . Nizet, V. (2012). Importance of Toll-like receptor 9 in host defense against M1T1 group A Streptococcus infections. *Journal of Innate Immunity, 4*(2), 213-218.

Zinkernagel, A. S., Timmer, A. M., Pence, M. A., Locke, J. B., Buchanan, J. T., Turner, C. E., . . . Nizet, V. (2008). The IL-8 protease SpyCEP/ScpC of group A Streptococcus promotes resistance to neutrophil killing. *Cell Host Microbe, 4*(2), 170-178.